WAVE INTERACTION OF THE H-TYPE FLOATING BREAKWATER

by

MARK DEXTER M TAN

Supervisor: DrTehHee Min

Civil Engineering Department

Wave Interaction of the H-Type Floating Breakwater

by

Mark Dexter M Tan

Dissertation submitted in partial fulfillment of
the requirements for the
Bachelor of Engineering (Hons)
(Civil Engineering)

MAY 2013

UniversitiTeknologi PETRONAS
Bandar Seri Iskandar
31750 Tronoh
Perak DarulRidzuan

CERTIFICATION OF APPROVAL

Wave Interaction of the H-Type Floating Breakwater

By

Mark Dexter M Tan

A project dissertation submitted to the

Civil Engineering Department

of Universiti Teknologi PETRONAS

in partial fulfillment of the requirement for the

Bachelor of Engineering (Hons)

(Civil Engineering)

Approved by,

_____

(Dr. Teh Hee Min)

UNIVERSITI TEKNOLOGI PETRONAS

TRONOH, PERAK

May 2013

CERTIFICATION OF ORIGINALITY

This is to certify that I am responsible for the work submitted in this project, that the original work is my own except as specified in the references and acknowledgements, and that the original work contained herein have not been undertaken or done by unspecified sources or persons.

_____

(MARK DEXTER M TAN)

ABSTRACT

Suppression of wave energy has been a challenge to many coastal engineers and researchers. Numerous efforts have been taken in the development of both hard and soft strategies in protecting coastal infrastructures from the intrusion of destructive waves. Breakwater is one of the most widely used structures in offering some degree of protection to the shoreline. Despite excellent wave dampening ability, the fixed breakwaters may pose several drawbacks mostly to the environment, i.e. interruption to sediment transport, interference to fish migration, water pollution and the downcoast erosions. This study aims at developing the H-type floating breakwater in providing an alternative to the bottom-seated breakwaters. A large scale (1:5) test model constructed using plywood and fiberglass coating was extensively tested in a 25-m wave flume equipped with measuring wave probes in its vicinity. Regular and random wave conditions were generated by the wave generator in the flume. Some of the important test parameters were breakwater immersion depth, wave period and wave height. In total, 108 tests were conducted in this study. The hydraulic performance of the H-type floating breakwater was quantified by the coefficients of transmission, reflection and energy loss. In general, the test model is an effective wave attenuator (with wave attenuation up to 95%), strong wave reflector (reflection of 42 - 87% of incident waves) and good energy dissipater (as high as 85%). In comparison with other types of floating breakwater, the H-type floating breakwater outperforms the others in terms of wave attenuation. This indicates that the configuration of the H-shape floating breakwater is effective in enhancing its overall hydraulic performance.

ACKNOWLEDGEMENT

The author would like to express his sincere gratitude to the supervisor, Dr. Teh Hee Min; lecturer of Civil Engineering Department, Universiti Teknologi PETRONAS for the guidance throughout this project. Thank you for the continuous supports and motivation.

To my Laboratory partner; Mr Awang Khairul Amzar who has been conducting the experiment together with the author, thank you for willing to contribute endlessly in helping the author. This special appreciation was also extended to Miss Nadia Aida and Mr Mohd Syahmi for their support.

Special appreciation to two postgraduate students; Miss Nur Zaidah and Miss Noor Diyana, for their guidance in analyzing of the experimental results as well as the preparation and conducting the experiment.

To the Offshore Laboratory technicians and staffs, particularly Mr. Meor Asnawan, Mr Iskandar and Mr. Mohd Zaid that have been assisting the author throughout the experiment. Without them, this project would've been a complete failure. Thank you for the help given when the author were facing difficulties during the experiment.

To Universiti Teknologi PETRONAS, thank you for giving this opportunity to the author to conduct this final year project with the help of various wonderful people and thus gaining the most wonderful experience in this institution.

To my family, thank you for your prayers and moral support. And last but not least, millions of thanks to the lecturers, technicians and friends who have been contributing for this project.

Thank you.

MARK DEXTER M TAN

Civil Engineering Department

TABLE OF CONTENT

SYMBOLS

H_i	incident wave height
H_r	reflected wave height
H_t	transmitted wave height
C_r	reflection coefficient
C_t	transmission coefficient
C_l	energy loss coefficient
E_i	incident wave energy
E_r	reflected wave energy
E_t	transmitted wave energy
E_l	energy loss
L	wavelength
T	wave period
f	frequency
B	width of breakwater
h	height of breakwater
l	length of breakwater
D	draft of breakwater
d	water depth
B/L	relative breakwater width
H_i/L_p	incident wave steepness
H_i/gT^2	wave steepness parameter
D/d	breakwater draft-to-water depth ratio

LIST OF FIGURES

LIST OF TABLES

CHAPTER 1

INTRODUCTION

1.1 Background Study

Coastal areas often need protection against excessive wave action. Some of the natural protection features are island, shoals and spits. However the degree of protection provided by these coastal features might not be adequate in suppressing the energy of waves. In such case, manmade structures such as breakwaters are constructed to reduce the height of the incident wave at the sheltered zone. These breakwaters reduce wave energy mainly through wave breaking, wave overtopping and wave reflection. The breakwater functions almost the same like those of natural topographies at the sea but breakwater offers a more promising results. Over the years, there are various types of fixed breakwater that have been used such as the sloping (mound) type, vertical (upright) type, composite type, and the horizontally composite type (Takahashi, 1996). The most common type of fixed breakwater used is the sloping (mound) type. An example of this type of breakwater will be the rubble mound which can be found not too far away from the shore. It is undeniable that fixed structure breakwater perform much better than the floating breakwater. However, the potential drawbacks of the fixed breakwater are it is not environmentally friendly. The fixed breakwater can be a total barrier to close off a significant portion of waterway or entrance channel, thereby causing a faster river flow in the vicinity as well as potentially trapping debris on the updrift side. The presence of these gigantic structures may also create unacceptable sedimentation and poor water circulation behind the structure.

Another shortcoming of a fixed breakwater is that its wave dampening power decreases rapidly as the tide level rises due to the fact that wave dissipation over the breakwater is mainly caused by wave breaking on the slope. It is often uneconomical and impractical to build a fixed breakwater in water deeper than about 20 feet as the construction cost of the breakwater is proportional to the square of the water depth (Sorensen, 1978; McCartney, 1985). Very careful thought must be given to the design of fixed

breakwaters and its effects on the physical system in which it is to be placed because, once constructed, very few are ever removed. They become a permanent part of the landscape and any environmental damage they may cause must either be accepted or the breakwater must be removed. This may be a very expensive penalty for a mistake.

Floating structure breakwaters have been developed as an alternative to fixed breakwater. Various types of floating breakwater were reported by Hales (1981) and McCartney (1985). Floating breakwaters offers advantages over the conventional fixed structure as they are inexpensive, reusable, movable and more environmental friendly. Previously many researchers had developed and tested various floating breakwaters (McCartney, 1985) and the design of the box-type floating breakwater (Nece and Skjelbreia, 1984; Isaacson and Brynes, 1988) had become the basis for the constructions of the H-shape floating breakwater (Teh and Nuzul, 2013). Due to its impressive performance over other previously experimented floating breakwaters, the H-shape configuration was chosen in this study as it will be improve further with the development of a novel breakwater. This novel breakwater will have a larger scales, will be tested with various test conditions and data obtained will be measured with enhanced measurement technique.

1.2 Problem Statement

Floating breakwater are structures that are used to protect marinas and harbor from the destructive sea waves. They offer many advantages over the fixed structure breakwaters. The previous study was conducted by the means of a small-scale physical modeling using a 10-m wave flume due to inadequate laboratory facilities and budget constraints. Even though the experimental study revealed that the H-shape breakwater was able to attenuate the incident wave height up to 80% (Teh *et al*., 2005), it was subjected to several drawbacks:

1) Width effect

Previous H-shape design were concentrated on the effect of higher draft and porosity but the effect of width was not investigated due to time constrain.

2) Limited test cases

Due to budget constrain, both the models were subjected to small test cases such as small range of wave period in the presence of monochromatic water waves

3) Scale effects

The scale used for the physical modeling was 1:30. It may result in significant scale effect that would not give actual representation of the physical processes taking place at the breakwater

4) Inadequate measurement technique

Reflection characteristics of the H-shape models were determined by the moving probe method, this method is prone to instrumental and human errors.

5) Poor understanding of hydrodynamic and motion responses of the breakwater

Energy dissipation mechanisms taking place at both the models and the motion responses were not measured.

The solution for the above problem is to develop a novel breakwater based on the design of H-shape floating breakwater but with larger scale. The novel breakwater is expected to perform better in attenuating wave energy.

1.3 Significance of the Study

The need to protect shoreline from erosion, valuable lives and also structures around the shore from the destructive wave energy had lead researchers and engineer constantly experimenting and developing floating breakwaters because they perform well and of low production cost. Over the past few years, many

marinas and recreational resorts as well as ports were developed in Malaysia. The harsh condition of the sea often poses threat to these coastal structures and at the same time the life of human being. In line with these developments, the need for coastal protection also increases. Fixed breakwaters were built to serve this purpose but it offers more potential drawback. An option to use floating breakwater to replace fixed breakwater has made this study more significant because when compared to fixed breakwater, floating breakwaters are inexpensive, environmentally friendly, flexible, removable, applicable in poor soil condition, and has more aesthetic value. Thus, the author decided to research and develops a novel breakwater locally which will perform better and hopefully will be cheaper than the existing breakwaters.

1.4 Objective of the Study

For this project, the objectives of the study are as follows:

1. To evaluate the hydraulic performance of the proposed breakwater with respect to the typical sea states in Malaysia using large scale physical modeling
2. To compare the novel floating breakwater performance with other existing breakwaters performance.

1.5 Scope of Study

The scopes of study are outlined as follows:

1. Literature review

   Thorough study will be conducted to explore the development of the previous floating breakwater designs.

2. Fabrication of the newly proposed floating breakwater

   The H-shape floating breakwater (FBW) is modified and scaled up with the aim to improve its wave breaking performance as shown in Figure 1.1 and Figure 1.2.

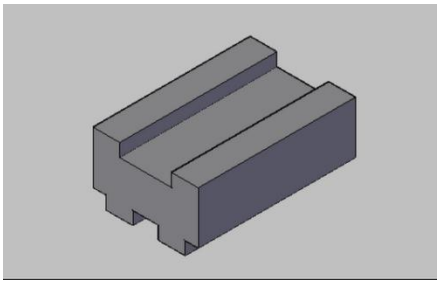

Figure 1.1: H-shape FBW

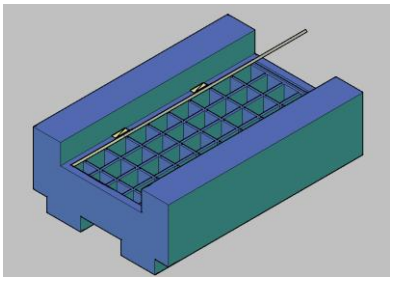

Figure 1.2: H-type FBW

3. Laboratory set up

   The operations of the test facilities such as wave flume and wave generator are studied properly. Accuracy and precision of the apparatus and equipments used in the experiment are checked.

4. Experiments

   Experiments will be conducted in a wave flume to assess the hydraulic performance of the novel floating breakwater.

5. Analysis of results

   Experimental results will be analyzed and discussed. Comparison with previous floating breakwaters will also be made.

CHAPTER 2

LITERATURE REVIEW

2.1 General

This chapter provide wave attenuation feature for the box, pontoon, mat and tethered type floating breakwaters as well as other configurations of floating breakwaters. The study on the breakwaters would provide some performance rule-of-thumb in developing a breakwater design that offer high hydraulic efficiency in the present study. This chapter also includes the discussion on parameters used to quantify the amount of wave reflection, wave transmission and energy loss.

2.2 Evaluation of Breakwater Performance

2.2.1 Wave Reflection

Wave reflection occurs when wave energy is reflected as the waves hit into a rigid obstruction such as a breakwater, seawall, cliff, etc. This is especially obvious where the surface is a smooth vertical wall. The amount of reflected wave can be quantified by reflection coefficient, C_r.

$$C_r = \frac{H_r}{H_i} \tag{2.1}$$

where, H_r and H_i are the reflected and incident wave height respectively

If 100% of wave energy is reflected (total reflection), the C_r is equal to 1. This is generally valid for impermeable vertical wall of infinite height. The reflection coefficient for sloping, rough or permeable structures are smaller.

2.2.2 Wave Transmission

The effectiveness of a breakwater in attenuating wave energy can be measured by the amount of wave energy that is transmitted past the floating structure. The greater the wave transmission coefficient, the lesser will be the wave attenuation ability. Wave transmission is quantified by the wave transmission coefficient, C_t .

$$C_t = \frac{H_t}{H_i} \tag{2.2}$$

where,H_t and H_i are the transmitted and incident wave height respectively.

2.2.3 Energy Loss

When a wave interact a floating structure, some of the wave energy is reflected to the lee side of the structure; some is used to excite the structure in motions; some is transmitted to the lee of the structure and form a new wave. The remaining energy are lost through the wave dissipation mechanisms for instance wave breaking, turbulence, heat and sound.

The energy loss of the system that passes through an obstruction can be represented by

$$E_i = E_r + E_t + E_l \tag{2.3}$$

Where,

E_i is the incident wave energy

E_r is the reflected wave energy

E_t is the transmitted wave energy

E_l is the energy loss

In other terms,

$$\frac{(pgH)^2{}_i}{8} = \frac{(pgH)^2{}_r}{8} + \frac{(pgH)^2{}_t}{8} + \frac{(pgH)^2{}_l}{8} \tag{2.4}$$

The equation above can be simplified as,

$$H_i{}^2 = H_r{}^2 + H_t{}^2 + H_l{}^2 \quad (2.5)$$

By dividing the incident wave heights at the both terms, it yields

$$\frac{H_i{}^2}{H_i} = \frac{H_r{}^2}{H_i} + \frac{H_t{}^2}{H_i} + \frac{H_l{}^2}{H_i} \quad (2.3)$$

$$1 = C_r{}^2 + C_t{}^2 + C_l{}^2 \quad (2.3)$$

Where,

C_r is the reflection coefficient

C_t is the transmission coefficient

C_l is the loss coefficient

Rearranging this equation will yield;

$$C_l{}^2 = 1 - (C_t)^2 - (C_r)^2 \quad (2.3)$$

2.2.4 Regular Waves

Regular waves are waves that repeat itself over time wherein the vertical displacement of the water surface is the same over a certain period and distance. The vertical displacement of the sea surface is described as a function of horizontal coordinates *x* and *y*, and time *T*. This T is called the period of the waves. The frequency of the waves is $f = \frac{1}{T}$, the angular frequency is $\omega = \frac{2\pi}{T}$, its unit is rad/s. The propagation speed of the waves depends on the period, the waves with the longer period propagate faster than the ones with a smaller period.

The classical example of a regular wave on constant depth (and current velocity) is the sinusoidal wave: $\eta = a\cos(kx - \omega t)$ where a is the amplitude, ω is the angular

frequency (as measured at a fixed location in space), and k is the wave number ($k = \frac{2\pi}{\lambda}$ where λ is the wavelength).

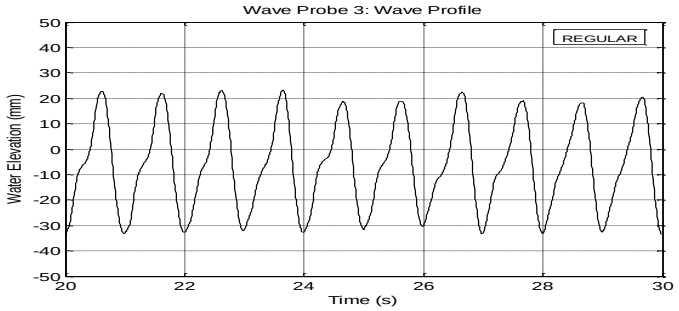

Figure 2.1: Regular wave train

2.2.5 Random Waves

Random waves are waves that are made up of a lot of regular plane waves. Random waves do not have a constant wavelength, constant water level elevation and it also has a random wave phase. When the waves are recorded, a non-repeating wave profile can be seen and the wave surface record will be irregular and random. From the profile, some of the individual waves can be identified but overall the wave profile will show significant changes in height and period from wave to wave as shown in Figure 2.2. The spectral method and the wave-by-wave analysis were used to treat random waves. Spectral approaches are based on Fourier Transform of the water waves. In wave-by-wave analysis, a time history of the water waves are used and a statistical record are developed.

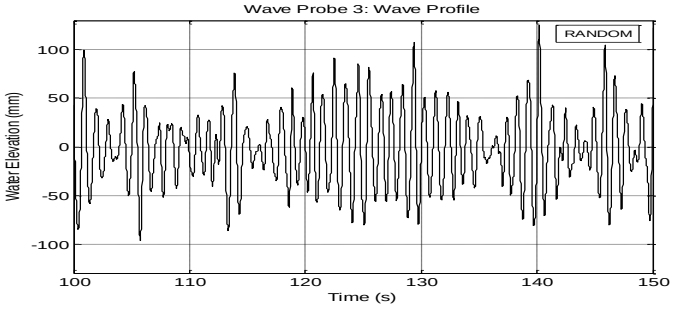

Figure 2.2: Random wave train

2.3 Floating Breakwater

In the past, fixed breakwaters were used widely in the attempt of protecting the shoreline from being eroded or destroyed by massive waves. These structures has some limitation: (a) it is costly when the structure need to be build further and deeper from the shore (Sorensen, 1978; McCartney, 1985), (b) it is not environmentally friendly as it can be a total barrier to trap debris from the updrift side and at the same time affect the sediment transport behind the structure, (c) its effectiveness in dampening incoming wave energy decreases as tide level increases, and (d) it has poor aesthetic value as it will block the view to the beautiful ocean from the beach. To overcome the above mentioned problems, floating breakwaters have been recommended by a number of researchers (Hales, 1981; McCartney, 1985; Mani, 1991; Murani and Mani, 1997; Sannasiraj, 1997; William and Abul-Azm, 1997; Koftis and Prinos, 2005). Floating breakwaters offer a number of desirable properties over fixed breakwater such as:

a. Low construction cost: Compared to the fixed breakwater, construction of floating breakwaters are inexpensive because as depth increases, its construction cost hardly increases (Fousert, 2006).
b. Rapid construction and transportation: Floating breakwater can be mass produced on land into various shapes and sizes by casting them inside a mould or by constructing them using recyclable materials. It can be stack on a big vessel or towed to the open ocean easily as it's a readily floating structure.
c. Less interference to the ecosystem: The presence of floating breakwater poses less interference to the environment. It allows fish migration and sediment transport beneath the structure and preserves the water quality in the vicinity of the breakwater.
d. Applicability at poor foundation sites: Floating breakwater often constructed at areas that are hard to reach by fixed breakwater such as offshore areas with water depth more than 20ft. Mooring the breakwater by cables or chains in the environment could greatly reduce the construction cost.
e. High mobility: Floating breakwater can be easily relocated to accommodate the change of sea condition.

f. High aesthetics value: Floating breakwaters have relatively low profiles that will preserve the natural beauty of the beach.
g. Interchangeable layout: Floating breakwaters are easy to assemble and dissemble. Rearranging them into new layout will take minimum effort.

2.3.1 Classification of Floating Breakwater

Hales(1981) review the five concepts namely pontoons, sloping floats, scrap tires, cylinders, and tethered floats which are the dominant floating breakwater types while McCartney (1985) introduced four types of FBW for instance, box, pontoon, mat, and tethered float. A brief description of those floating breakwater are as follow:

a) Box type floating breakwater

This type of breakwater is the commonly used because of its simple configuration. It is constructed from reinforced concrete modules which has a density lower than that of sea water. It has a solid or hollow body. The floating module is then moored to the sea floor with flexible or tensioned connectors. The common shapes of the box type floating are square, rectangle and trapezoidal shape.

b) Pontoon type floating breakwater

Pontoon type floating breakwater (also called Alaska or ladder type) takes on the design of the catamaran used by fishermen in the past as the structure are very stable and rigid. It comprises two units of rectangular or box shaped breakwater connected together by a plate or a wooden deck. This structure offers a great option if increasing the draft of a structure is permitted. The width and spacing between the pontoons can be increased so as to offer a double protection against waves. The pontoons are made of reinforced concrete embedded with light buoyant materials for instance, polystyrene.

c) Mat type floating breakwater

Mat type floating breakwater consists of a series of scrap tires or log raft chained on cable together and moored to the sea floor. Rubber tires float well in water and their arrangement provides a permeable surface to allow some wave energy to be reflected and some to pass through them for the dissipation of wave energy. Floating mat type breakwater offer disadvantage such as lack of buoyancy. Marine growth and silt accumulation in tire can sink the breakwater. They pose the ability to attract and accumulate floating debris due to their configurations. The main reason for the usage of this type of breakwater is because of low material and labor cost.

d) Tethered float type floating breakwater

Tethered type breakwaters often made up of spherical floats or steel drums with ballasts that are individually tethered to a rigid submerged frame. It is appropriate to be used in a small fishing village where the waves are not too violent. If needed for deep sea, the size of the float needs to be decrease and to offer a better performance (Vethamony *et al*., 1993).

And after that, various researchers such as Gesraha (2006), Williams and Abul-Azm (1995), Hedge *et al*. (2007), Wang and Sun (2009) and Vethamony (1994) had improved these floating breakwaters design since then.

2.3.2 Drawbacks of Floating Breakwater

Although the floating type breakwater offer various advantages over the fixed type breakwaters, there are some disadvantages and limitations. Overall floating breakwater offer lesser wave attenuating performance compared to fixed breakwater. Moored breakwater can offer protection up to some extent, but huge waves might just overtop and even destroy the structure. One of the mechanisms for wave energy dissipation is by reflection but extensive wave reflection on the structure might cause problems to the small floating vessels. Moored breakwaters are subjected to uneven tensile force when operating at sea. If the breakwater is damaged by waves, it could not

be repaired at site but to tow to the land for the repairing process. Besides that, they have shorter design life as it will deteriorate easily over time because of the effect of heat and the raging sea water. Most of the floating breakwaters are designed to withstand waves of smaller period in shallow waters.

The limitations of floating breakwaters have led researchers to further investigate the optimal features and configurations of the floating breakwater with increased performance and economically feasible.

2.4 Performance of existing floating breakwater

A number of floating breakwaters (FBW) have been developed and tested by different researchers in the past. Hales (1981) reviewed five concepts of FBW which are the pontoon, sloping floats, scrap tires, cylinders, and tethered float. He suggested that the designs of FBW should be kept as simple, durable and maintenance free as possible; avoiding highly complex structures that are difficult and expensive to design, construct and maintain. Later on, McCartney (1985) introduced four types of FBW, including the box, pontoon, mat, and tethered float. Some example of the floating breakwater that have been developed and tested as shown in Figure 2.3, will be discussed in this section as follows.

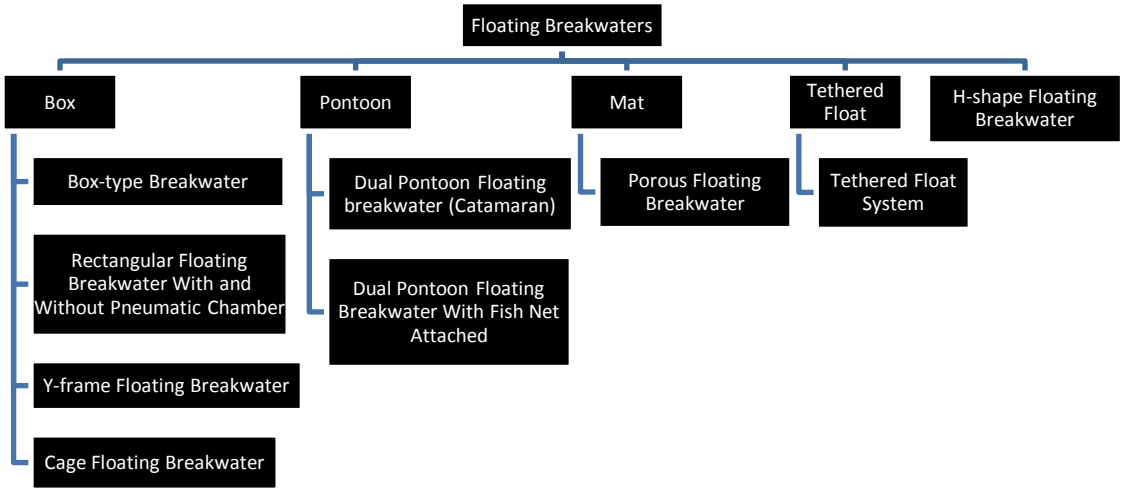

Figure 2.3: Various types of floating breakwater configuration

2.4.1 Box, Rectangular, and Trapezoidal Type Floating Breakwater

2.4.1.1 Box Floating Breakwater

McCartney (1985) introduced the box floating breakwater which was constructed of reinforced concrete module. It could be of barge shape or rectangular shape as shown in Figure 2.4 and Figure 2.5 respectively. The modules either have flexible connections or are pre- or post-tensioned to make them act as a single unit. The advantages of the box-type breakwater are it has 50 years design life, its structure allow pedestrian access for fishing and temporary boat moorage. The shape of the box breakwater is simple to build but a high quality control is needed. It is effective in moderate wave climate. However, the cost of constructing the box type breakwater is very high, if maintenance is needed for the breakwater, it has to be tow to dry dock. In Figure 2.6, it shows that the box-type breakwater that was tested at Olympia Harbor, Washington attenuate wave energy more as it only allows 40% of the wave energy to be transmitted as the breakwater relative width increases.

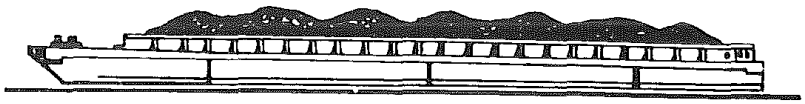

OPEN HOPPER BARGES

TYPE	LENGTH FEET	BREADTH FEET	DRAFT FEET	CAPACITY TONS
STANDARD	175	26	9	1000
JUMBO	195	35	9	1500
SUPER JUMBO	250 - 290	40 - 52	9	2500 - 3000

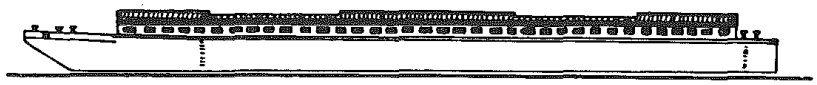

COVERED HOPPER BARGES

TYPE	LENGTH FEET	BREADTH FEET	DRAFT FEET	CAPACITY TONS
STANDARD	175	26	9	1000
JUMBO	195	35	9	1500

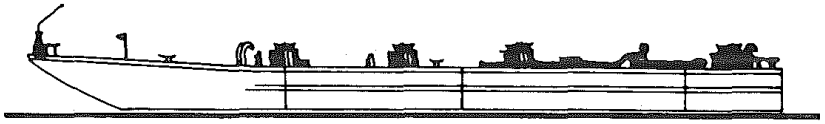

INTEGRATED CHEMICAL AND PETROLEUM BARGES

LENGTH FEET	BREADTH FEET	DRAFT FEET	CAPACITY TONS
150 - 300	50 - 54	9	1900 - 3000

Figure 2.4: Predominate barge sizes in United States (source: McCartney, 1985)

Figure 2.5: Solid rectangular box-type floating breakwater (source: McCartney, 1985)

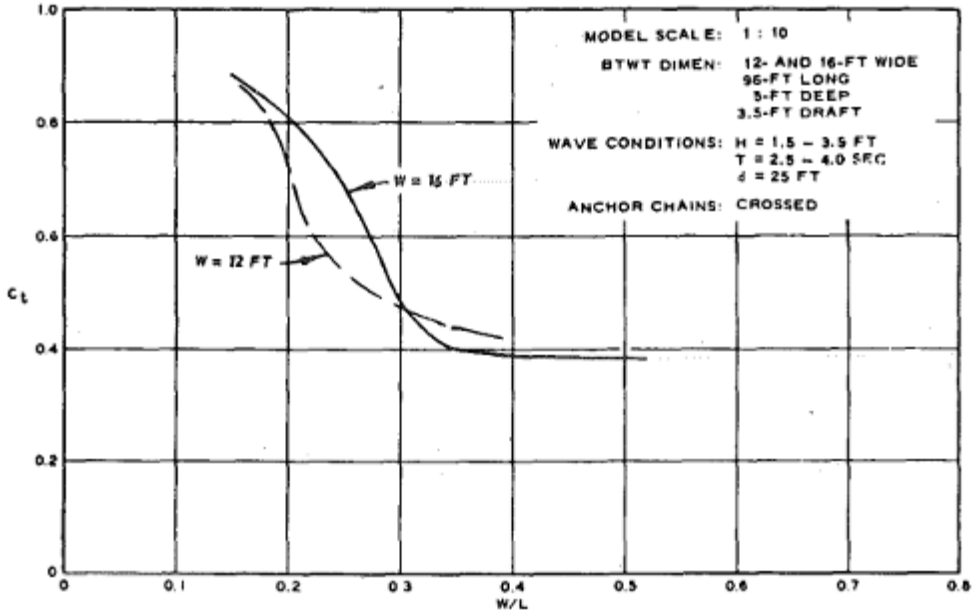

Figure 2.6: Wave transmission coefficient C_t, versus breakwater relative width for box type breakwater tested for Olympia Harbor, Washington (source: McCartney, 1985)

2.4.1.2 Rectangular Floating Breakwater With and Without Pneumatic Chamber

He *et al*. (2011) studied the performance of rectangular shaped breakwaters with and without pneumatic chambers installed on them. He *et al*. (2011) propose a novel configuration of a pneumatic floating breakwater for combined wave protection and potential wave energy capturing. Pneumatic is a system that uses compressed air trapped in a chamber to produce mechanical motion for instance, a vacuum pump.

The development of the concept originates from the oscillating water column (OWC) device commonly used in wave energy utilization (Falcao, 2010). The configuration consists of the box-type breakwater with a rectangular cross section as the base

structure, with pneumatic chambers (OWC units) installed on both the front and back sides of the box-type breakwater without modifying the geometry of the original base structure as shown on Figure 2.7. The pneumatic chamber used in this experiment is of hollow chamber with large submerged bottom opening below the water level. Air trapped above the water surface inside the chamber is pressured due to water column oscillation inside the chamber and it can exit the chamber through a small opening at the top cover with energy dissipation. The aim for this experiment is to provide an economical way to improve the performance of the box-type floating breakwater for long waves without significantly increasing its weight and construction cost. The performance was compared with that of the original box-type floating breakwater without pneumatic chambers. With the comparison of these two configurations, the wave transmission, wave energy dissipation, motion responses, the effect of draught and air pressure fluctuation inside the pneumatic chamber were studied.

As shown in Figure 2.8 (a), wave reflection of model 1 was stronger for relatively shorter period waves but weaker for longer period waves. The minimum reflection coefficient occurred around B/L = 0.23. In contrast, Figure 2.8 (b) shows the reflection coefficient for model 2 varied in narrow ranges roughly between 0.2 and 0.5.

In Figure 2.9 (a), when installing the pneumatic chambers for model 1, wave transmission coefficient was reduced for the whole range of B/L. Increasing B/L reduces transmission coefficient from 0.71 to 0.15. In contrast, Figure 2.9 (b) shows that the transmission coefficient for model 2 was high for long period waves and eventually decreased at shorter period waves but at a higher value compared to model 1.

In Figure 2.10 (a) and (b), comparing model 1 and model 2, model 1 was able to dissipate more energy for longer period waves but no significant changes for shorter period waves. This might be due to the vortex shedding at the tips of the chamber front walls and the air flow through the slot openings at the top of the chambers.

From this study, with the installation of the pneumatic chambers, wave transmission coefficient was reduced in the whole range of B/L. This is because the pneumatic chambers changed the wave scattering and energy dissipation of incoming waves.

Draughts were adjusted by extra ballast wherein model with deeper draught had a larger mass and larger moment of inertia and the amount of water in the pneumatic chamber were also increased. Deepening the draught reduced the wave transmission beneath the breakwater but increased the wave reflection. Pneumatic chamber can also turned breakwaters into energy generator by installing Wells turbines to the chambers.

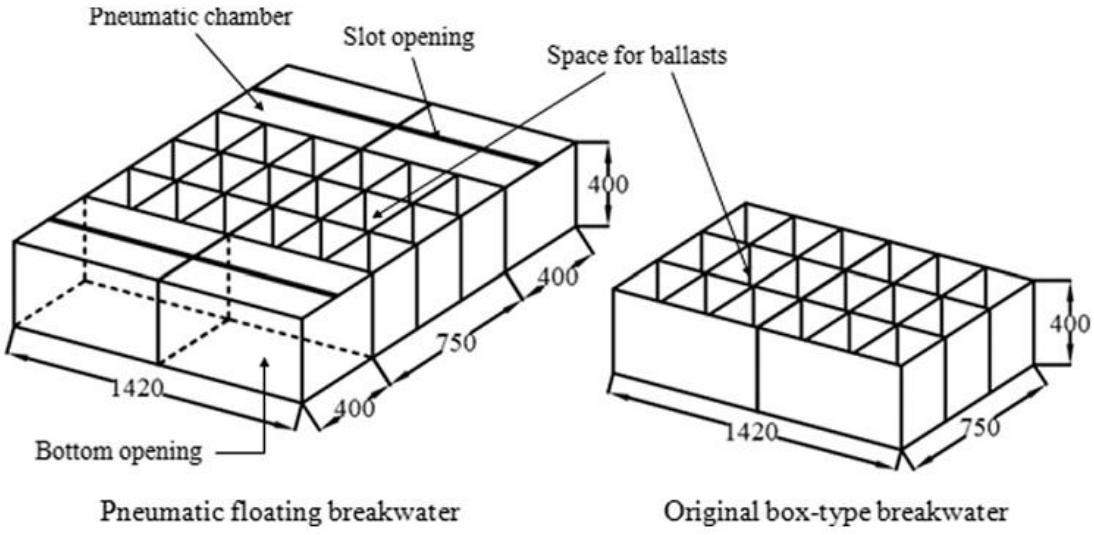

Figure 2.7: Pneumatic floating breakwater and box-type rectangular model. (Source: He *et al.*, 2011)

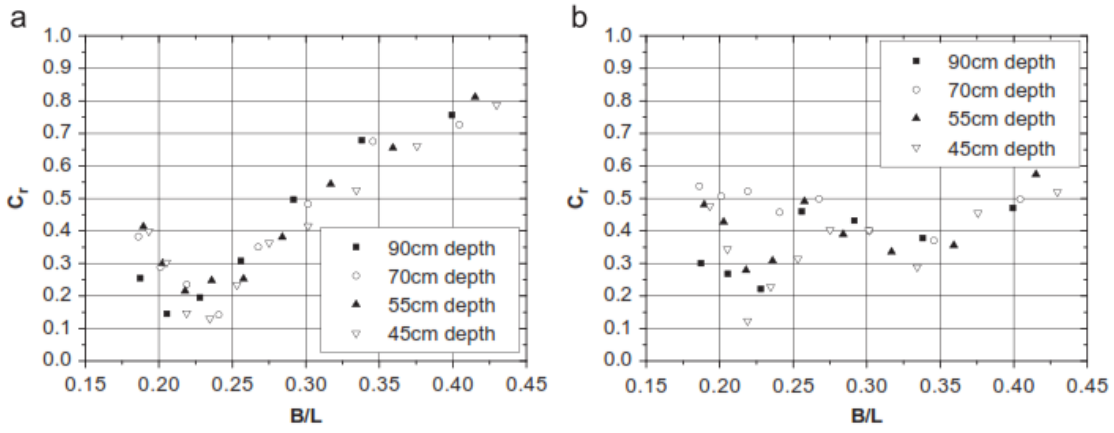

Figure 2.8: Variation of reflection coefficient, C_r versus B/L under 4 water depth: (a) Model 1 with chambers, 0.235m draught; (b) Model 2 without chambers, 0.235m draught. (Source: He *et al.*, 2011)

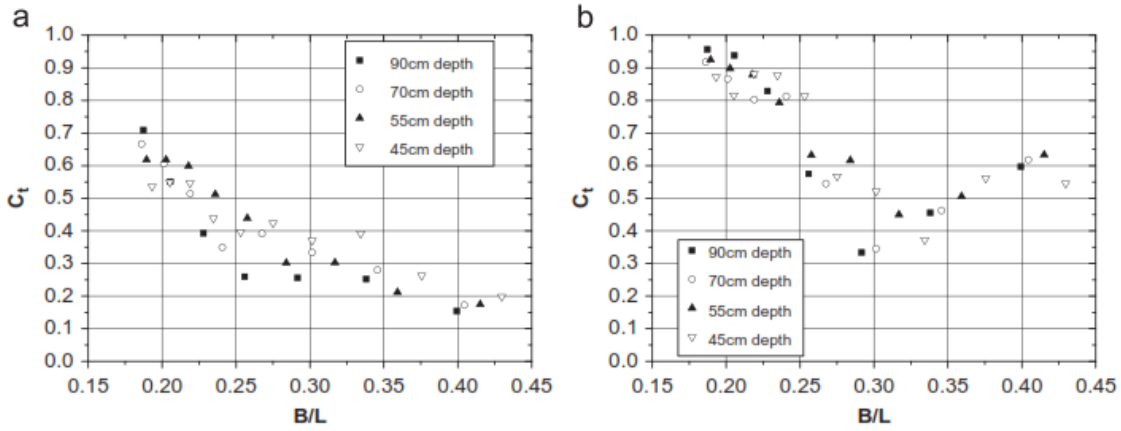

Figure 2.9: Variation of transmission coefficient, C_t versus B/L under 4 water depth: (a) Model 1 with chambers, 0.235m draught; (b) Model 2 without chambers, 0.235m draught. (Source: He *et al*., 2011)

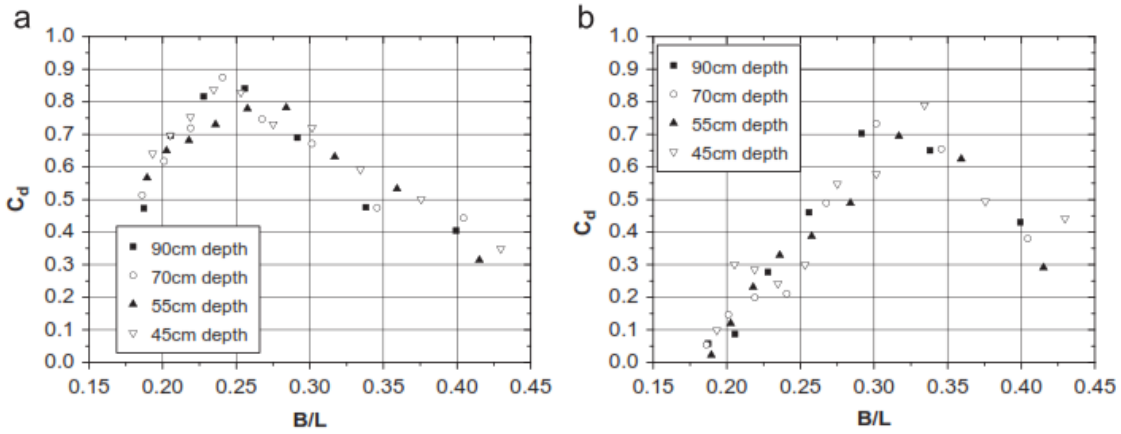

Figure 2.10: Variation of energy loss coefficient, C_l versus B/L under 4 water depth: (a) Model 1 with chambers, 0.235m draught; (b) Model 2 without chambers, 0.235m draught. (Source: He *et al*., 2011)

2.4.1.3 Y-Frame Floating Breakwater

Mani (1991) studied different types of existing breakwaters performance in reducing transmission coefficient. Figure 2.11 shows the different types of floating breakwater reported by various investigators in the past (Kato *et al.*, 1966; Carver 1979; Seymour and Harnes, 1979; Brebner and Ofuya 1968; Mani and Venugopal 1978). It was determine that the "relative width" which is the ratio of width of the floating breakwater (*B)* to the wavelength (*L*) influence greatly the wave transmission

characteristic. It was suggested that *B/L* ratio should be greater than 0.3 to obtain transmission coefficient below 0.5. Increasing the width will cause the construction of the breakwater to be expensive and handling and installation of the breakwater to be difficult.

The aim of this experiment is to reduce the width of the floating breakwater by changing its shape thus improving the performance of the breakwater in reduction of the transmission coefficient. The inverse trapezoidal pontoon was selected and a detail drawing of the floating breakwater with a row of pipe installed underneath is shown in Figure 2.12. The aim for the installation of the row of pipes is to reduce *B/L* ratio and at the same time increasing the draft of the breakwater.

This study shows that closer spacing between pipes reduce transmission coefficient due to the improved reflection characteristic of breakwater and dissipation of wave energy due to turbulence created because of flow separation in the vicinity of the pipe.

Comparison of floating breakwater width requirements by various studies for a given prototype condition, *d*= 6m, *T*= 10 sec and C_t = 0.5 *is* given in Figure 2.13. From Figure 2.13, present breakwater need smaller width (11.8m) compared to other breakwater to achieved C_t = 0.5. Thus attaching pipes at the bottom of the breakwater resulted in smaller *B/L* ratio, easy handling, minimum space occupied and acceptable value of transmission coefficient.

Mani (1991) also made a cost comparison for different types of floating breakwater. The details were based on cost analysis provided by Adee (1976). Figure 2.14shows the cost comparison between different types of breakwater and it was concluded that the Y-frame floating breakwater with a row of pipes attached is cost effective compared to the existing floating breakwater.

Mani (1991) also compared his results with similar experimental studies (Kato et al., 1966; Carver and Davidson, 1983; Brebner and Ofuya; 1968; Bishop, 1982) as shown in Figure 2.15. From the comparison, it was deduced that the Y-frame floating breakwater performed well with row of pipes attached to the bottom of the trapezoidal float compared to other studies. The performance of the Y-frame floating breakwater

attenuates waves better as transmission coefficient was decreased when the relative width ratio increased.

S. number (1)	Type of floating breakwater (2)	Wave height (m) (3)	Wave period (sec) (4)	d/h (5)	W/L (6)	Transmission coefficient for $W/L = 0.15$ (7)	Reference (8)
1	Inverse trapezoid pontoon	0–0.4	0.6–2.2	0.12–0.32	0.1–1.77	0.6–0.8	Kato et al. (1966)
1	Trapezoid pontoon	0–0.4	0.6–2.2			0.75–1.0	
1	Rectangle pontoon	0–0.4	0.6–2.2			0.5–1.0	
1	Triangle pontoon	0–0.4	0.6–2.2			0.6–0.8	
2	Box type	0.45–1.05	2.5–4.0	0.27	0.15–0.50	0.8	Carver (1979)
3	Tethered	0.11–0.28	1.14–5.26	0.56	0.03–0.48	0.2–0.90	Seymour and Hanes (1979)
4	A-frame	0.12	1.12	0.78	0.45–1.25	0.80 ($W/L = 0.45$)	Brebner and Ofuya (1968)
5	Square	0.06–0.12	1.0–2.0	0.30–0.60	0.05–0.16	0.40–0.60	Mani and Venugopal (1987)

Figure 2.11: Characteristics of laboratory type floating breakwater (Source: Mani, 1991)

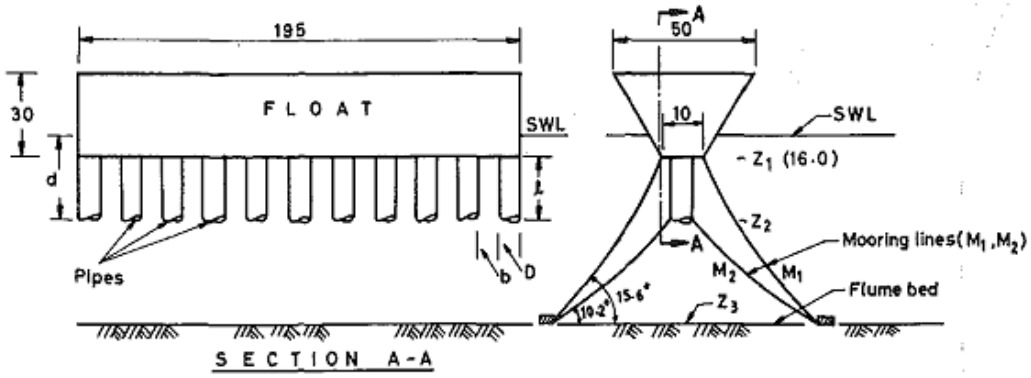

Figure 2.12: Details of the Y-frame floating breakwater (Source: Mani, 1991)

S1 number (1)	Author (2)	d/h (3)	W/L (4)	Width (m) (5)	Percentage (6)
1	Bishop (1982)	0.16	1.13	83.17	+700
2	Bishop (1982)	0.32	1.07	78.75	+667
3	Carver and Davidson (1983)	0.27	0.62	45.62	+387
4	Kato et al. (1966)	0.213	0.25	18.4	+156
5	Present study without pipes	0.16	0.54	39.7	+336
6	Brebner and Ofuya (1968)	0.78	0.54	39.7	+336
7	Present study with pipes	0.46	0.16	11.8	—

Figure 2.13: Comparison of breakwater width requirement for C_t= 0.5 (Source: Mani, 1991)

S1 number (1)	Breakwater type (2)	Maximum beam (m) (3)	Approximate present cost/m ($) (4)	Material (5)	Comment (6)
1	A-frame	8.58	3,400 (755 in 1965)	Steel frame and wooden planking	Period of incident wave is 2 sec
2	Alaska type	6.40	6,600 (1,395 in 1972)	Open-well made of lightweight reinforced concrete over foam core	T = 2 sec
3	Friday Harbor	7.62	4,900 (1,050 in 1972)	Plastic floatation containers supporting continuous wooden deck	T = 2 sec
4	Holmes Harbor	8.83	2,900 (646 in 1973)	Foam-filled aluminium drainage pipe	T = 2 sec
5	Port Orchard	3.65	2,500 (574 in 1974)	Rectangular cross section with lightweight reinforced concrete over foam core	T = 2 sec
6	Scrap tire	9.14	1,300 (328 estimated)	Scrap tires held together in bundles	T = 2 sec
7	Tethered float	—	2,300 (574 estimated)	Plastic floating spheres anchored to submerged frame	T = 2 sec
8	Maze scrap tire	60	20,000	Scrap tires held together in bundles	T = 10 sec ($d/h \approx 0.3$)
9	Maze scrap tire	120	36,000	Scrap tires held together in bundles	T = 10 sec ($d/h \approx 0.3$)
10	Pontoon	120	13,000–23,000	Mild steel	T = 10 sec ($d/h \approx 0.3$)
11	Y-frame	7	1,340	Concrete float with suitable pipes	T = 10 sec (d/h = 0.46)
12	Y-frame	14	2,600	Concrete float with suitable pipes	T = 10 sec (d/h = 0.46)

Figure 2.14: Comparison of cost of floating breakwaters (Source: Mani, 1991)

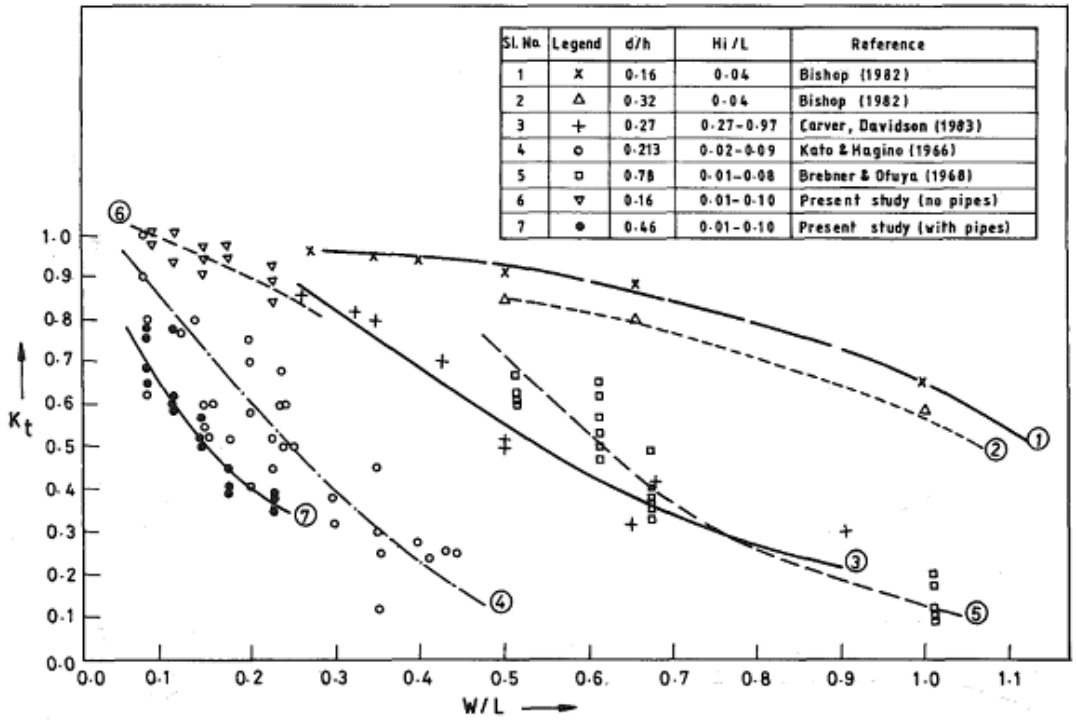

Figure 2.15: Variation of transmission coefficient with *B/L* – comparison (Source: Mani, 1991)

2.4.1.4 Cage Floating Breakwater

Murali and Mani (1997) adopted the cost-effective Y-frame floating breakwater (Mani, 1991) in designing the cage floating breakwater which comprises two trapezoidal pontoons connected together with nylon mesh with two rows of closely spaced pipes as shown in Figure 2.16. The breakwater offers advantages such as easy on land fabrication, quick installation, less maintenance, and environmental friendly. The aim of this study is to investigate the effect of the new cage floating breakwater configuration on wave transmission coefficient

Murali and Mani (1997) also compared their present design with previous studies (Kato *et al*., 1966; Brebner and Ofuya, 1968; Yamamoto, 1981; Bishop, 1982; Carver and Davidson, 1983; Mani, 1991) on the effects of *B/L* on C_t as shown in Figure 2.17. In Figure 2.17, curve 8 is the cage gloating breakwater and it shows for C_t to be below 0.5, the recommended *B/L* ratio is 0.14-0.60. Comparison with the previous Y-frame breakwater design (Mani, 1991), curve 7 reveals that the cage floating breakwater is 10-20% more efficient in controlling the transmission coefficient.

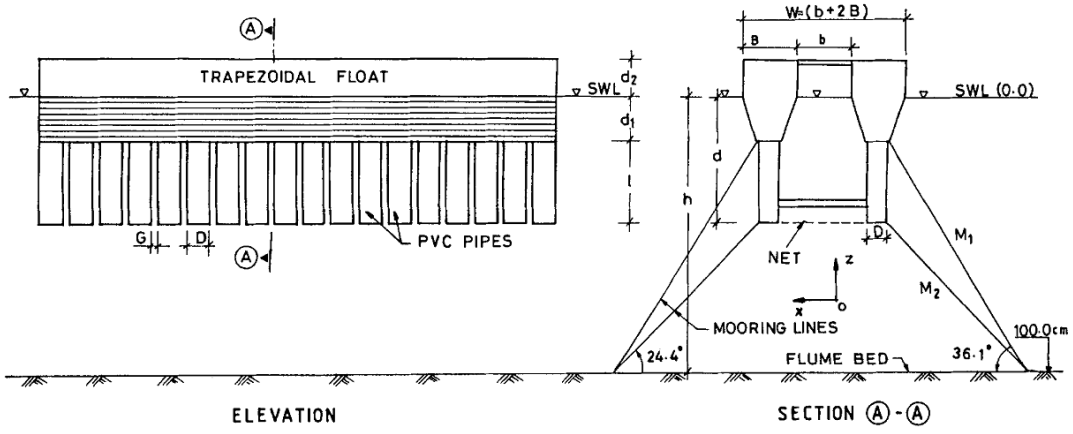

Figure 2.16: Cage floating breakwater (Source: Murali and Mani, 1997)

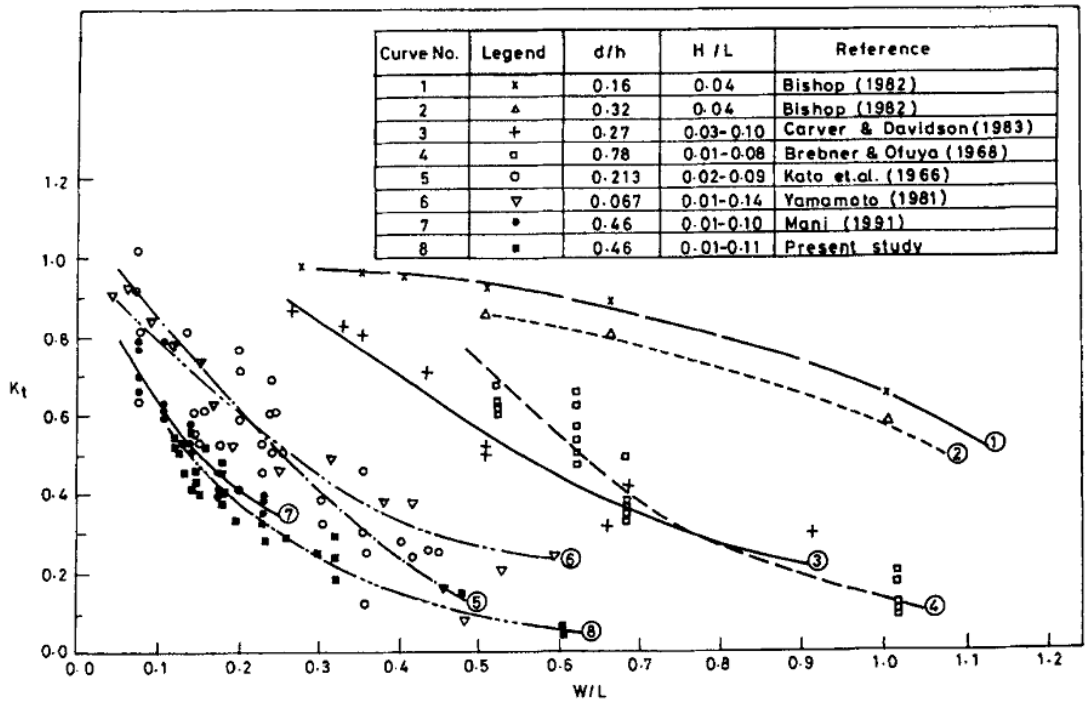

Figure 2.17: Comparison of the performance of floating breakwater. (Source: Murali and Mani, 1997)

2.4.2 Pontoon Type Floating Breakwaters

2.4.2.1 Dual Pontoon Floating Breakwater (Catamaran)

Williams and Abul-Azm (1995) investigated the hydrodynamic properties of a dual pontoon breakwater consisting of a pair of floating cylinder of rectangular section connected by a rigid deck as shown in Figure 2.18. The effects of various waves and structural parameters on the efficiency of the breakwater as a wave barrier were studied. A boundary element technique was utilized to calculate the wave transmission and reflection characteristics.

The performance of the dual pontoon structure depends upon the width (*2a*), draft (*b*), and spacing (*2h*) of the pontoons. Figure 2.19 shows the influence of pontoon draft on the reflection coefficient which shows that the larger the draft, the higher will be the reflection coefficient. Figure 2.20 present the influence of pontoon width on the reflection coefficient which shows that as the width of pontoon increased, the reflection

coefficient of the pontoon also increases. Figure 2.21 show the effect of pontoons spacing on the reflection coefficient. The bigger the spacing between pontoon, the better will the breakwater perform because it acts as a continuous barrier in long waves and act independently in short waves. When compared with the dual (lines) and single pontoon (dots) (Figure 2.22), Williams and Abul-Azm (1995) found that the dual pontoon exhibit high reflection coefficient in low frequency (C_l<0.75 or C_l <1.0) and mid frequency (1.5 < C_l < 3.0) range which shows that the dual pontoon is a more efficient wave barrier in lower and mid range frequency compared to the single pontoon. Williams and Abul-Azm (1995) found that wave reflection properties of the structure depend strongly on the draft and spacing of the pontoons.

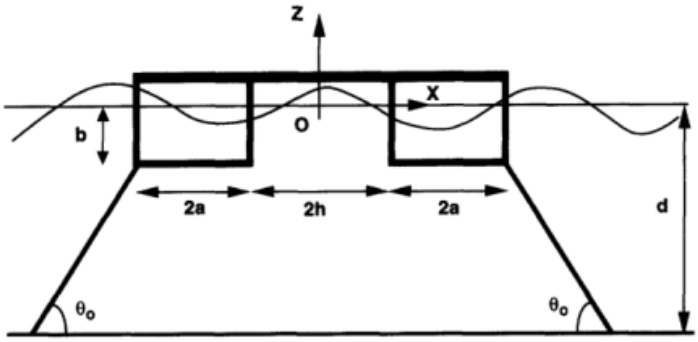

Figure 2.18: Dual pontoon breakwater sketch (Source: Williams and Abul-Azm, 1995)

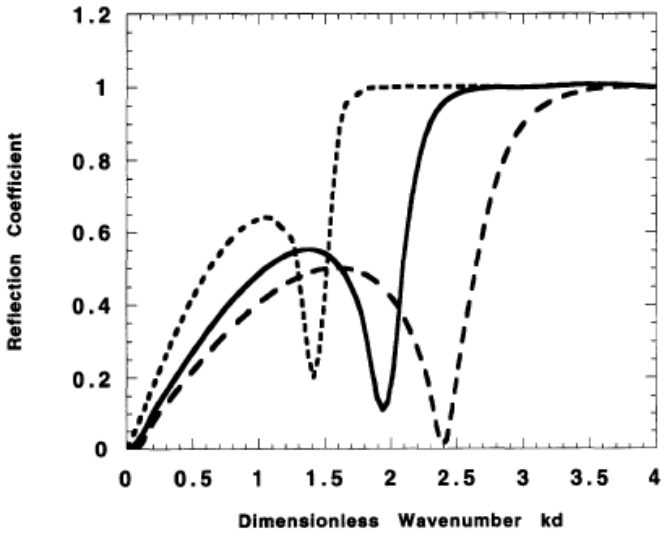

Figure 2.19: Influence of pontoon draft on reflection coefficient. Notations: -- -- -- -- *b/a*=0.5; ---------- *b/a*=1; - - - - - - *b/a*=2. (Source: Williams and Abul-Azm, 1995)

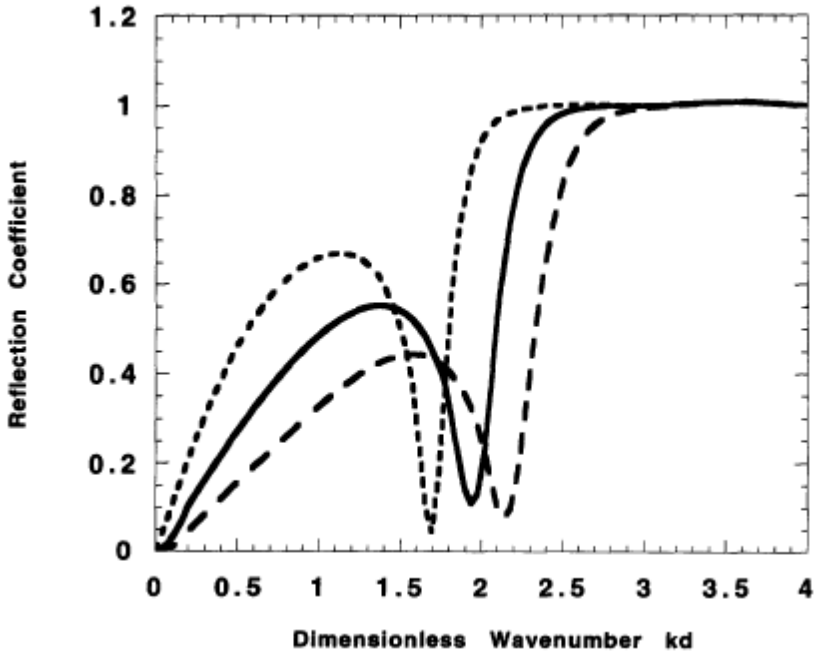

Figure 2.20: Influence of pontoon width on reflection coefficient. Notations: -- -- -- -- *b/a*=0.5; ---------- *b/a*=1; - - - - - - *b/a*=2. (Source: Williams and Abul-Azm, 1995)

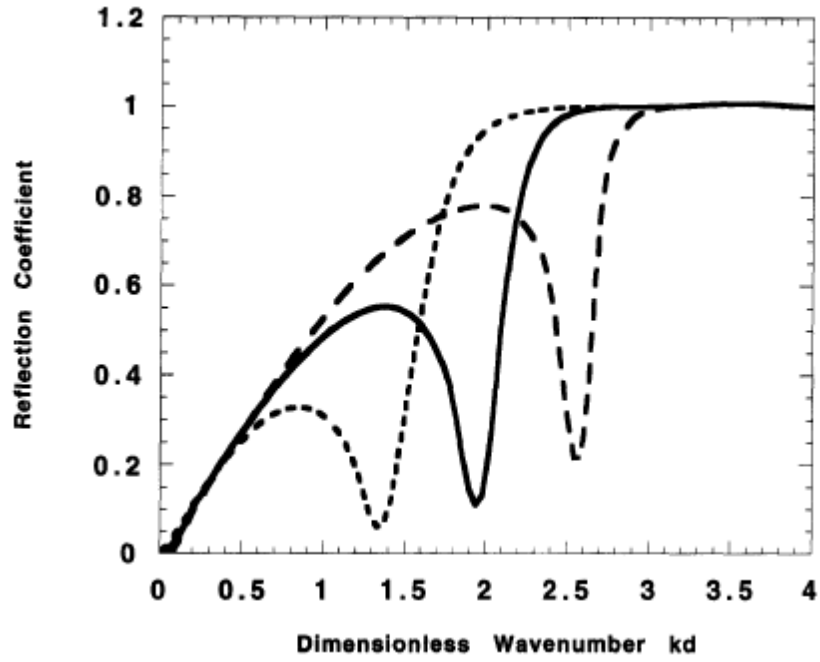

Figure 2.21: Influence of pontoon spacing on reflection coefficient. Notations: -- -- -- -- *h/a*=0.5; ---------- *h/a*=1; - - - - - - *h/a*=2. (Source: Williams and Abul-Azm, 1995)

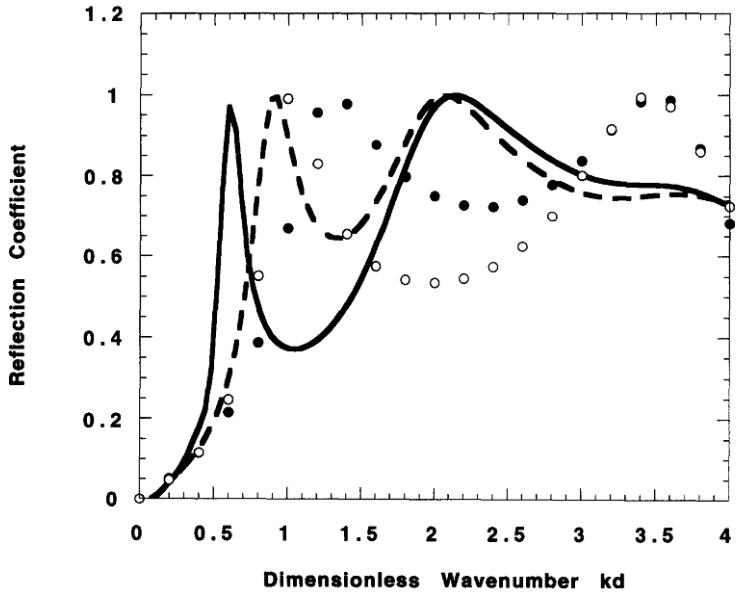

Figure 2.22: Comparison of reflection coefficient for dual pontoon structure (line) and single pontoon structure (symbols) of draft *b* and width *(4a+2h)* for *d/a*=5, *b/a*=1, *h/a*=1, and *p*=0.25. (Source: Williams and Abul-Azm, 1995)

2.4.2.2 Dual Pontoon Floating Breakwater with Fish Net Attached

Tang *et al*. (2010) investigate the dynamic properties of a dual pontoon floating structure (DPFS) with and without a fish net attached as shown in Figure 2.23 by using physical and numerical models. In Figure 2.23, *a* is the pontoon width, *b* is the spacing between two pontoons, *d* is the draft, and *h* is the water depth. The purpose for attaching the fish net is to increase the draft of the structure and at the same time offering a room for marine aquaculture. Figure 2.24 shows the comparison of the reflection coefficient with different net depths. The trend seems to be that the DPFS with deeper net has the lower reflection coefficient at the peaks due to the energy dissipated in the fluid-net interaction. Figure 2.25 shows the comparison of the reflection coefficient of DPFS with different net width. Enlarging the width of the net would reduce the reflection coefficient because most of the wave energy was absorbed by the structure.

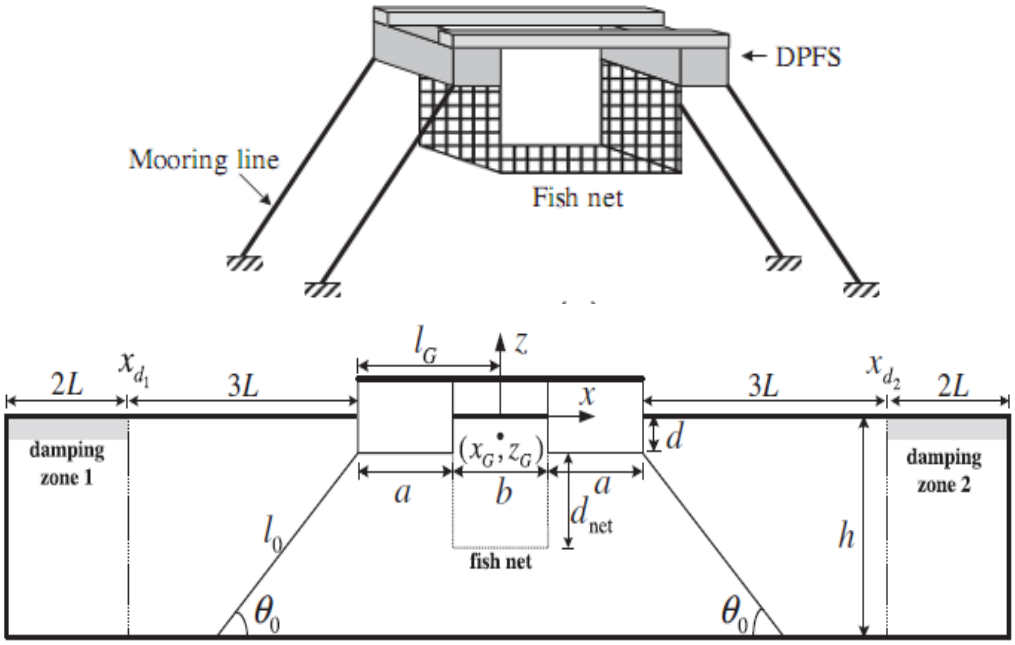

Figure 2.23: Dual pontoon floating breakwater with fish net attached (Source: Tang *et al.*, 2010)

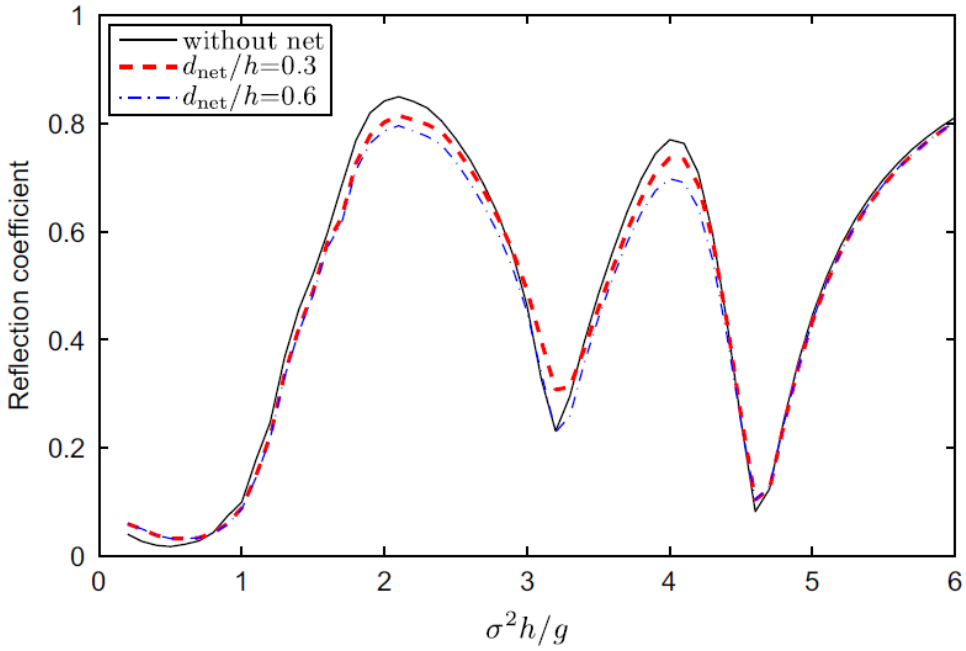

Figure 2.24: Comparison of reflection coefficient for the DPFS with different net depth. (Source: Tang *et al.*, 2010)

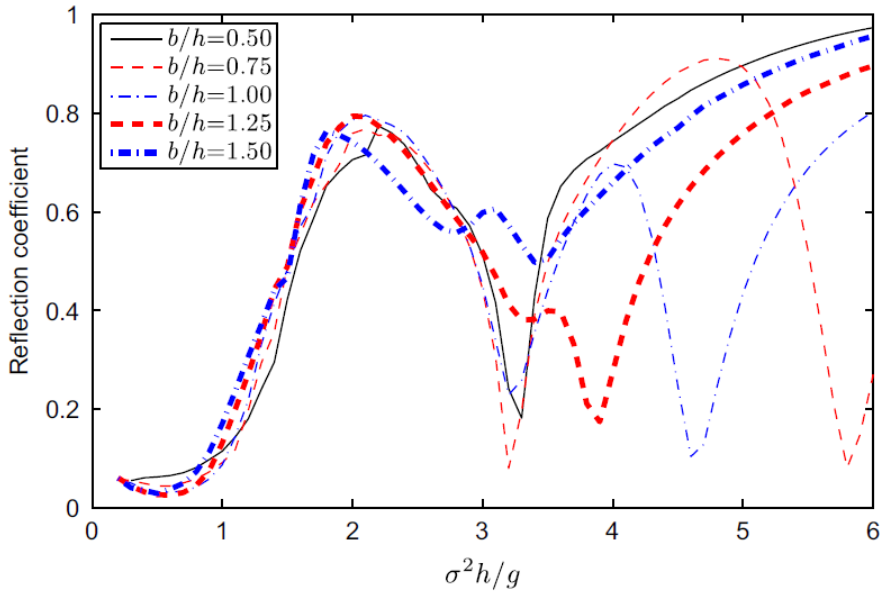

Figure 2.25: Comparison of reflection coefficient for the DPFS with different net widths. (Source: Tang *et al.*, 2010)

2.4.3 Mat Type Floating Breakwater

2.4.3.1 Porous Floating Breakwater

Wang and Sun (2009) developed a mat-type floating breakwater that was fabricated by a large number of diamond-shaped blocks so arranged to reduce transmitted wave height as showed in Figure 2.26. They also considered mooring models for instance, directional mooring and bidirectional mooring as shown in Figure 2.27 and Figure 2.28 respectively. For the directional mooring, the incident wave energy (E_{loss}) varies from 0.29 to 0.99 as *B/L* increases while in the bidirectional mooring, the (E_{loss}) varies from 0.69 to 0.99 which shows that the bidirectional mooring which fraps the floating body tighter than the directional mooring, brings not only preferable E_{loss} but also enhanced mooring force. The transmission coefficient of the floating breakwater decreased and the dissipation of wave energy increases with the increase of *B/L* (C_t is less than 0.5 and E_{loss} is higher than 0.78 as *B/L* is higher than 0.323).

Wang and Sun (2009) also did a comparison with the conventional pontoon floating breakwater (Rahman *et al.*, 2006) on transmission, reflection and energy dissipation as shown in Figure 2.29. It was shown that for the directional mooring, the reflection coefficient and transmission coefficient of porous floating breakwater are lower and higher than that of conventional pontoon breakwater. However there is no significant E_{loss} between them. The porous floating breakwater with bidirectional mooring present lower C_r , higher E_{loss} and lower C_t when compared with the pontoon breakwater (Rahman *et al.*, 2006).

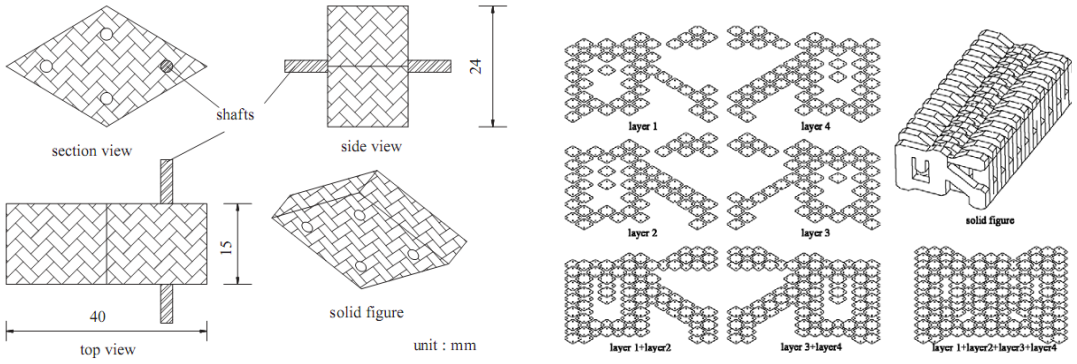

Figure 2.26: Sketch of diamond shape block (left) and arrangement of the blocks (right). (Source: Wang and Sun, 2009)

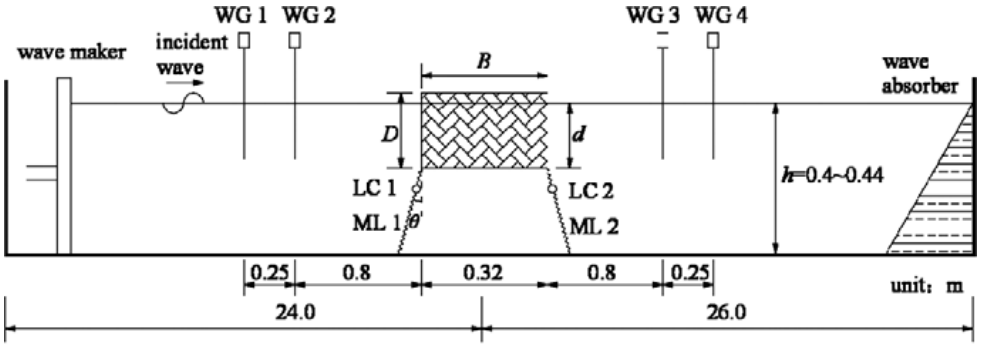

Figure 2.27: Experimental set-up with directional mooring (Source: Wang and Sun, 2009)

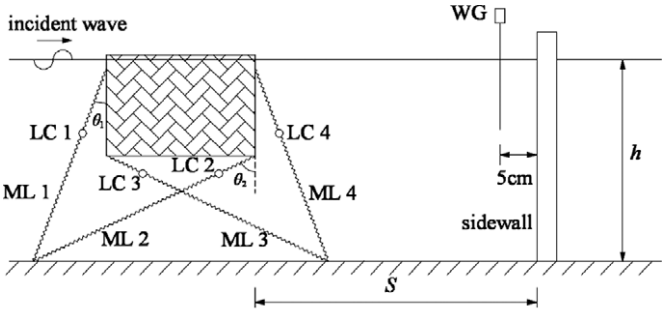

Figure 2.28: Bidirectional mooring. (Source: Wang and Sun, 2009)

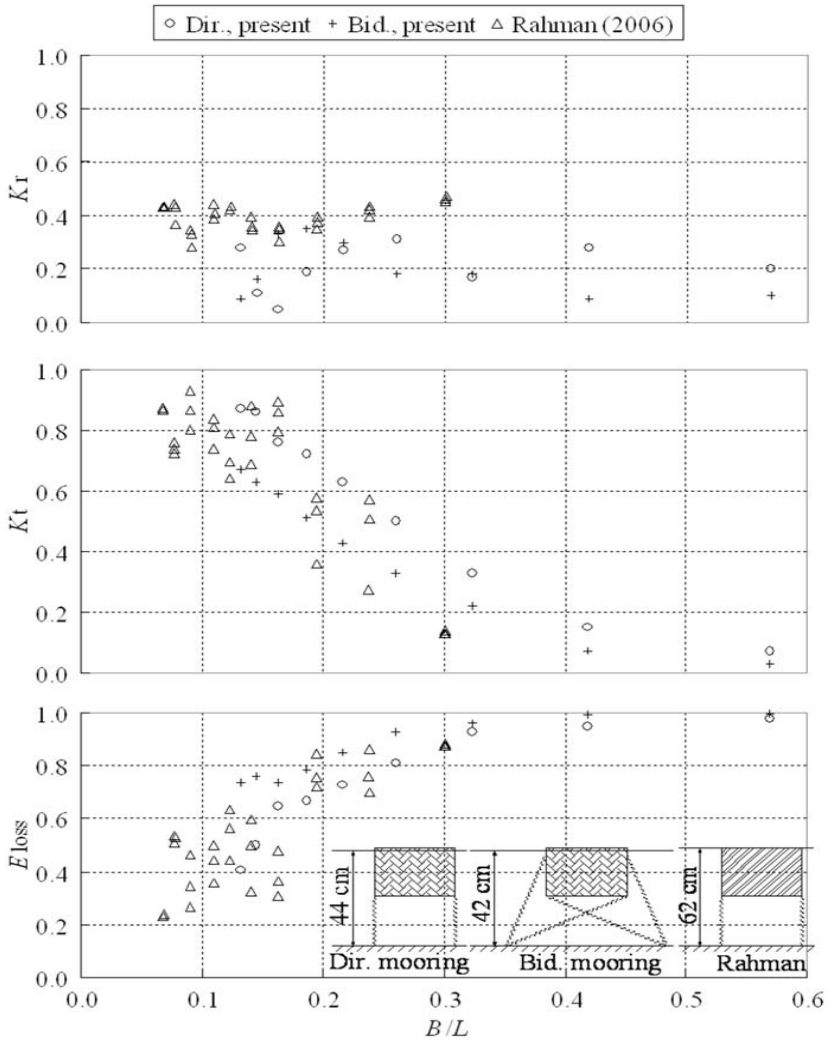

Figure 2.29: Comparison between Wang and Sun result, and that of the conventional pontoon breakwater (Rahman *et al.*, 2006) on reflection coefficient (C_r), transmission coefficient (C_t) and wave energy dissipation (E_{loss}). (Source: Wang and Sun, 2009)

2.4.4 Tethered Float

2.4.4.1 Tethered Float System

Vethamony (1994) studied the wave attenuation characteristics of a tethered float system as shown in Figure 2.30, with respect to wave heights, wave periods, wave depths, depths of submergence of float and float size. From the experiment, it was determined that the efficiency of the tethered float system was at maximum when it was just submerged but decreased when depth of submergence (d_s) of float increases as shown in Figure 2.31. Figure 2.32 shows that wave attenuation denoted by transmission coefficient (C_t) decreased with the increase in float size (r). For any level of wave attenuation, float array size decrease with decrease in float size (Figure 2.33). The smaller the float size, the higher will be the wave attenuation, since small floats undergo maximum excursion and interfere with the orbital motion of the fluid particles.

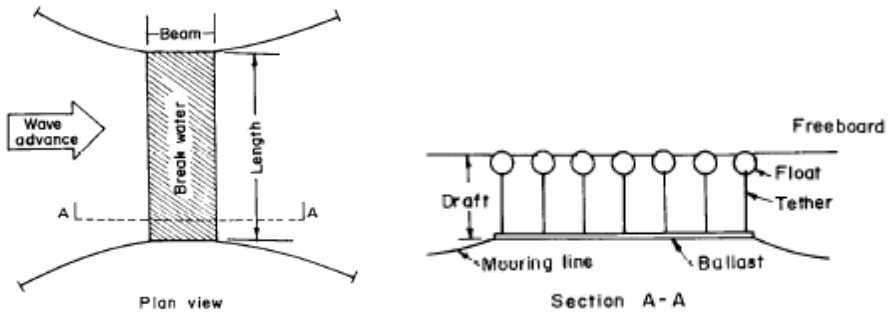

Figure 2.30: Tethered float breakwater (Source: Vethamony, 1994)

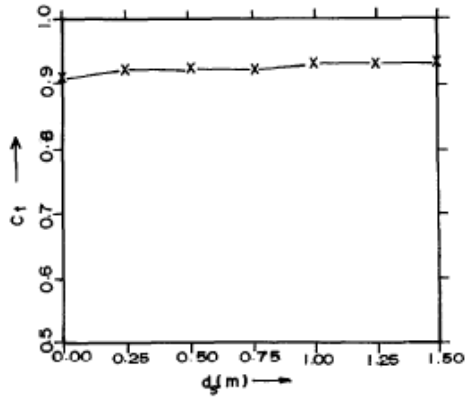

Figure 2.31: Variation of transmission coefficient with depth of submergence (Source: Vethamony, 1994)

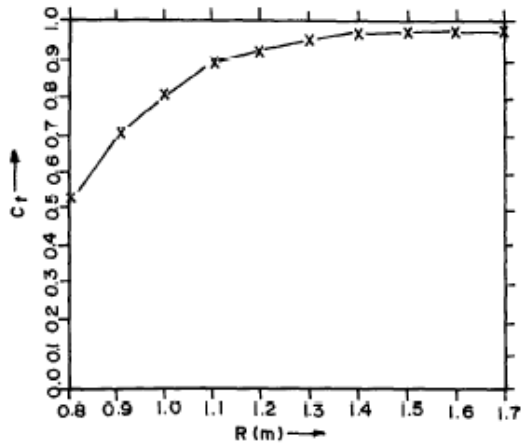

Figure 2.32: Variation of transmission coefficient with float size (Source: Vethamony, 1994)

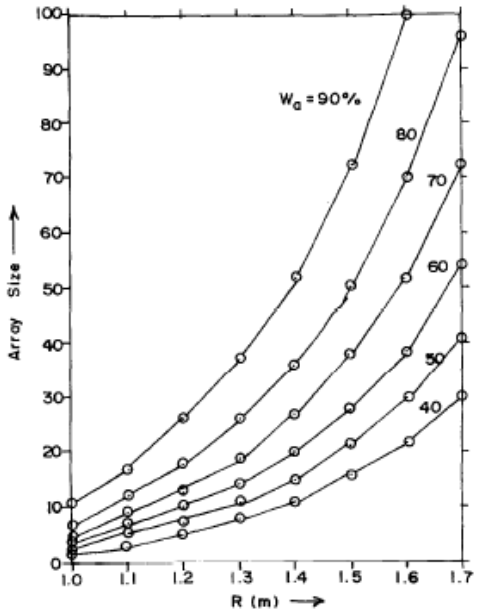

Figure 2.33: Variation of float array size for desired level of wave attenuation with float size. (Source: Vethamony, 1994)

2.4.5 H-shape Floating Breakwater

Teh and Nuzul (2013) studied the hydraulic performance of a newly developed H-shape floating breakwater (Figure 2.34) in regular waves. The aim of this study was to conduct a laboratory test to determine the wave transmission, reflection and energy dissipation characteristics of the breakwater model under various wave conditions. The breakwater was previously developed by a group of UTP students for their Engineering Team Project in 2004. The breakwater was designed to reduce wave energy through reflection, wave breaking, friction and turbulence. The two "arms" at the top of the main body was create to facilitate wave breaking at the structure; whereas the two "legs" at the bottom was created to enhance the weight of the breakwater barrier against wave actions.

The overall density of the system is *650 kg/m*^{3}. The breakwater model was made of autoclaved lightweight concrete (ALC) with fiberglass coating. According to Teh and Nuzul (2013), wave transmission coefficient, C_t decrease with the increasing *B/L* ratio. The H-shape breakwater was capable of dampening the incident wave height by almost 80% when the breakwater was designed at *B/L*= 0.5. The H-shape breakwater was less effective in dampening longer waves in the flume. The H-shape breakwater was capable in attenuating *90%* of the incident wave height when *B/L* is approaching *0.4*. However, the experiment were conducted in limited wave range due to time constrains.

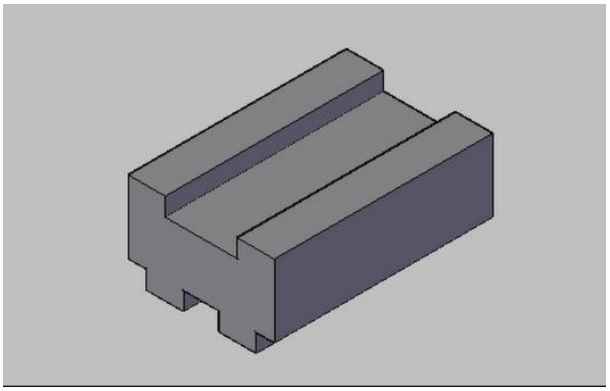

Figure 2.34: H-shape floating breakwater

2.4.6 Summary of the Investigation of the Floating Type Breakwaters

Table 2.1: Summary of the various types of floating breakwater

No.	Breakwater type	Ref.	Type of analysis	Model dimension	Test parameters					Dimensionless parameters				Energy coefficient		
					wave	*d*(m)	*D*(m)	H_i	*T(s)*	d/L	*D/d*	H_i/L	*B/L*	C_t	C_r	C_l
Box, rectangular and trapezoidal type floating breakwater																
1	Box	McCartney (1985)	Experimental	*B = 4.0 & 4.8, l = 29.7, h = 1.5*	Irr	7.6	1.1	0.5-1.1	2.5-4..0	n.a.	n.a.	n.a.	n.a.	0.42-0.88	n.a.	n.a.
2	Rectangular with and without pneumatic chambers	He *et al*., (2011)	Experimental RAOs	Model 1,2,3 & *4: L = 1.42m B = 0.75m H = 0.4m*	reg	0.9 0.7 0.55 0.45	0.235 0.235 0.299 0.177	0.04	1.1-1.8	n.a.	n.a.	n.a.	0.18 – 0.45	0.18-0.91	0.15-0.72	0.05-0.88
3	Y-frame	Mani (1991)	Experimental	*Top B = 0.5m Btm B = 0.1m Pipe dia = 0.09m Pipe L = 0.36-0.56m*	Reg	1.0	0.16 0.36 0.46 0.56	0.054-0.24	1.2-2.0	n.a.	0.46	0.01-0.1	0.095-0.224	0.31-0.79	n.a.	n.a.
4	Cage	Murali & Mani (1997)	Experimental	*B = 0.6, 0.8, 1.0, l = 0.2, 0.3, 0.4, h = 0.3*	Reg	1.0	0.36-0.56	n.a.	5.0-10.0	n.a.	0.36-0.56	n.a.	0.12-0.60	0.08-0.58	n.a.	n.a.
Pontoon type floating breakwater																
1	Dual pontoon	William & Abul-Azm (1995)	Numerical	n.a.	n.a.	n.a.	n.a.	n.a.	n.a.	n.a.	n.a.	n.a.	n.a.	n.a.	0.5 -0.75	n.a.
2	Dual pontoon	Tang *et al*. (2010)	Experimental Numerical RAO	*B=0.25m* Spacing=0.5m	n.a.	0.8	0.153	n.a.	n.a.	n.a.	n.a.	n.a.	n.a.	n.a.	0.05-0.95	n.a.
Mat Type floating breakwater																
1	Porous	Wang & Sun (2009)	Experimental	*L=0.32m B=0.68m H=0.2m* Porosity=0.63	reg	0.44	0.4-0.44	0.06	0.6-1.4	n.a.	n.a.	0.025-0.107	0.132-0.569	0.01-0.94	0.09-0.28	0.4-1.0
Tethered float floating breakwater																
1	tethered float	Vethamony (1994)	Theoretical	Diameter = 0.15m	n.a.	n.a.	n.a.	n.a.	6	n.a.	n.a.	n.a.	n.a.	0.85-0.88	n.a.	n.a.
Other type of floating breakwaters																
1	H-shape	UTP students (2004)	Experimental	*B=0.2m L=0.3m H=0.1m*	Reg	0.2-0.3	0.065	0.005-0.075	n.a.	n.a.	0.22-0.325	0.025-0.125	0.1-0.5	0.18-0.70	0.22-0.25	0.5-0.95

2.4.7 Concluding Remarks

Literature reviews were done on various types of floating breakwater such as the box, pontoon, mat and tethered float type floating breakwater. Besides offering advantages over the conventional fixed type breakwaters, there are also some drawbacks associated with them. Nevertheless due to its practicality, reliable performance and its reasonable price tags, researchers around the world continue to research on the new designs, materials and construction method to further improve these floating breakwaters. The aim of this study is to research on the existing floating breakwaters as well as the floating breakwater that were developed by UTP students which is the H-shape floating breakwater, and based on this study, a novel breakwater will be develop incorporating the properties of various breakwaters for further performance enhancement.

Table 2.1 shows the summary of various floating breakwater that was discussed earlier in the literature review. In this summary all of the model are of different scales and measurements and were being analyzed by various method such that of experimental, theoretical and numerical. From the Table 2.1, it shows that the width and draft of the breakwater affect the reflection and transmission coefficient and thus resulted in energy loss. Some of the breakwater that has a vertical face such as the box and pontoon reflect waves more thus reducing the transmitted wave energy. Whereas, for the porous floating breakwater, it reflect and transmit less wave energy due to its unique configuration.

The novel breakwater that will be develop must have a large surface are facing the incident waves for the purpose of wave reflection. But not all wave energy must be reflected because total reflection at the seaward side of the breakwater will pose danger to small vessels at sea, thus, there should be some wave energy that should be transmitted either through the top, middle or bottom of the structure. Sufficient porosity can further help in wave energy transmission through the breakwater. At deep sea, the floating breakwater should be rigid because as waves hit the structure with less rigidity, it will tend to move in multiple direction thus instead of attenuating waves, the breakwater will only help to transfer the energy to the leeside with less energy loss.

Rigidity can be achieved by cable mooring or restraining the structure using piles but using piles will be costly.

Besides that, the draft or draught and width of the breakwater are also an important part in wave energy attenuation. Low draft and larger width will eventually reduce wave energy transmission to the other side because with lower draft, wave energy will have to move underneath the structure and overtop the structure where surface friction will provide the resistance needed to attenuate wave energy. The large width will tend to prolong the passing of wave energy to the other side of the breakwater.

CHAPTER 3

METHODOLOGY

3.1 General

This chapter introduces an innovative floating breakwater that is designed to provide optimal hydraulic efficiency for instance, high energy dissipation and low wave reflection. This chapter will describe the physical properties of the breakwater as well as the materials used for its construction. The geometrical properties of the floating breakwater will be thoroughly presented. This chapter will also deliver the introductions of the facilities and equipments used in the experiments, experimental set-up and test procedures.

3.2 Floating Breakwater Model

3.2.1 Breakwater Design

In this study, an H-shape floating breakwater was developed according to model scale. The general dimensions of the test model are 1000 mm width x 1440 mm length x 500 mm height. The breakwater was constructed by plywood and was made waterproof by a layer of fiberglass coating on the surfaces of the body. Plywood is chosen as the primary construction material because it is a lightweight material that provides high resistance to external force impacts. The fiberglass coating was injected with yellow coloring pigment for better visibility of the model during experiment.

The breakwater has a pair of upward arms and a pair of downward legs, with both connected to a rectangular body as shown in Figure 3.1. The seaward arm, body and leg act as the frontal barrier in withstanding the incident wave energy mainly by reflection. Some wave energy is anticipated to be dissipated through vortices and turbulence at the 90^{o} frontal edges of the breakwater. When confronted by storm waves, the H-type floating breakwater permits water waves to overtop the seaward arm and reaches the U-shape body as seen in Figure 3.2. The overtopped water trapped within the U-shape

body heavily interacts with the breakwater body, and the flow momentum is subsequently retarded by shearing stresses (frictional loss) developed along the body surfaces. The excessive waves in the U-shape body may leap over the shoreward arm and reaches the lee side of the floating body, making a new wave behind the breakwater which is termed as the transmitted waves.

Apart from the energy dissipation mechanisms exhibited at the upper body of the breakwater, both seaward and leeward legs, which are constantly immersed in water, are particularly useful in intercepting the transmission of wave energy beneath the floating body through formation of bubbles and eddies near the sharp edges as well as underwater turbulence. The remaining undisturbed energy past underneath the floating body and contributes to the transmitted waves behind the breakwater.

As breakwater immersion depth is an important parameter controlling the hydrodynamic performance of the floating breakwater, a ballast chamber located within the breakwater body was designed for adjustment of immersion depth of the breakwater with respect to still water level, in a freely floating condition. For the breakwater model, a 5 x 9 matrix wooden grid system as shown in Figure 3.7 was developed for the placement of sandbags for weight control of the breakwater. The ballast chamber was covered by transparent lid made of Plexiglas, as shown in Figure 3.3. The gap between the breakwater body and the transparent lid was tightly sealed by adhesive tapes so as to prevent the seepage of water to the ballast chamber.

The sides of the floating body facing the flume walls were coated with polystyrene foams to prevent direct collision between the concrete wall and the fiberglass coated breakwater body. The implementation of the polystyrene foams at both sides of the breakwater would not pose significant disturbance to the movement of the floating body.

Four hooks were attached to the bottom corners of the floating model, as shown in Figure 3.4, for mooring purposes. A taut-leg mooring was adopted in this study as it provides greater efficiency to the performance of floating breakwaters. A thin metal rope with low elasticity was tied to each hook beneath the breakwater and the other end

was attached to the floor of the wave flume. The taut-leg mooring lines were almost straight with minimal slacking when in operation in water. For the present experiment, the pre-tensile stress of the mooring cables was set as zero in still water level. The build-up of the tensile stress in the mooring cables during the experiment is mainly posed by the wave force acting on the floating breakwater. The setting of present experiment allows heave, surge and pitch responses to the floating breakwater, and the other motion responses (*i.e.* sway, yaw and roll) were restricted.

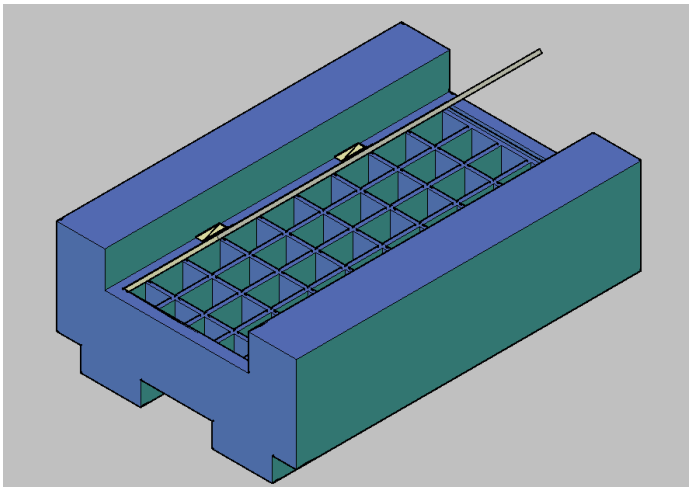

Figure 3.1: Design of the H-type floating breakwater (isometric view)

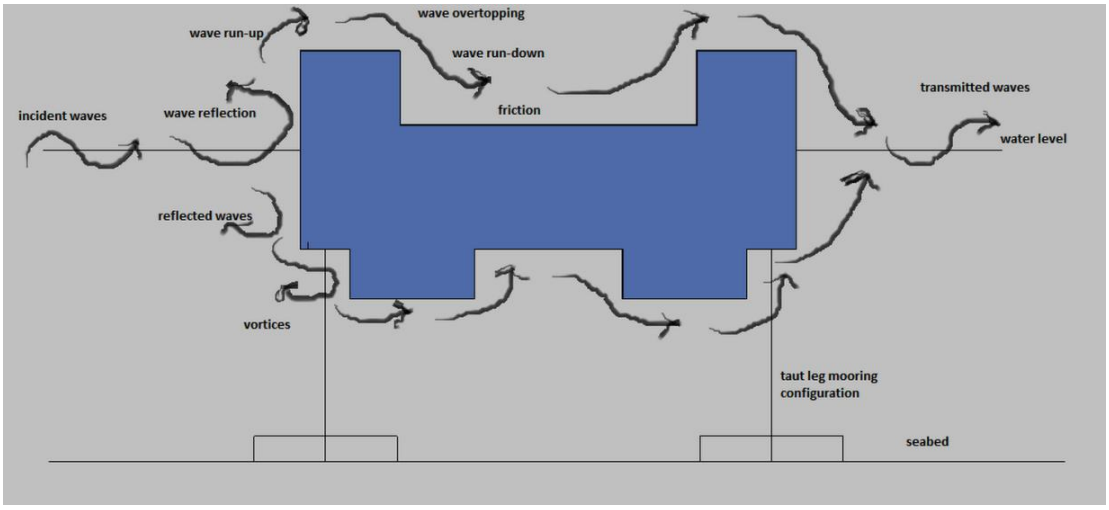

Figure 3.2: Primary wave dissipation mechanism of the H-type floating breakwater.

Figure 3.3: Model with the transparent lid on the top

Figure 3.4: Hooks at bottom corners of the model

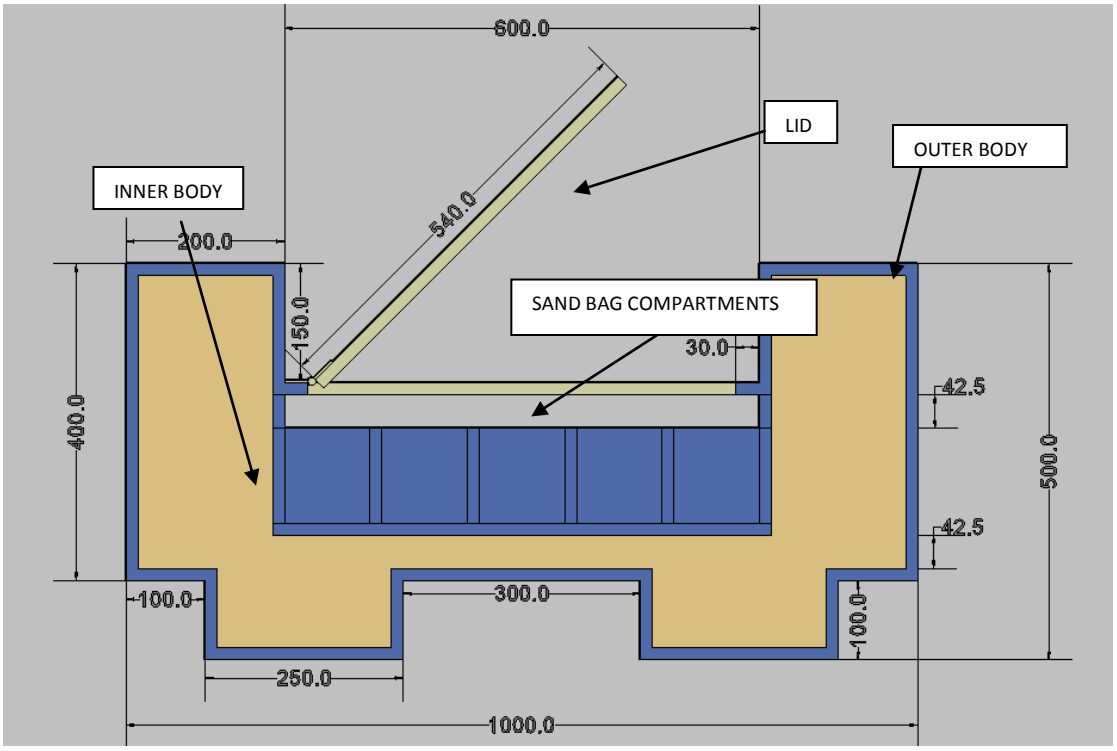

Figure 3.5: Side view of the H-type floating breakwater

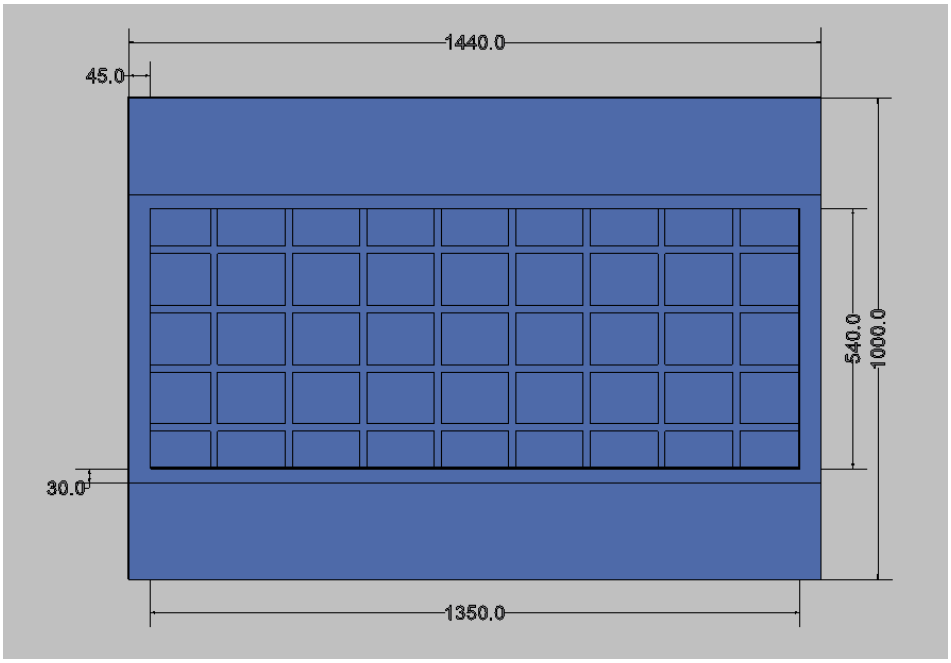

Figure 3.6: Top view of the H-type floating breakwater

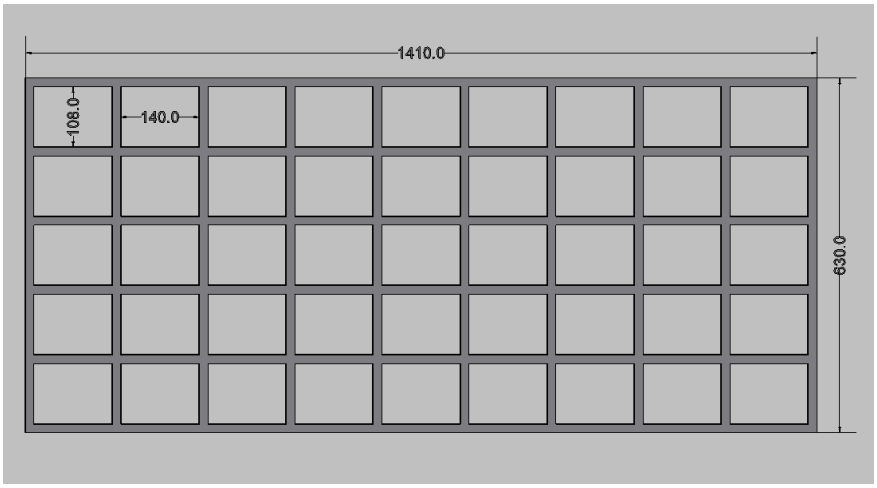

Figure 3.7: Top view of the sand bags compartment of the H-type floating breakwater

3.3 Test Facilities and Instrumentations

3.3.1 Wave Flume

The Ocean and Coastal laboratory in UTP have a large wave tank and a wave flume. For this experiment, we will be using the wave flume which is 25 m long, 1.5 m wide and 3.2 m high as seen in Figure 3.8. The maximum water level that can be fill in the flume will be 0.7 m high. The wave flume was constructed using reinforced concrete for its wall and 6 strong Plexiglas panel are embedded around the body of the flume. The presence of these glasses will make it easier for us to observe the wave interaction with the structure as seen in Figure 3.9.

Figure 3.8: Wave flume.

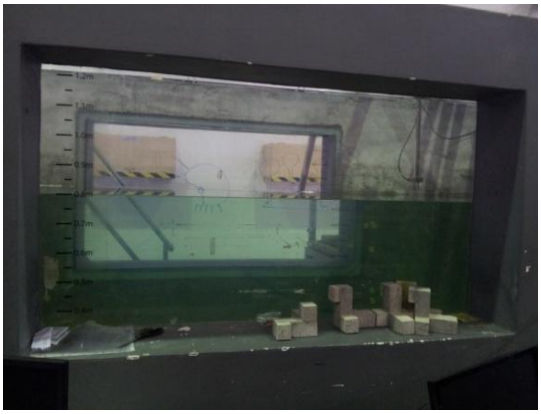

Figure 3.9: Plexiglas panel

3.3.2 Wave Paddle

The wave will be generated by using a wave paddle (Figure 3.10) which is a piston type wave generator (pneumatic-type) driven by an electric motor. The wave paddle was fabricated by Edinburgh Design Ltd, UK. The wave paddle will be able to generate regular and irregular wave but user can also define their preference. This wave paddle can generate a maximum wave height of 0.3 m and maximum wave period of 2 second. The wave paddle was made from anti-corrosive materials and is able to absorb re-reflected waves.

Figure 3.10: Wave paddle

Figure 3.11: Wave absorber.

3.3.3 Wave Absorber

At the end part of the wave flume, there will be a removable wave absorber installed there as shown in Figure 3.11 to absorb the incoming wave energy and reduce the reflection of wave energy. It is 3 m in length and made up of anti-corrosion material. This wave absorber has the ability to absorb a minimum of 90% of wave energy. It can also be remove for the modeling of river flow.

3.3.4 Wave Probe

In this experiment, wave probes as shown in Figure 3.12, will be used to measure the incident wave height, reflected wave height and transmitted wave height at the seaward and leeward side of the model. Three wave probes will be install in front of the model which faces the incident waves to measure the incident and reflected wave data while at the leeward side of the breakwater, another 3 wave probes will be placed there to measure the transmitted wave height. Calibration of the probes must be made prior to every test that will be conducted later.

Figure 3.12: Wave probes

3.3.5 Data Acquisition System

In this experiment, the required parameters will be measured using the 3-points method that was developed by Mansard and Funke (1980). This method is based on least square analysis where the incident and reflected wave spectra are resolved from the co-existing wave spectra. Previously, the 2-points method was used in the previous generations floating breakwater but in this experiment, the 3-points method was utilized as it is superior to 2-points method. This is mainly because it has wider frequency range, reduced sensitivity to noise and deviation from the linear theory and lesser sensitivity to critical probe spacing.

3.4 Experimental Set-Up

The complete experimental set-up is presented in Figure 3.13 (A) and (B). The test model was located at the mid-length of the wave flume, which is 13 m apart from the wave paddle. The test model was anchored to the floor of the wave flume by the means of metal cables and hooks. Load cells were installed at the mid-point of the respective mooring lines for the measurement of the mooring forces.

Three wave probes were located both seaward and shoreward of the model (with the nearest probe located away from the model at 3 m) for the measurement of water level fluctuation at the respective locations. These time series data were then further analyzed using computer tools to yield some significant wave parameters, *e.g.* significant wave height, peak wave period, etc. Mansard and Funke's method (1983) was adopted to decompose the wave signals from the three probes into incident and reflected wave components. To achieve this, the probes were carefully arranged according to the spacing requirement set by Mansard and Funke (1980).

A number of reflective balls were attached to the test model. The movement of these balls, which is equivalent to the movement of the model, was captured by three optical tracking cameras located at close proximity of the model.

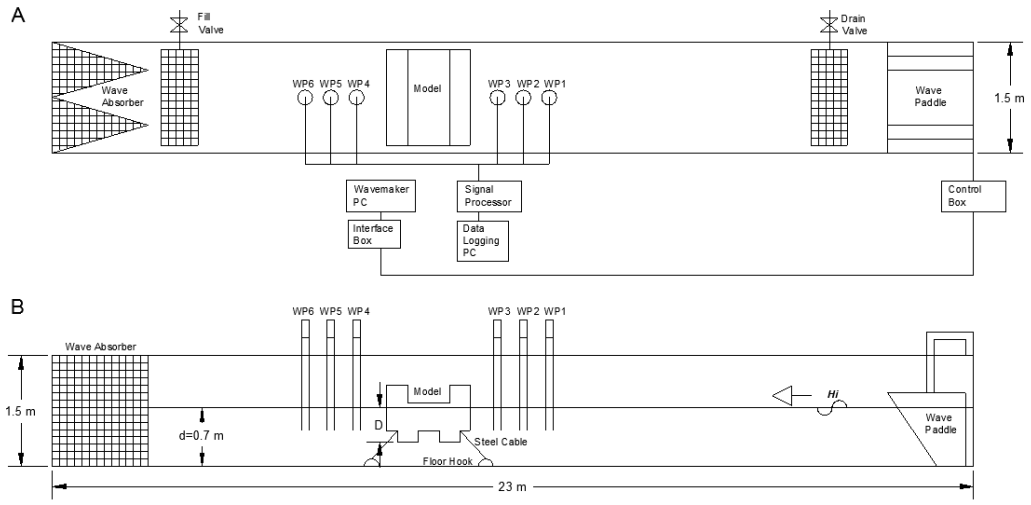

C

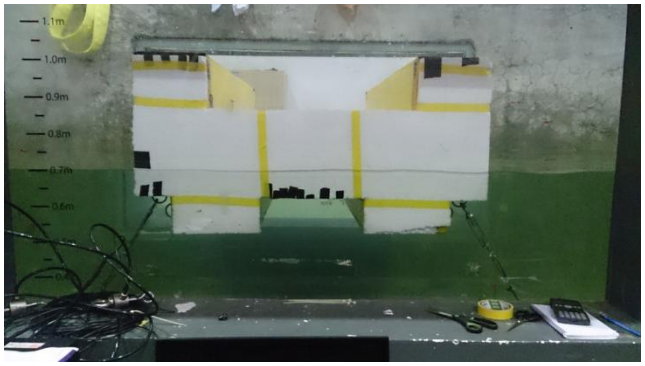

Figure 3.13: (A) plan view of the experimental set-up, (B) side view of the experimental set-up, (C) side view of the floating breakwater in the wave flume.

3.5 Test Program

In this study, the novel breakwater will be subjected to various wave conditions to simulate the sea states in Malaysia. The model will be subjected to regular and random wave condition. The dependent variables in this study are wave period and wave steepness. These are the variables that will be changed throughout the experiment to study their effects on the performance of the H-type floating breakwater. There will only be 1 water depths that will be used in this experiment which is 0.7 m. Upon

increasing the water level in the wave flume, the placement of the wave probes must also be adjusted. Water depth of 0.7 m was used to assess the model performance in deep sea depths. There will be 6 wave period in this experiment which will range from 1.0 s to 2.0 sec with the interval of 0.2 s. The wave period can easily be adjusted by using the computer at the laboratory. In this experiment, three wave heights will be used correspond to the wave steepness of H_i/L_p= 0.04, 0.06 and 0.07. The draft of the model will also be adjusted to determine what level of submergence of the model will have the optimum reflection, transmission and energy loss coefficient. The model will have 3 drafts which is 0.24 m, 0.27 m and 0.31 m Thus, the total numbers of runs that will be conducted are as follow;

Total number of runs = 1 water depth x 6 wave periods x 3 wave heights x 3 model draft x 2 waves condition

= **108 runs**

The parameters that need to be measured are as follows:

1. Maximum and minimum wave height in front of the structure for the calculation of reflected wave height, H_r.
2. Wave height at the back of the structure for the calculation of transmitted wave height, H_t
3. After the wave heights were obtained, the reflection coefficient, transmission coefficient and energy loss coefficient can be calculated.

3.6 Analyzing the Obtained Results

The results obtained will be analyzed by first plotting the water elevation from each wave probes against time which comprised the superimposed of both incident and reflected waves. This incoming wave signal has to be decomposed into incident and reflected wave spectrum using Fast Fourier Transform method. This can be done by applying function and formulae in the MATLAB software as showed in Figure 3.14 below:

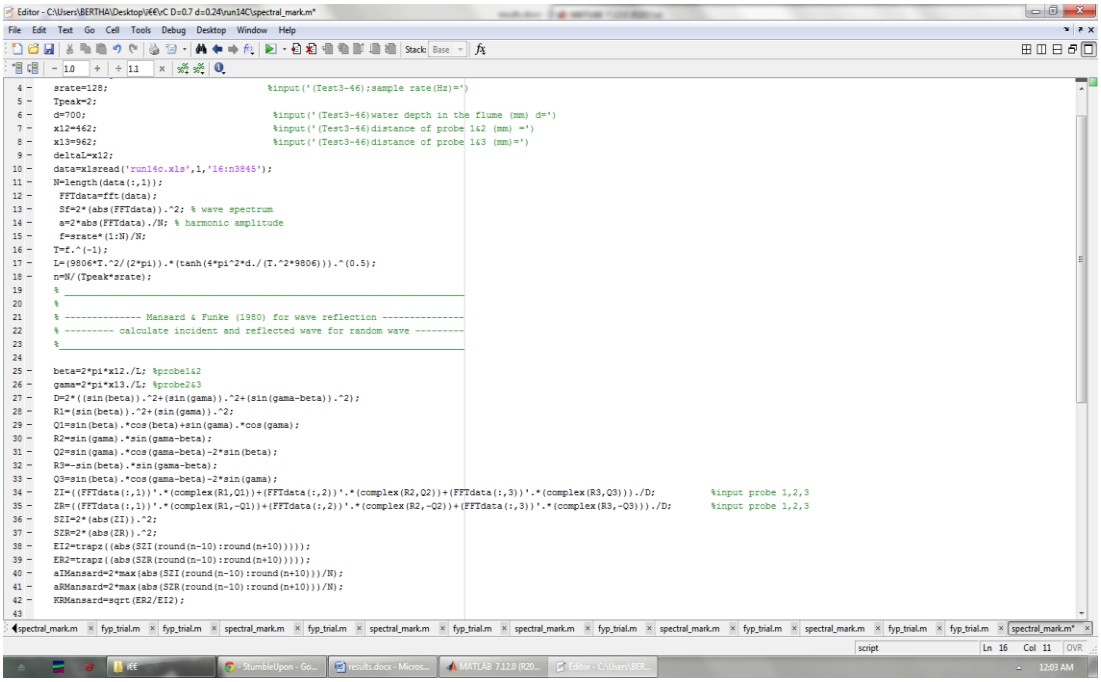

Figure 3.14: MATLAB codes sample

CHAPTER 4

RESULTS AND DISCUSSIONS

4.1 General

In this chapter, a brief explanation about the calibration of the wave flume and all other test instruments will be discussed here. The determination of the gain values corresponding to their wave height will also be discussed wherein the gain value will be used in the wave generation program to generate irregular waves. This chapter will also discuss the determination of the parameters required to quantification the hydraulic performance of the floating breakwater. After the results were obtained, the hydraulic performance of the floating breakwater will also be analyzed in this chapter.

4.2 Calibration of Wave Flume

The calibrations of the wave flume will be done by using the three-point method proposed by Mansard and Funke (1980), as being mentioned in the previous chapter. The basis of this method is to measure simultaneously the waves in the flumes at three different points with an adequate distance between one set of probe to another. The wave probes will be located parallel to the wave's direction inside the wave flume. The set up of all the equipments for the calibration is shown in the Figure 4.1, where it indicates the length of the probes from the wave paddle (*X1*), the length of first probe to the second probe ($X1 = L_p/102$) and the length of first probe to the third probe ($L_p/6 < X13 < L_p/3$).

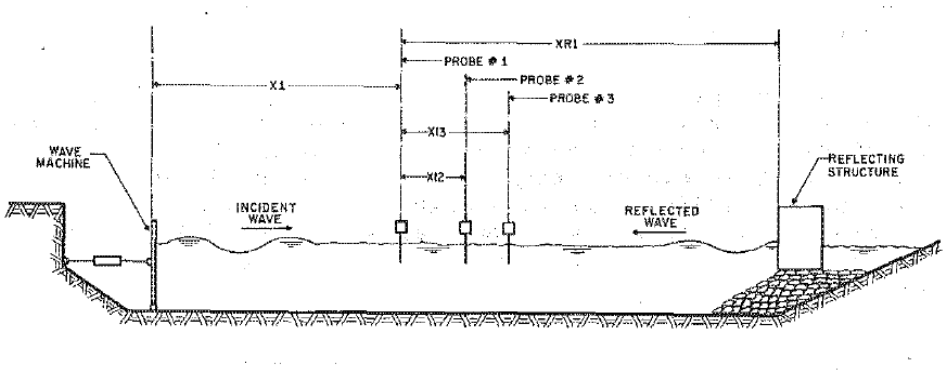

Figure 4.1: Three-point method calibration set up (Source: Mansard and Funke, 1980)

Where L_p is the overall length of the wave flume. The importance of following the spacing requirement as stated in the study is to ensure that there are no singularities in the wave probe readings. The spacing of the wave probes correspond to their wave period is shown in Table 4.1.

Table 4.1: Distance of each wave probes from each other for different wave period.

T (s)	f (Hz)	Distance of probe 1 and 2 (cm)	Distance of probe 2 and 3 (cm)	Distance of probe 1 and 3 (cm)
1.0	1.000	15.5	28	43.5
1.2	0.833	21.7	28	49.7
1.4	0.714	28.1	40	68.1
1.6	0.625	34.3	40	74.3
1.8	0.556	40.3	50	90.3
2.0	0.500	46.2	50	96.2

The distance between the final wave probes and the reflective structures is also being defined. The recommended distance between the two points must be at least one wave length away from each other.

This study will deal with both regular and random waves. For regular waves, there are two options in which calibrations of the wave flume can be done which are by directly selecting the pre-determined values of wave height and wave period as prepared by the

wave generation software. The wave paddle will then be automatically adjusted to suit the numbers that have been commanded in the computer. However, the drawback of such method is that there might be some irregularities with the waves that will be produced. The actual reading of the wave that will be generated by the wave paddle might vary from the input values. This happens due to the limitation of the software to get a fully accurate value of the wave properties in the wave flume, as well as other external factors that might affect these values. In order to overcome this drawback, the manual command method can be used.

In manual command method, the values of the wave parameters, such as the wave height and the frequencies, can be independently defined by the user itself. The advantage of using the command method is that the user can check the accuracy of the wave being generated by the wave paddles and then adjust them accordingly. This is done in a series of trial-and-error method until the desired value is achieved. This method proved to be more reliable and it helps to maintain the accuracy of the generated waves. The command that will be key-in into the software is in a script method, depending on the type of wave wanted to be produced by the user. To generate random waves, the manual method will also be used.

The following scripts are an example of producing regular and random waves:

For regular waves:

"begin
run "1 Hz 6 cm wave for 64 secs (1)" with (10)
makewave x=1.0*single (1, 0.06) on 1;
end; "

In the command given, the wave paddle is expected to produce a regular wave with 6 cm wave height, at the frequency of 1Hz, or 1 second of wave period. However, the generated wave that being recorded by the wave probes might not give the similar values as the commanded values. Thus, the values must be corrected accordingly by introducing a gain value, represented by *x*, in which will adjust the wave parameters value. Since there are no definite ways to determine gain values, trial-and-error method

is going to be used to calibrate the wave paddle until the reading on the wave probes result in the desired value. Based on this command, the data that have been collected can be synthesized and plotted in a series of graph and the pattern of the graph is represented in Figure 4.2. Based on the graph, the final gain value that will be used to get the desirable wave height can be found.

For random waves:

```
“begin
 run "1.0 sec 1.00 hz Hs=0.0620 g=1.45 random wave" with (13)
 wave x=1.45*jonswap(1.00,0.0081, 3.3, 0.07, 0.09);
 makewave x on 1;
end;”
```

In the command given, the wave paddle is expected to produce a JONSWAP wave of 0.06 m tall with a peak frequency of 1Hz, or 1 second of wave period. The gain value used in this command to produce 0.06 m tall waves in 1 sec wave period is 1.45. The introduction of the gain value will create an accurate wave that is required in this experiment. However, as observed in Figure 4.2, the gain values produced has its own limitation. Gain values could not be obtained for wave height that is more than 27cm due to the limitation posed by the laboratory apparatus such that of the wave paddle and also the wave probes.

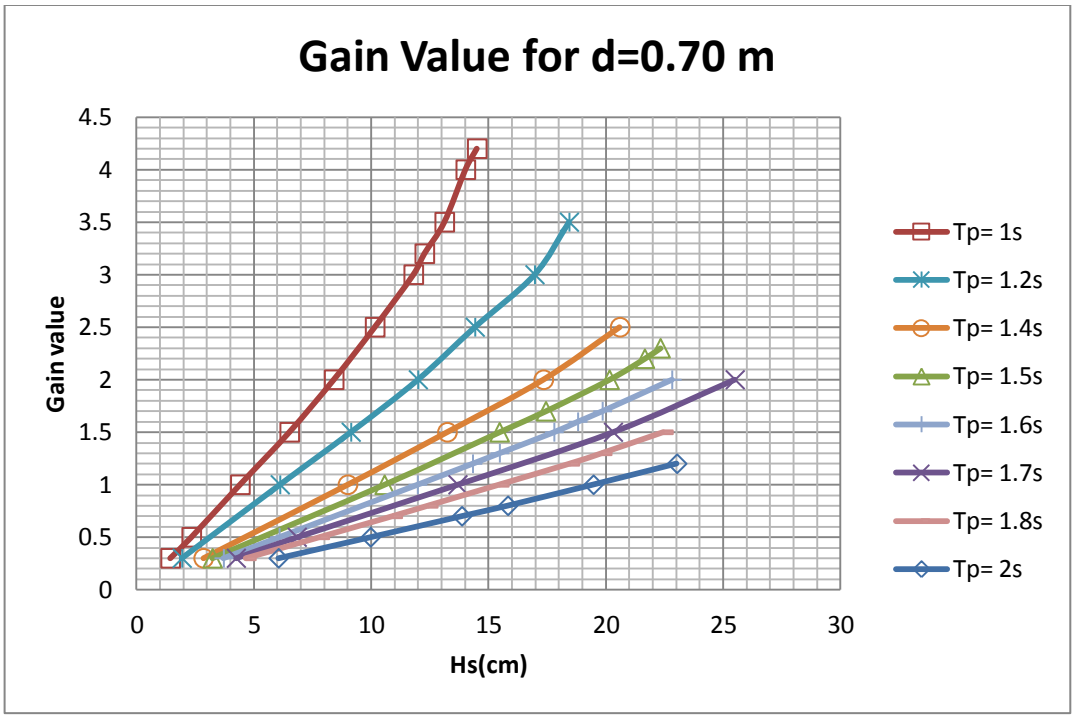

Figure 4.2: Gain value with respect to wave height reading on probes

4.3 Experimental Results

Series of experiments were rigorously conducted in the wave flume to study the wave responses on the H-type floating breakwater in both regular and random waves. The details of these wave types are presented in section 2.2.4 and section 2.2.5. Some examples of raw data and the related wave analysis are demonstrated according to the wave type in the following sections.

4.3.1 Regular Waves

Regular waves are waves that repeat itself over time wherein the vertical displacement of the water surface is the same over a certain period and distance. Profiles of 1-s waves with steepness H_i/L_p = 0.04, 0.06 and 0.07 recorded by the wave probes (WP) at the closest proximity to the test model (i.e. WP3 and WP4) are presented in Figures 4.3- 4.5. Note that WP3 is located in front of the test model of

immersion depth of 0.24 m and WP4 is located behind the model. The corresponding energy density spectra for incident, reflected and transmitted waves are also presented with respect to wave frequency.

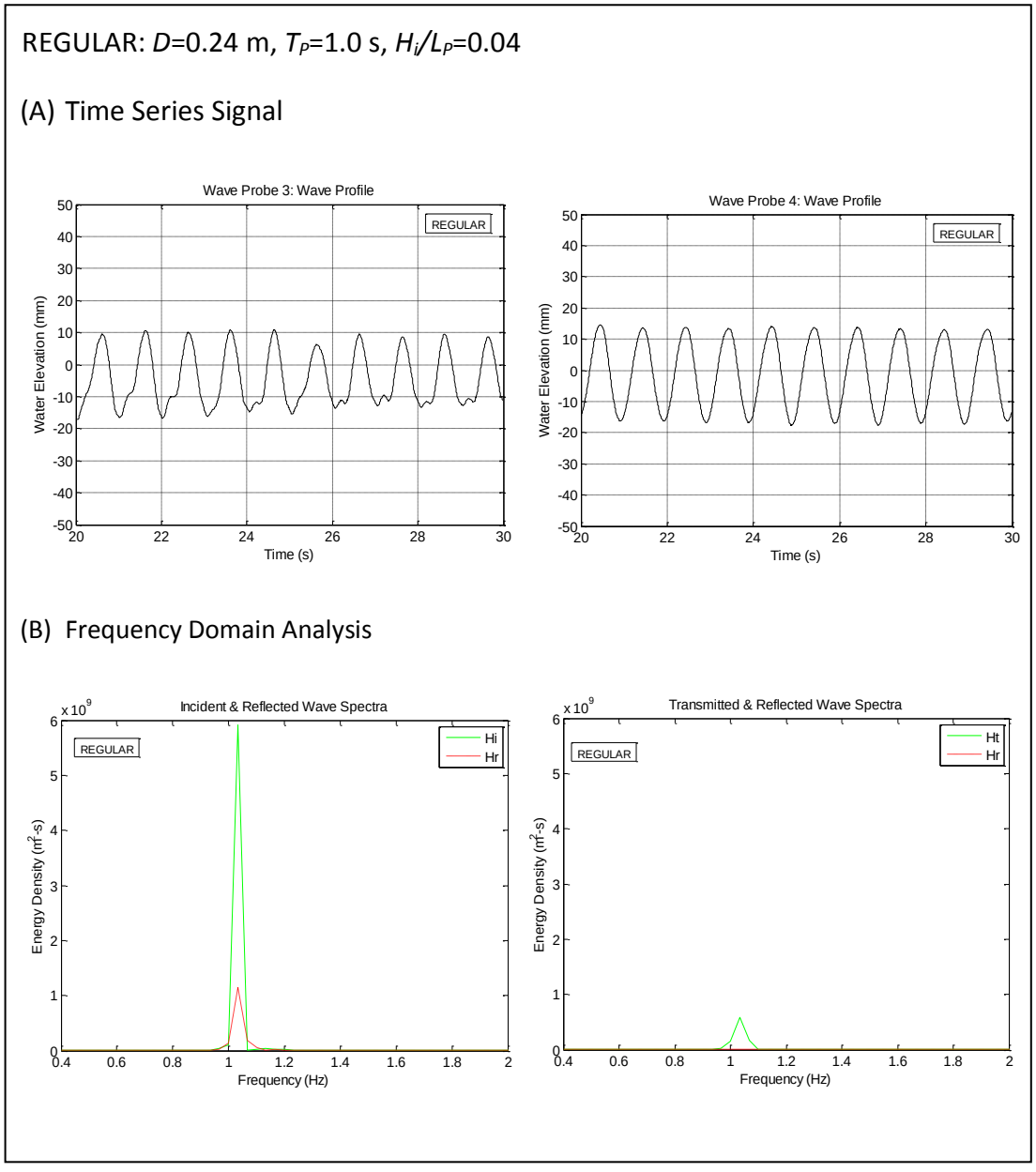

Figure 4.3: Time Series Signal and Frequency Domain Analysis for Regular Waves (D=0.24 m, T_P=1.0 s, H_i/L_P=0.04)

REGULAR: D=0.24 m, T_P=1.0 s, H_i/L_P=0.06

(A) Time Series Signal

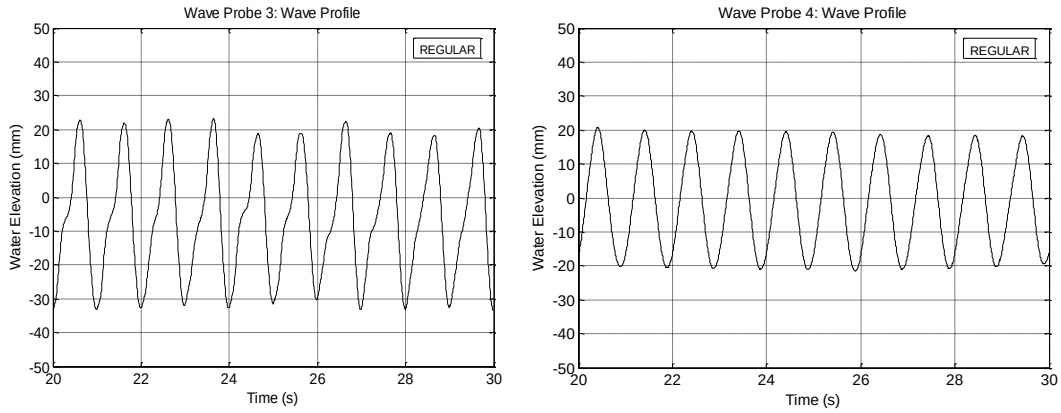

(B) Frequency Domain Analysis

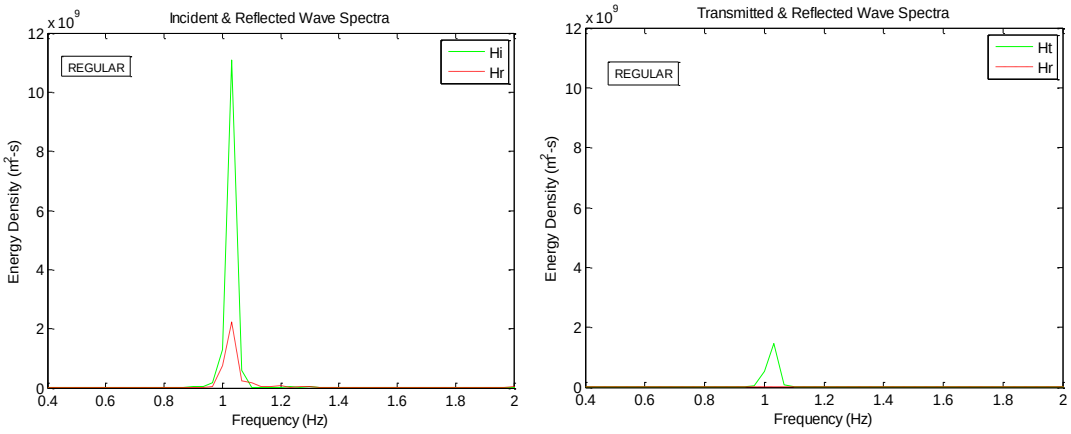

Figure 4.4: Time Series Signal and Frequency Domain Analysis for Regular Waves (D=0.24 m, T_P=1.0 s, H_i/L_P=0.06)

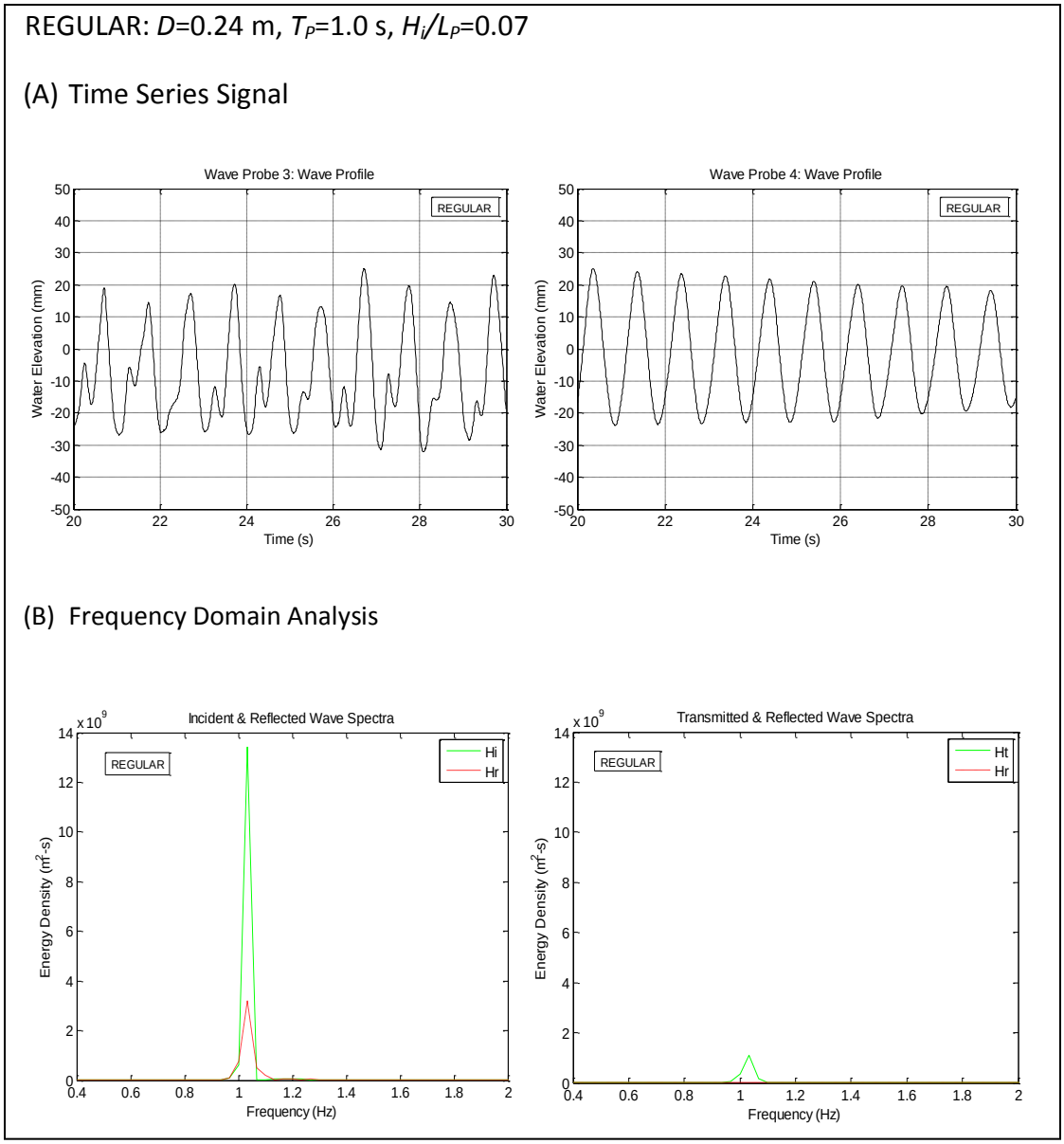

Figure 4.5: Time Series Signal and Frequency Domain Analysis for Regular Waves (D=0.24 m, T_P=1.0 s, H_i/L_P=0.07)

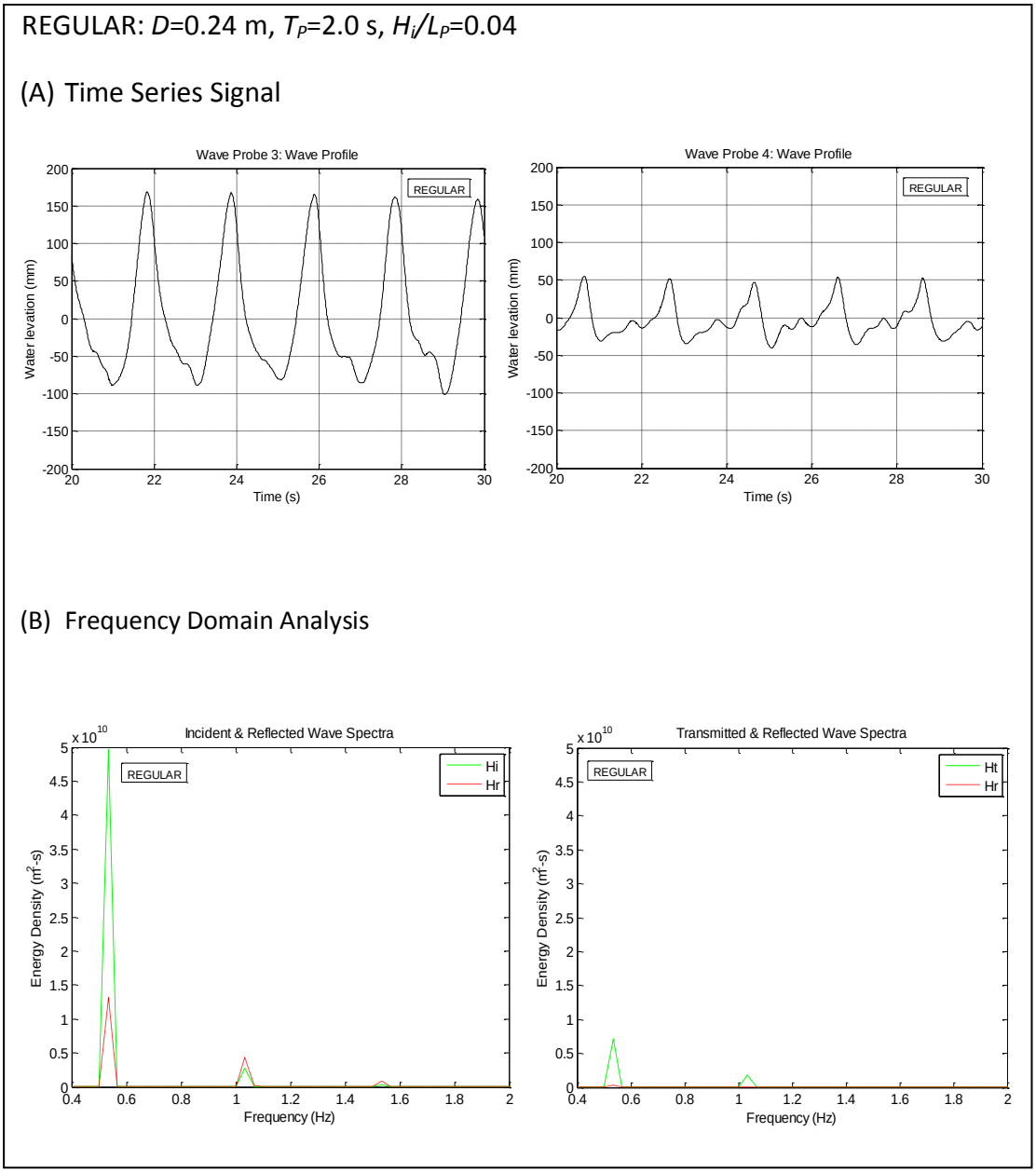

Figure 4.6: Time Series Signal and Frequency Domain Analysis for Regular Waves (D=0.24 m, T_P=2.0 s, H_i/L_P=0.04)

The time series signal measured by WP3 and WP4 for H_i/L_p = 0.04, 0.06 and 0.07 are respectively plotted in a 10-s window with a start-up time of 20 s, as shown in Figures 4.3- 4.5. It is seen from the time series plots in the figures that the wave signals are regular in terms of wave period and height throughout the sampling period. Some

irregularities are observed in the signals recorded by WP3. This is attributed to the wave interference effect resulted by both incident and reflected waves in front of the test model. The detailed information of the measured waves is reflected by the energy spectra plots as shown in Figures 4.3- 4.5. These energy spectra demonstrate peak frequency T_p close to 1 Hz (equivalent to wave period of 1 s). A single peak of the wave signal is seen in each plot at wave frequency close to 1 Hz due to uniformity of the period of the waves generated by the wave paddle. It is apparent from the plots that the incident waves carry more energy than the reflected waves from the test model. At the rear of the breakwater, the transmitted wave energy is considerably dampened by the test model due to abrupt reduction of the energy density level. It is also noted from the figures that the reflected wave energy behind the test model is so small that it can be ignored in the experiments.

Figure 4.6 presents the time series and the related wave spectra analysis of a longer waves on the H-type floating breakwater subjected to immersion depth D = 0.24 m, wave period T_p = 1.9 s and wave steepness H_i/L_p = 0.04. The corresponding peak frequency of 1.9-s wave is 0.53 Hz. Similar trends and relationship between H_i, H_r and H_t are seen in the wave spectra plots. It is interesting to notice a number of spectra peaks for H_i, H_r and H_t at n x T_p where n = 1, 2, 3….This phenomena is expected in longer period waves due to interference of harmonic waves of different orders induced by the reflected waves. Analyses of other test series were also conducted; however, these outcomes of the analysis are not displayed here due to the page constraint of the thesis. It is worth mentioning that the trends of the results resemble those presented here.

4.3.2 Random Waves

Random waves are waves that are made up of a lot of regular plane waves with random wavelength, water level elevation and also wave phase. Figures 4.7-4.9 present the profiles of 1-s peak period waves with steepness H_i/L_p = 0.04, 0.06 and 0.07 recorded by the wave probes at the closest proximity to the test model (i.e. WP3 and

WP4) and the corresponding energy density spectra for incident, reflected and transmitted waves in random waves described by JONSWAP.

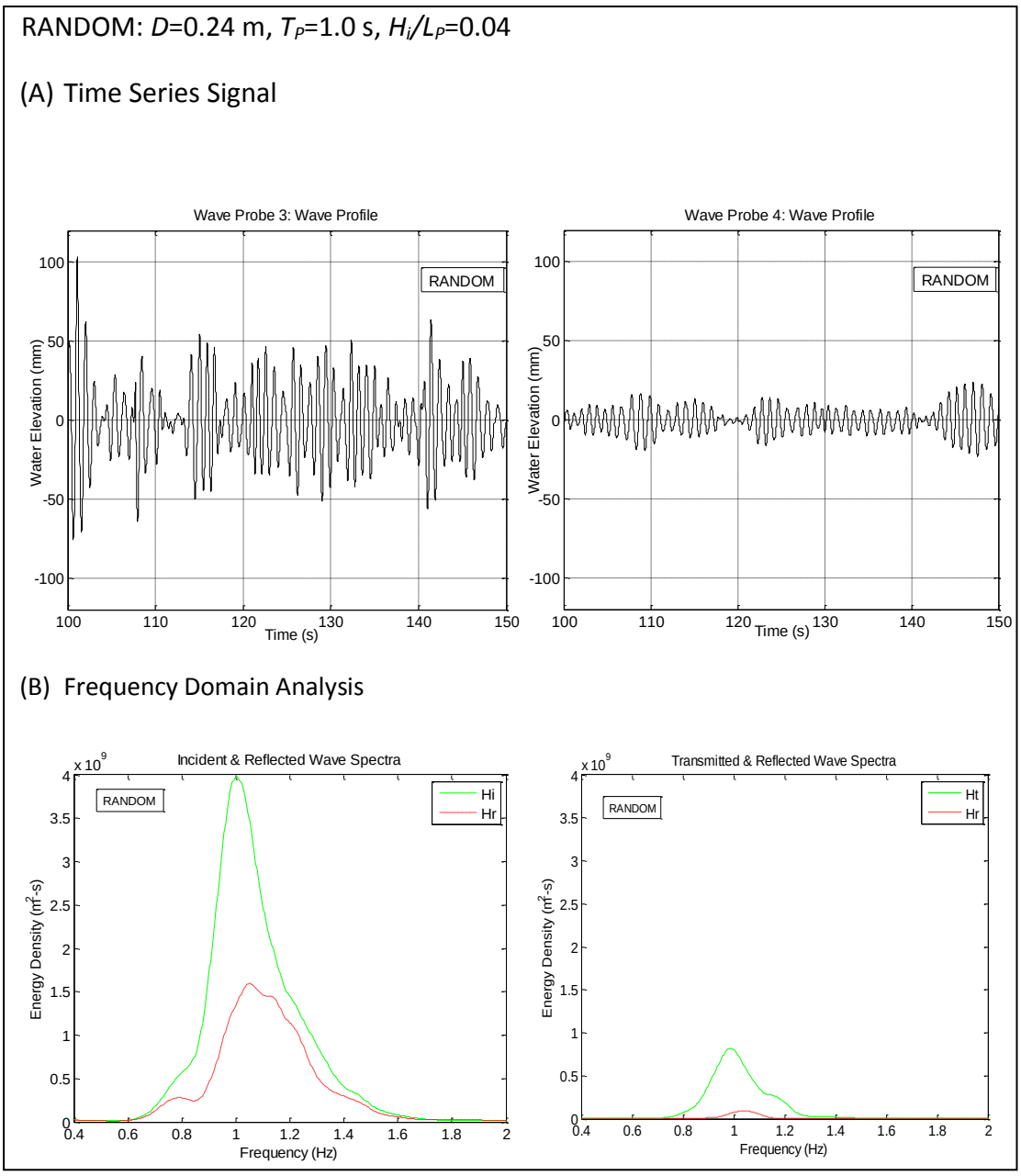

Figure 4.7: Time Series Signal and Frequency Domain Analysis for Random Waves (D=0.24 m, T_P=1.0 s, H_i/L_P=0.04)

RANDOM: D=0.24 m, T_P=1.0 s, H_i/L_P=0.06

(A) Time Series Signal

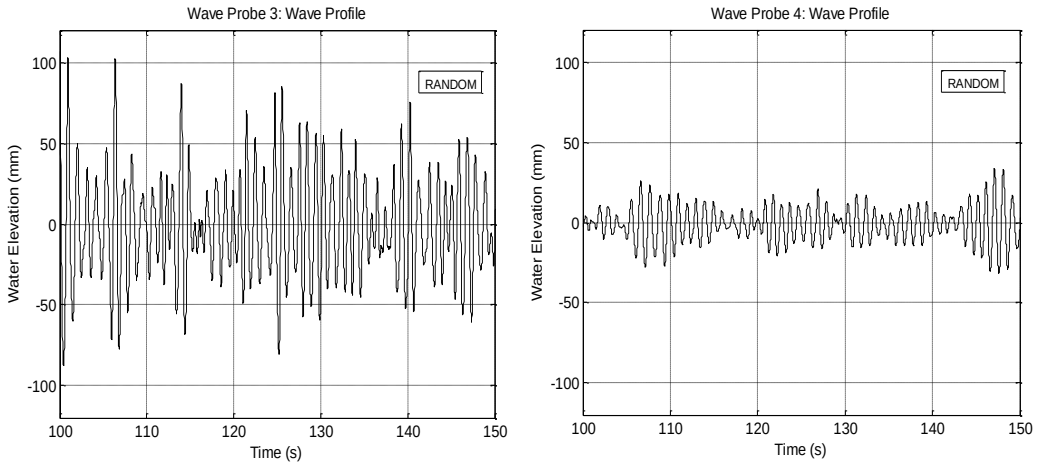

(B) Frequency Domain Analysis

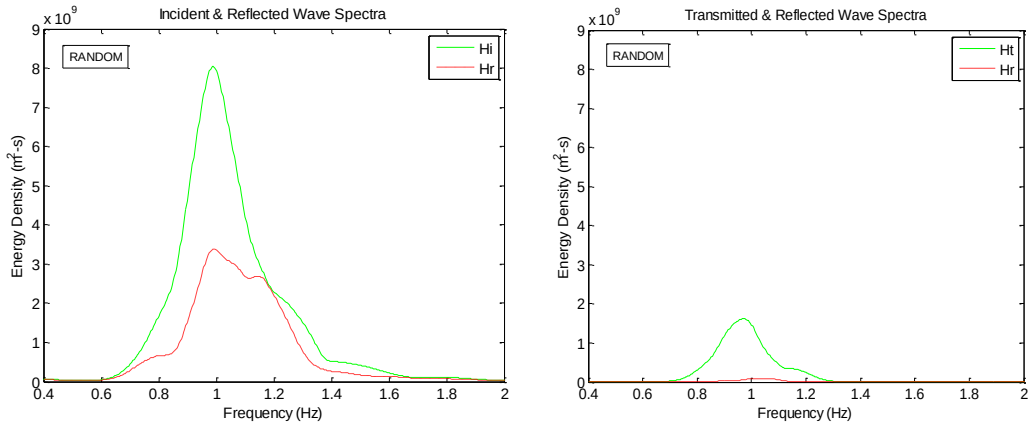

Figure 4.8: Time Series Signal and Frequency Domain Analysis for Random Waves (D=0.24 m, T_P=1.0 s, H_i/L_P=0.06)

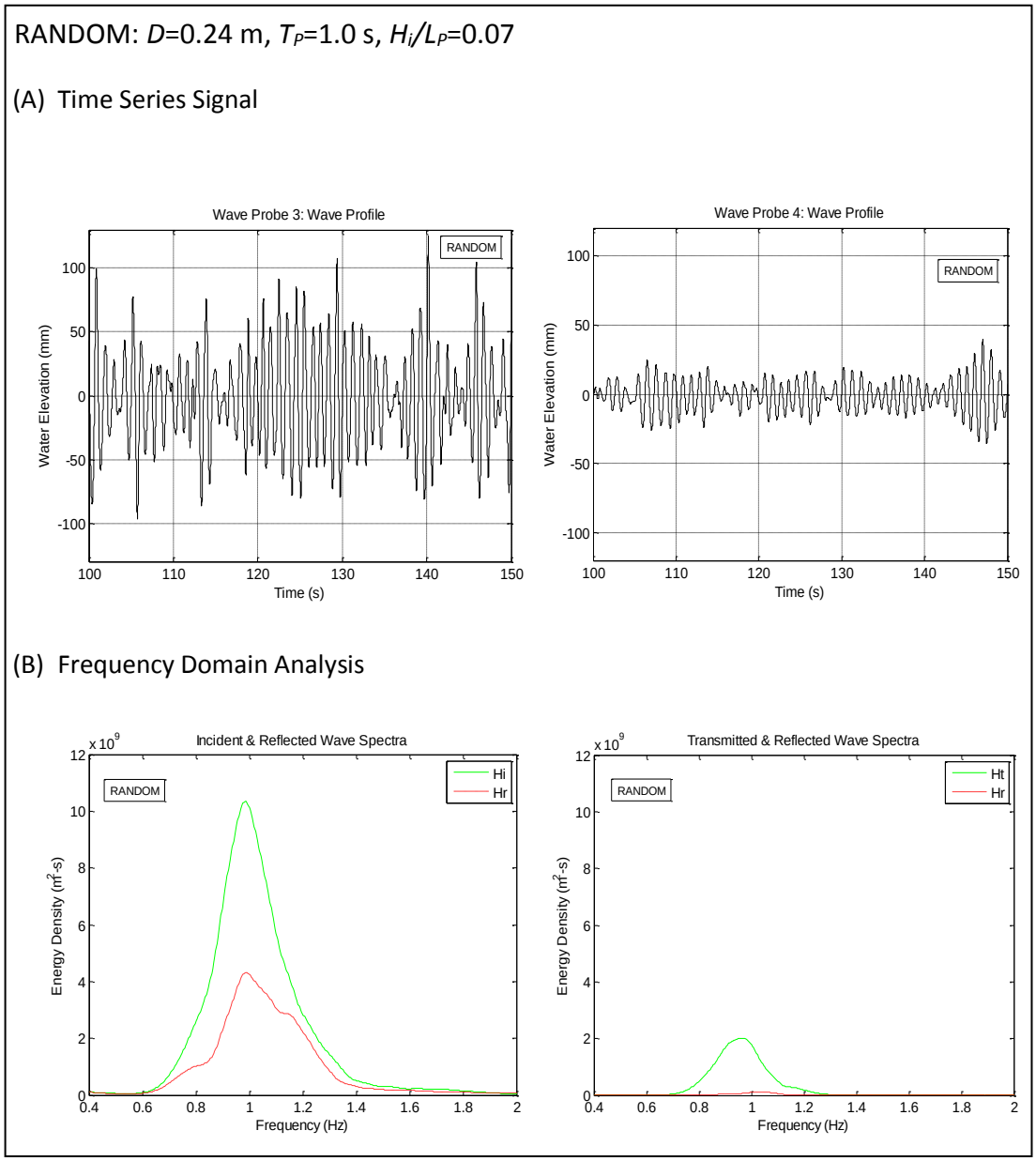

Figure 4.9: Time Series Signal and Frequency Domain Analysis for Random Waves (D=0.24 m, T_P=1.0 s, H_i/L_P=0.07)

RANDOM: D=0.24 m, T_P=2.0 s, H_i/L_P=0.04

(A) Time Series Signal

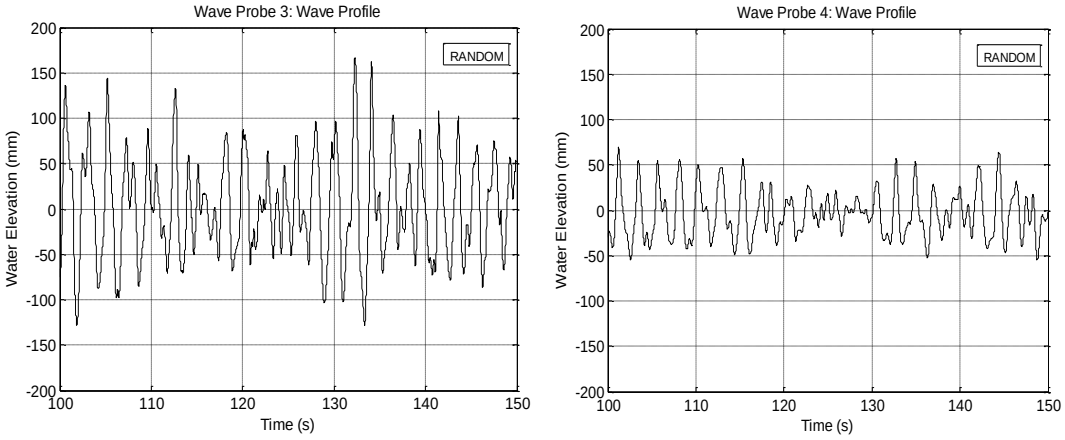

(B) Frequency Domain Analysis

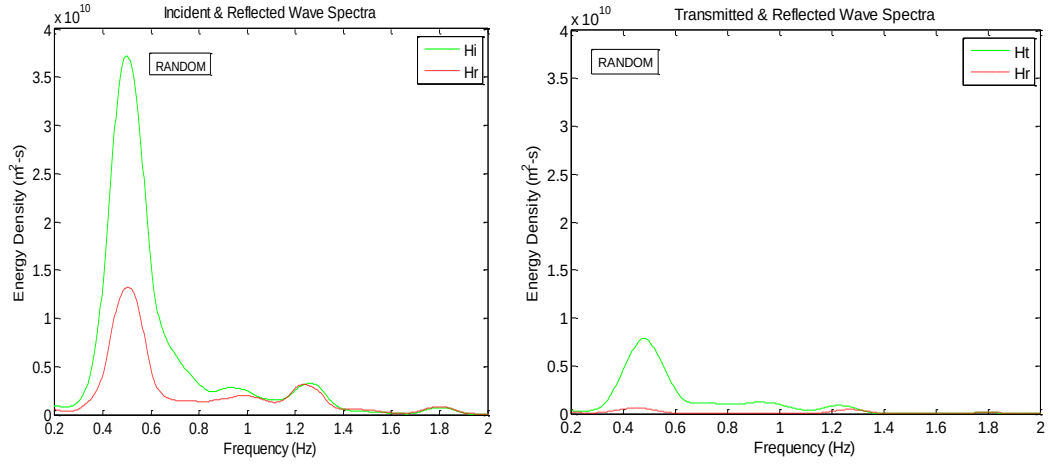

Figure 4.10: Time Series Signal and Frequency Domain Analysis for Random Waves (D=0.24 m, T_P=2.0 s, H_i/L_P=0.04)

Figures 4.7-4.9 show the time series signal measured by WP3 and WP4 for H_i/L_p = 0.04, 0.06 and 0.07 are respectively plotted in a 50-s window with a start-up time of 100 s. Compared with the time series signals of regular waves in Figures 4.3-4.5, the signal inputs for random waves are irregular with a range of wave periods and heights. The energy is unevenly distributed in a range of wave frequencies. The peak of the energy spectra indicates the peak frequency of the data set for incident, reflected and transmitted waves in random waves. Note that the area underneath the curves of energy spectra indicates the zeroth spectral moment m_0 whereby the energy is directly proportional to m_0. The findings obtained are similar to those of the regular waves in which the energy of the incident waves is being the greatest, followed by the reflected and transmitted waves in all test cases; whereas, the reflected waves at the lee of the test model is negligible.

Figure 4.10 displays the time series and the related wave spectra analysis of a longer waves on the H-type floating breakwater subjected to immersion depth D = 0.24 m, peak wave period T_p = 2.0 s and wave steepness H_i/L_p = 0.04. Once again, the results are identical to those of the regular waves as shown in Figure 4.10. Analyses of other test cases were performed separately. These results will not be included in this thesis.

4.4 Results Interpretation

4.4.1 Effect of the Relative Breakwater Width

The wave energy coefficients C_t, C_r and C_l are plotted against the breakwater width B/L where B and L are the breakwater width and the wavelength, respectively. The geometrical ratio of B/L is a well accepted dimensionless parameter used in the design of coastal engineering structures. Since B is fixed in this study and the fact that L is the only independent variable that is governed by the change of wave period or wave frequency, the B/L is often termed as the relative wave period or the relative wave length. Nevertheless, as far as this thesis is concerned, the B/L is consistently termed as the relative breakwater width throughout this writing.

4.4.1.1 Wave Transmission

Wave transmission performance of the H-type floating breakwater is quantified by the wave transmission coefficient, C_t. The lower the C_t values, the smaller the amount of wave transmission at the lee side of the breakwater which, in turn, leads to higher wave attenuation ability. Figure 4.11 displays the C_t of the H-type floating breakwater subjected to immersion depth ratios of D/d = 0.34, 0.39 and 0.44 in both regular and random waves. The wave steepness tested ranges from 0.04 – 0.07 for both wave conditions.

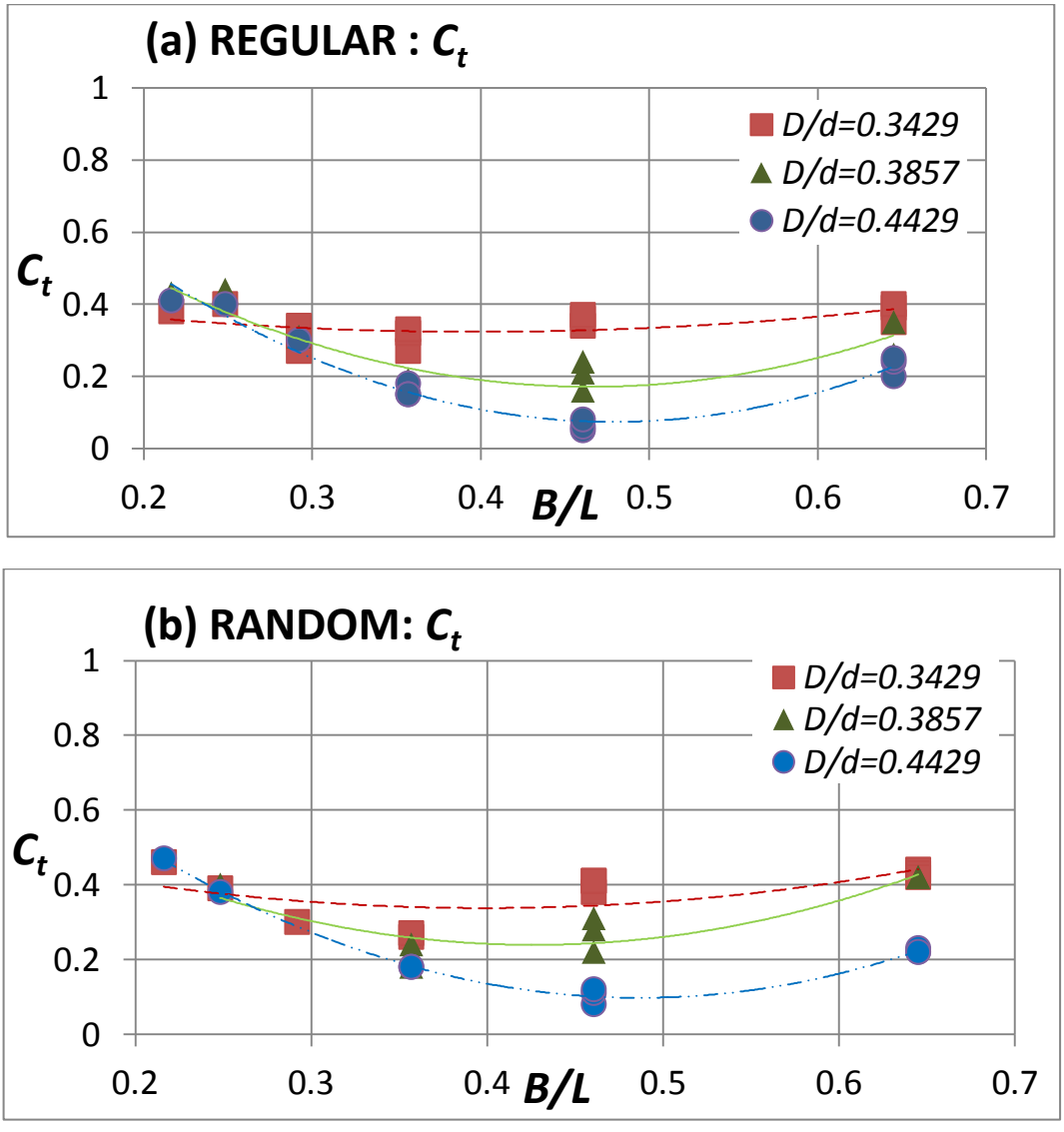

Figure 4.11: C_t vs. B/L of regular and irregular waves: (a) Regular waves and (b) Random waves

It is found that the C_t recorded are relatively small (C_t < 0.5), which indicates that at least 50% attenuation of wave height was attained by H-type floating breakwater in both regular and irregular waves. The C_t reduces as *D/d* increases from 0.34 to 0.44. The lowest C_t values recorded in regular and random waves are 0.05 and 0.11, respectively, with both happen at *D/d* = 0.44. It is also seen from the figure that the C_t values are rather constant with *B/L*, particularly for *D/d* = 0.34. This means that wave attenuation ability of the model does not alter much with the variation of wave period. Nevertheless, as *D/d* increases the C_t values gradually decrease with an increase in *B/L*, indicating that the breakwater restricts wave transmission more in shorter period waves. No significant change of the C_t plots when comparing the C_t of regular and random waves. This implies that wave attenuation characteristics of the H-type floating breakwater are not much governed by the wave climate type. The summary of C_t for regular and irregular waves is presented in Table 4.2.

Table 4.2: C_t of regular and irregular waves: (a) Regular waves and (b) Random waves

(a) Regular Waves

D/d	0.34	0.39	0.44
C_t range	0.27 - 0.40	0.16 – 0.44	0.05 – 0.41

(b) Random Waves

D/d	0.34	0.39	0.44
C_t range	0.26 – 0.46	0.18 – 0.42	0.11– 0.47

4.4.1.2 Wave Reflection

Wave reflection performance of the H-type floating breakwater is quantified by the wave reflection coefficient, C_r. The higher the C_r values, the greater will be the wave reflection effect. Figure 4.12 present the relationship between C_r and *B/L* at *D/d* = 0.34, 0.39 and 0.44 in both regular and random waves.

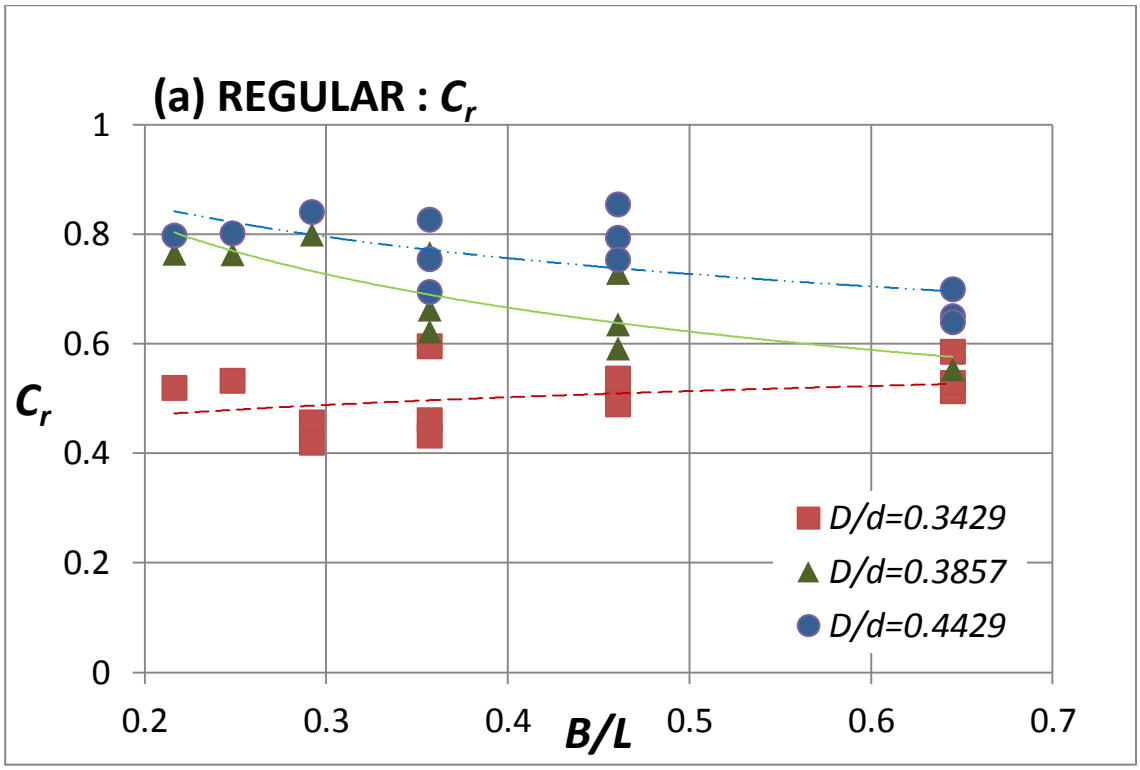

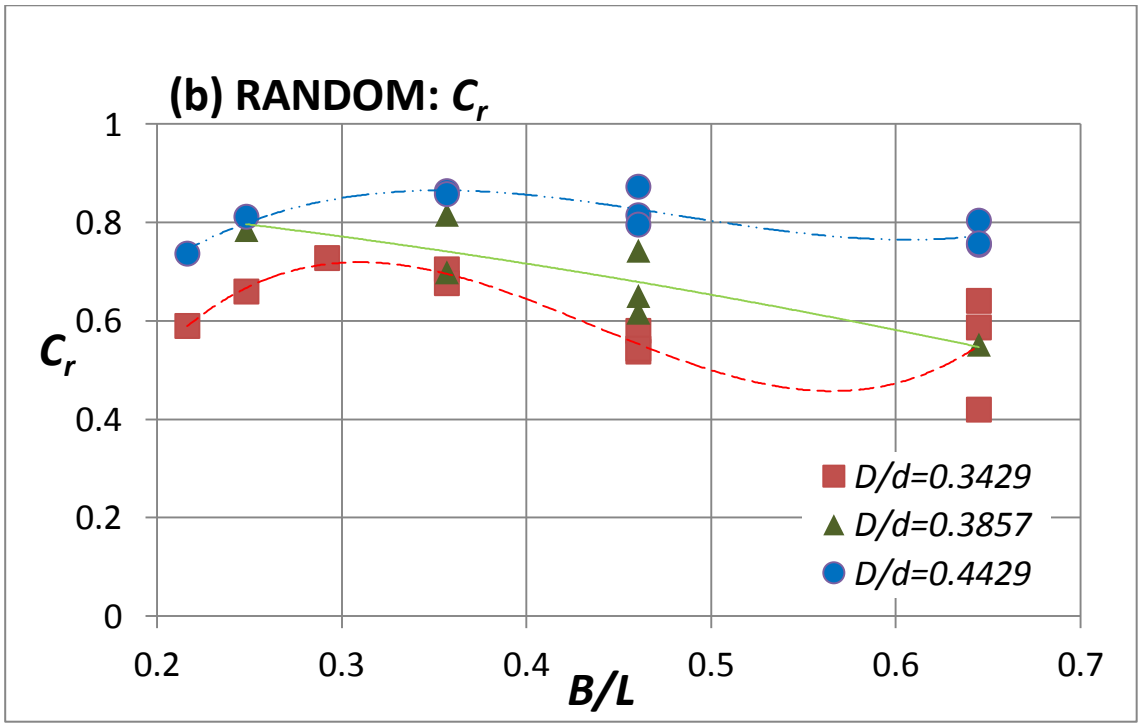

Figure 4.12: C_r vs. B/L of regular and irregular waves: (a) Regular waves and (b) Random waves

In general, the C_r has an uncertain relation with B/L for all the tested D/d cases. The highest C_r value recorded is about 0.87 at D/d = 0.44 and the smallest C_r happens at D/d = 0.34. The record shows that the H-type floating breakwater is a good wave reflector (with almost 77% of the incident wave energy get reflected) when it is deeply immersed. The range and average of C_r for D/d = 0.34, 0.39 and 0.44 in both regular and random waves are summarized in Table 4.3.

Table 4.3: C_r of regular and irregular waves: (a) Regular waves and (b) Random waves

(a) Regular Waves

D/d	0.34	0.39	0.44
C_r range	0.43 – 0.717	0.45 – 0.80	0.64 – 0.85
Average C_r	0.52	0.65	0.76

(b) Random Waves

D/d	0.34	0.39	0.44
C_r range	0.42 – 0.73	0.53 – 0.82	0.74 – 0.87
Average C_r	0.61	0.66	0.81

4.4.1.3 Energy Dissipation

Wave energy dissipation of the H-type floating breakwater is quantified by the energy loss/dissipation coefficient, C_l. The amount of energy loss due to the test model is reflected by the C_l values. The higher the C_l values, the greater will be the energy loss triggered by the H-type floating breakwater. The mechanisms identified to trigger energy loss are wave breaking, wave run-up and run down, formation of eddies underneath the test model, sound and heat. Since these phenomena are difficult to be measured physically, the loss of energy is often quantified based on the Principle of Conservation of Energy and the related formulation is presented in Section 2.2.3. Figure 4.13 present the C_l of the H-type floating breakwater plotted against B/L at D/d = 0.34, 0.39 and 0.44 in both regular and random waves.

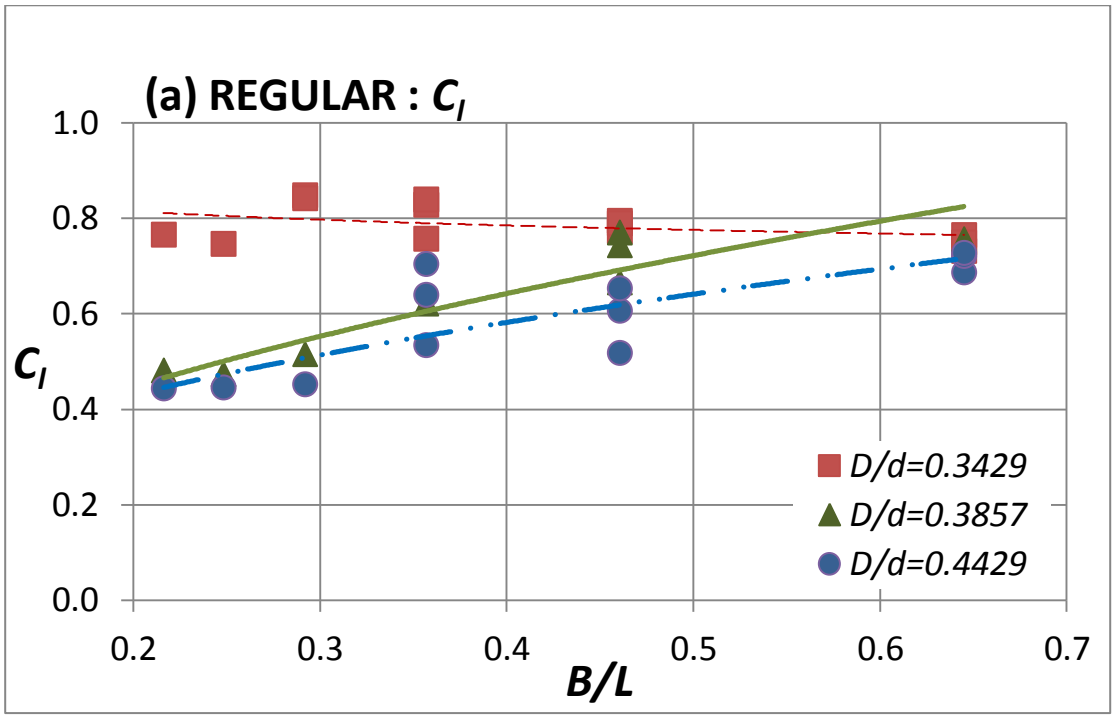

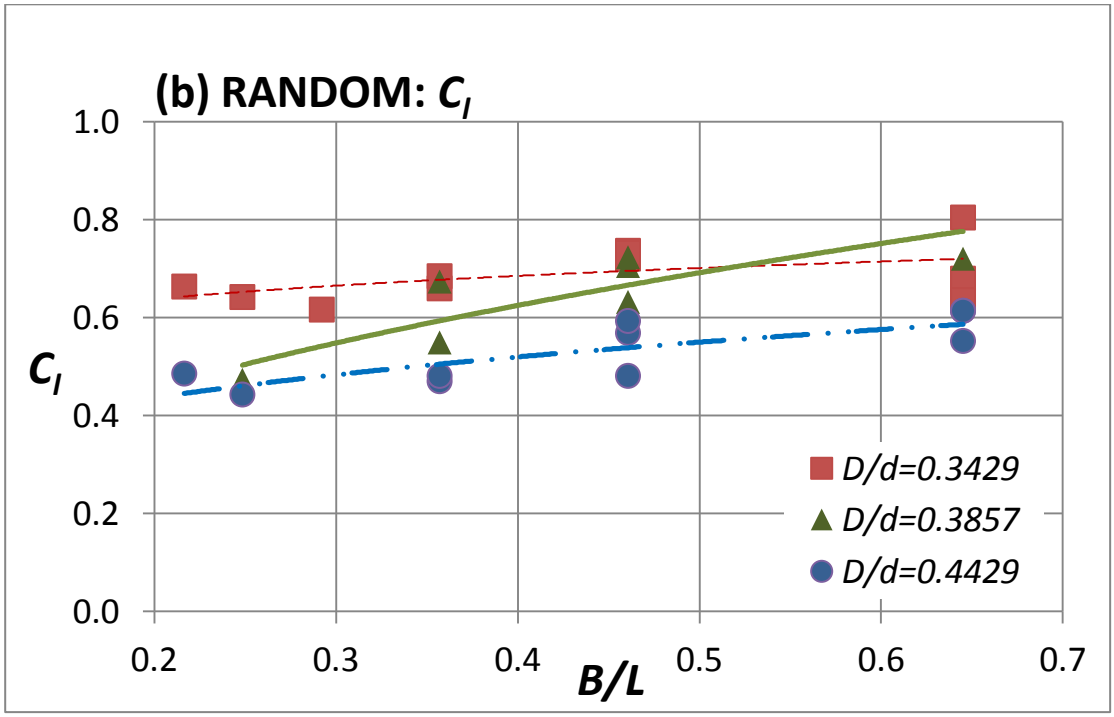

Figure 4.13: C_l vs. B/L of regular and irregular waves: (a) Regular waves and (b) Random waves

An increasing trend of C_l of the test model is seen with respect to *B/L*. This indicates that the configuration of the H-type floating breakwater is helpful in dissipating energy of the smaller period waves. The maximum C_l values attained in regular and random waves are 0.85 and 0.74, respectively, with both happen at *D/d* = 0.34. Therefore, it is safe to say that the H-type floating breakwater of shallow immersion depth is indeed a good energy dissipater particularly when exposed to shorter period waves. The range and average of C_l for *D/d* = 0.34, 0.39 and 0.44 in both regular and random waves are summarized in Table 4.4.

Table 4.4: C_l of regular and irregular waves: (a) Regular waves and (b) Random waves

(a) Regular Waves

D/d	0.34	0.39	0.44
C_l range	0.62 – 0.85	0.47 – 0.85	0.44 – 0.73

(b) Random Waves

D/d	0.34	0.39	0.44
C_l range	0.62 – 0.74	0.47 – 0.74	0.44 – 0.61

4.4.2 Effect of the Wave Steepness Parameter

The wave energy coefficients C_t, C_r and C_l are plotted against the wave steepness parameter $\frac{H_i}{gT^2}$ where g, H_i and T are acceleration due to gravity, the incident wave height and the wave period, respectively. The geometrical ratio of $\frac{H_i}{gT^2}$ is a well accepted dimensionless parameter used in the design of coastal engineering structures. Since H_i always depends on the change of the variable T in this study, the $\frac{H_i}{gT^2}$ often termed as the relative wave steepness. Nevertheless, as far as this thesis is concerned, the $\frac{H_i}{gT^2}$ is consistently termed as the relative wave steepness throughout this writing.

4.4.2.1 Wave Transmission

Wave transmission performance of the H-type floating breakwater is quantified by the wave transmission coefficient, C_t. The lower the C_t values, the smaller the amount of wave transmission at the lee side of the breakwater which, in turn, leads to higher wave attenuation ability. Figure 4.14 displays the C_t of the H-type floating breakwater subjected to immersion depth ratios of D/d = 0.34, 0.39 and 0.44 in both regular and random waves. The wave steepness tested ranges from 0.04 – 0.07 for both wave conditions.

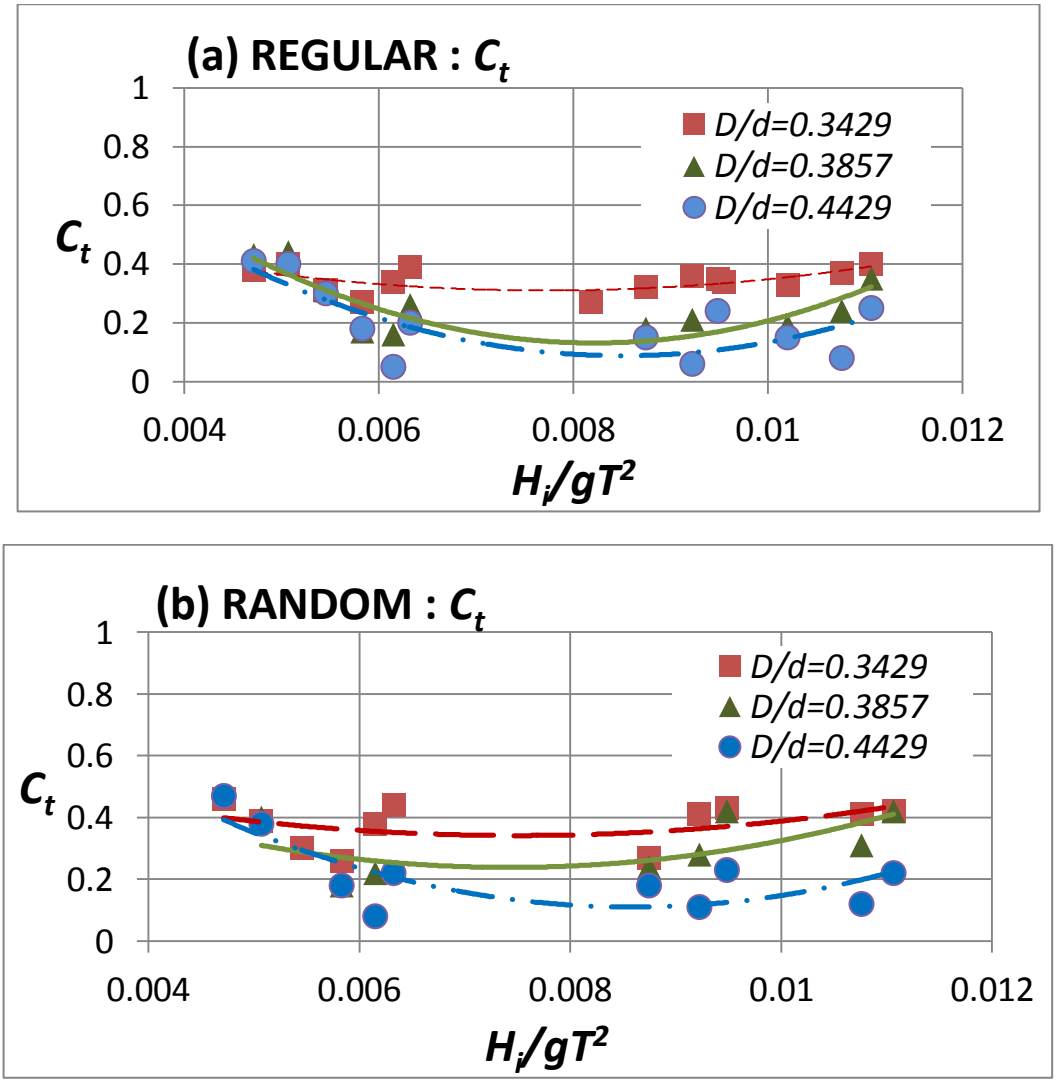

Figure 4.14: C_t vs. $\frac{H_i}{gT^2}$ of regular and irregular waves: (a) Regular waves and (b) Random waves

It is found that the C_t recorded are relatively small (C_t < 0.5), which indicates that at least 50% attenuation of wave height was attained by H-type floating breakwater in both regular and irregular waves. The C_t reduces as *D/d* increases from 0.34 to 0.44. The lowest C_t values recorded in regular and random waves are 0.05 and 0.11, respectively, with both happen at *D/d* = 0.44. It is also seen from the figure that the C_t values are rather constant with $\frac{H_i}{gT^2}$, particularly for *D/d* = 0.34. This means that wave attenuation ability of the model does not alter much with the variation of wave steepness. Nevertheless, as *D/d* increases the C_t values gradually decrease with an increase in $\frac{H_i}{gT^2}$, indicating that the breakwater restricts wave transmission more in steeper waves. No significant change of the C_t plots when comparing the C_t of regular and random waves. This implies that wave attenuation characteristics of the H-type floating breakwater are not much governed by the wave climate type. The summary of C_t for regular and irregular waves is presented in Table 4.5.

Table 4.5: C_t of regular and irregular waves: (a) Regular waves and (b) Random waves

(a) Regular Waves

D/d	0.34	0.39	0.44
C_t range	0.27 - 0.40	0.16 – 0.44	0.05 – 0.41

(b) Random Waves

D/d	0.34	0.39	0.44
C_t range	0.26 – 0.46	0.18 – 0.42	0.11– 0.47

4.4.2.2 Wave Reflection

Wave reflection performance of the H-type floating breakwater is quantified by the wave reflection coefficient, C_r. The higher the C_r values, the greater will be the wave reflection effect. Figure 4.15 present the relationship between C_r and $\frac{H_i}{gT^2}$ at *D/d* = 0.34, 0.39 and 0.44 in both regular and random waves.

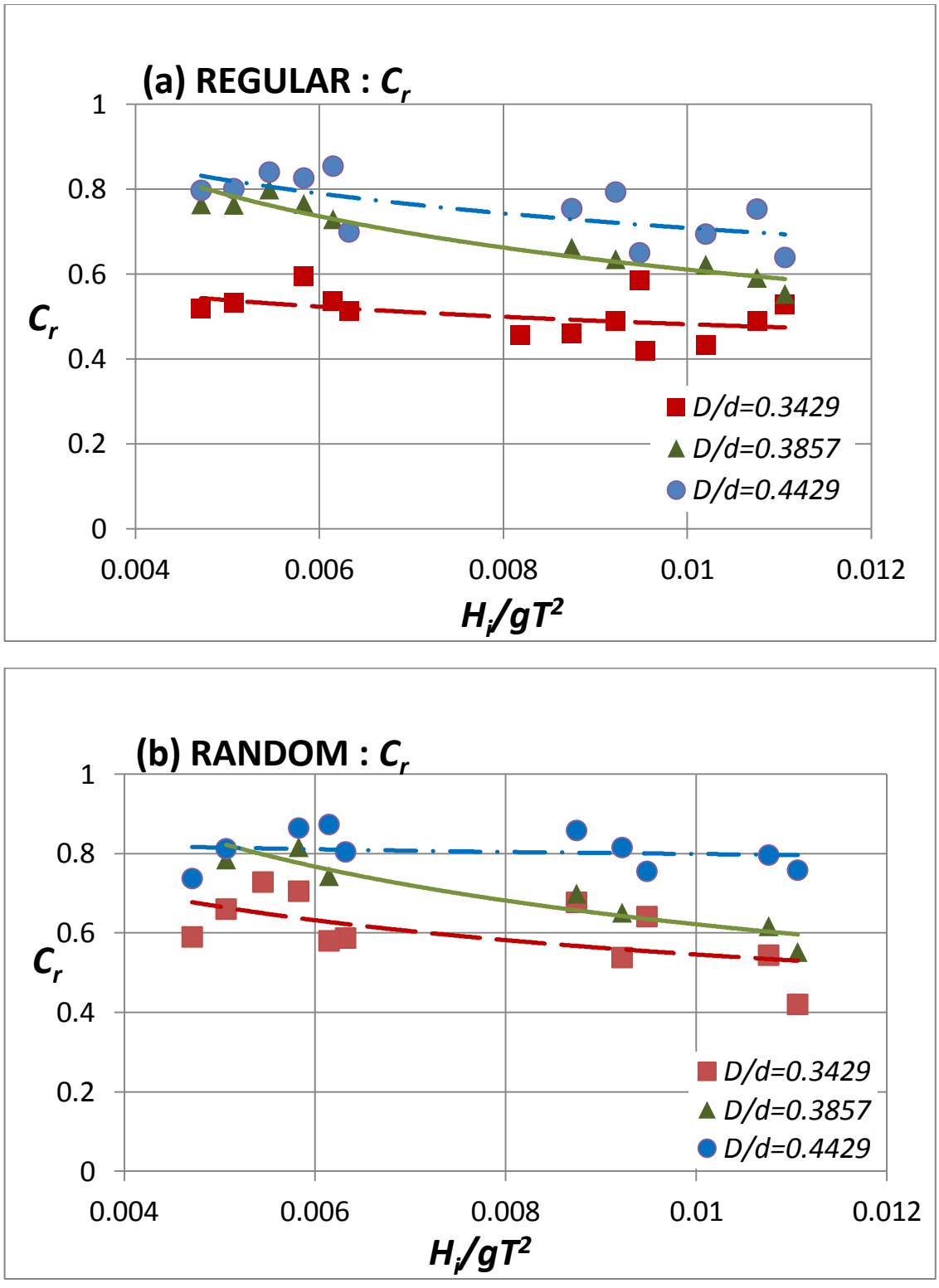

Figure 4.15: C_r vs. $\frac{H_i}{gT^2}$ of regular and irregular waves: (a) Regular waves and (b) Random waves

In general, the C_r has an uncertain relation with $\frac{H_i}{gT^2}$ for all the tested *D/d* cases. The highest C_r value recorded is about 0.87 at *D/d* = 0.44 and the smallest C_r happens at *D/d* = 0.34. The record shows that the H-type floating breakwater is a good wave reflector (with almost 77% of the incident wave energy get reflected) when it is deeply immersed. The range and average of C_r for *D/d* = 0.34, 0.39 and 0.44 in both regular and random waves are summarized in Table 4.6.

Table 4.6: C_r of regular and irregular waves: (a) Regular waves and (b) Random waves

(a) Regular Waves

D/d	0.34	0.39	0.44
C_r range	0.43 – 0.717	0.45 – 0.80	0.64 – 0.85
Average C_r	0.52	0.65	0.76

(b) Random Waves

D/d	0.34	0.39	0.44
C_r range	0.42 – 0.73	0.53 – 0.82	0.74 – 0.87
Average C_r	0.61	0.66	0.81

4.4.2.3 Energy Dissipation

Wave energy dissipation of the H-type floating breakwater is quantified by the energy loss/dissipation coefficient, C_l. The amount of energy loss due to the test model is reflected by the C_l values. The higher the C_l values, the greater will be the energy loss triggered by the H-type floating breakwater. The mechanisms identified to trigger energy loss are wave breaking, wave run-up and run down, formation of eddies underneath the test model, sound and heat. Since these phenomena are difficult to be measured physically, the loss of energy is often quantified based on the Principle of Conservation of Energy and the related formulation is presented in Section 2.2.3. Figure 4.16 present the C_l of the H-type floating breakwater plotted against $\frac{H_i}{gT^2}$ at *D/d* = 0.34, 0.39 and 0.44 in both regular and random waves.

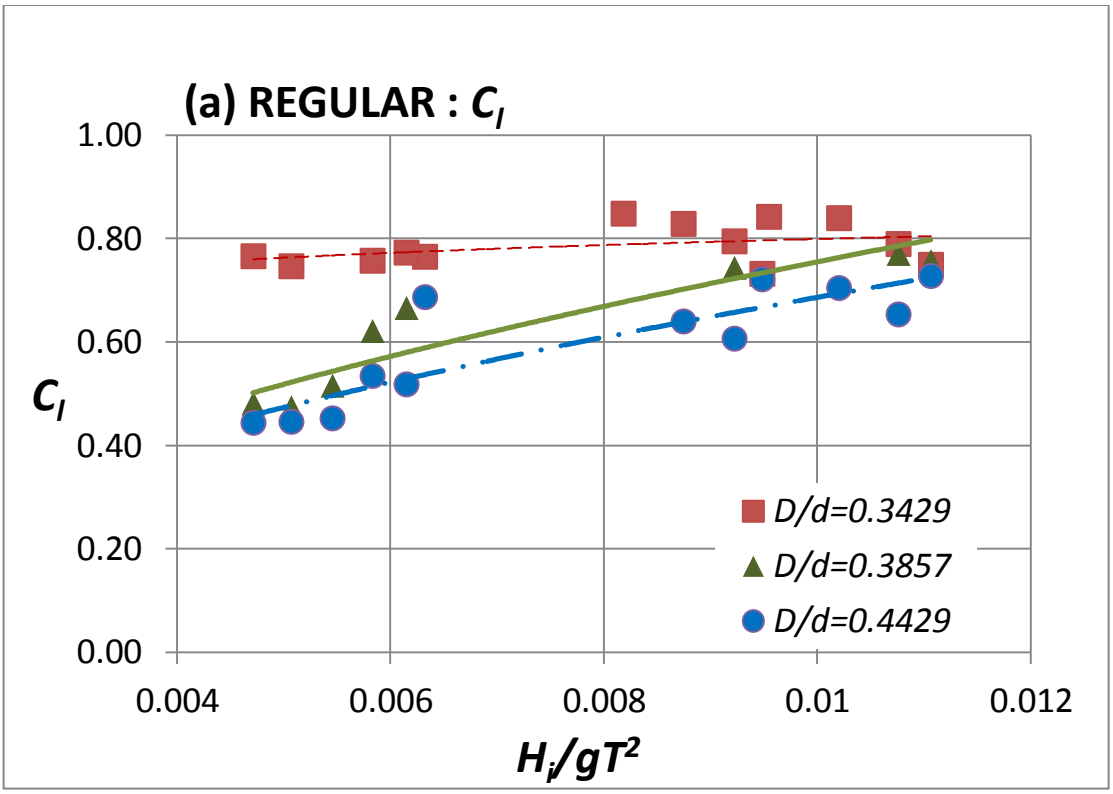

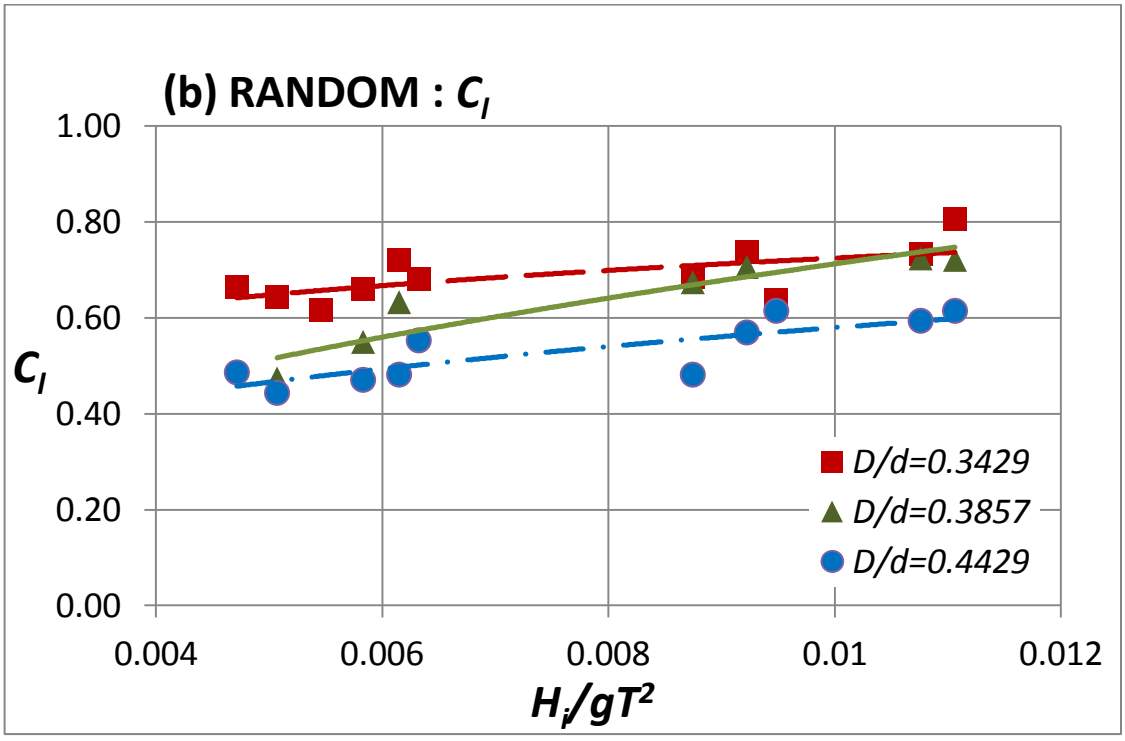

Figure 4.16: C_l vs. $\frac{H_i}{gT^2}$ of regular and irregular waves: (a) Regular waves and (b) Random waves

An increasing trend of C_l of the test model is seen with respect to $\frac{H_i}{gT^2}$. This indicates that the configuration of the H-type floating breakwater is helpful in dissipating energy of the steeper waves. The maximum C_l values attained in regular and random waves are 0.85 and 0.74, respectively, with both happen at D/d = 0.34. Therefore, it is safe to say that the H-type floating breakwater of shallow immersion depth is indeed a good energy dissipater particularly when exposed to high steepness waves. The range and average of C_l for D/d = 0.34, 0.39 and 0.44 in both regular and random waves are summarized in Table 4.7.

Table 4.7: C_l of regular and irregular waves: (a) Regular waves and (b) Random waves

(c) Regular Waves

D/d	0.34	0.39	0.44
C_l range	0.62 – 0.85	0.47 – 0.85	0.44 – 0.73

(d) Random Waves

D/d	0.34	0.39	0.44
C_l range	0.62 – 0.74	0.47 – 0.74	0.44 – 0.61

4.5 Comparisons of Results

A comparison on the performance of the previously studied floating breakwater in terms on the energy coefficient and relative breakwater width ratio are illustrated in Figure 4.17, 4.18 and 4.19. Relative width ratio is the ratio of width of the breakwater-to-wavelength. In this study, the energy coefficients that were used are transmission coefficient, reflection coefficient and energy loss coefficient. The H-type floating breakwater was compared with the breakwater developed by various researchers to illustrate the performance of the H-type breakwater in wave attenuation. For this study, the immersion depth ratio, D/d of 0.44 was chosen for the comparison for wave steepness ranges from 0.04 – 0.07 in random waves condition as this condition is relatively similar to the regular wave condition. The variation of energy coefficient will

be represented with *B/L* ratio. The characteristics of the experimental studies adopted by various researchers are shown in Table 4.8.

Figure 4.17 shows different floating breakwater model performed differently when compared to each other. The trend and shape of the FBW curves are quite similar to each other wherein when the relative width of the breakwater increases, their transmission coefficient decreases. The scattering of the performance of the different FBW attributed to the differences in the model geometry, model shape, test facilities and also test conditions. From the figure, it can be observed that the H-type FBW outperformed most of the previously developed FBW. It can be seen that as the wavelength decreases, the H-type FBW can perform better in attenuating wave energy. Less wave is allowed to be transmitted by the H-type FBW as the relative breakwater width increases.

Figure 4.18 shows the comparison the H-type FBW with other breakwaters developed by other researchers. As can be seen in the figure, the H-type floating breakwater doesn't follow the trend of the other breakwaters but it did shows that it has a high reflection coefficient value compared to the other floating breakwater which shows that it is a good reflector of waves. Apart from that, the figure also shows that as the relative width of the breakwater decreases, the H-type FBW tends to reflect less wave energy. It can be observed that the model can reflect about 80% of incoming wave energy.

Figure 4.19 shows the comparison of the energy loss coefficient of the H-type FBW with other types of previously studied breakwater. The present breakwater follow the trend and shape of the other breakwater but the H-type FBW dissipate less wave energy when compared to other floating breakwater.

Table 4.8: Characteristics of experimental studies used in the comparison in Figure 4.17 – 4.19.

Reference	Structure type	Dimension of model [m]	Experimental facilities [flume dimension & d in m]	Main parameters ranges	Hydrodynamics coefficients (C_t, C_r ,C_l)
Bruce L. McCartney (1985)	Box-type FBW (B = 12 FT)	B = 4.0, l = 29.7, h = 1.5, D = 1.1	Tested for Olympia Harbor, Washington, *d* = 7.6	H_i = 0.50-1.10, T=2.50-4.00	C_t = 0.42-0.88
Bruce L. McCartney (1985)	Box-type FBW (B = 16 FT)	B = 4.8, l = 29.7, h = 1.5, D = 1.1	Tested for Olympia Harbor, Washington, *d* = 7.6	H_i = 0.50-1.10, T=2.50-4.00	C_t = 0.39-0.89
Mani J.S. (1991)	Y-Frame FBW	B = 0.5, l = 0.2, 0.3, 0.4, h = 0.3, D = 0.16-0.46	30 x 2 x 1.5, *d* = 1.0	*D/d* =0.46, H_i/L = 0.01-0.10 *B/L* =0.095-0.224	C_t = 0.31-0.79
Murali K. and Mani J.S. (1997)	Cage FBW	B = 0.6, 0.8, 1.0, l = 0.2, 0.3, 0.4, h = 0.3, D = 0.36-0.56	30 x 2 x 1.5, *d* = 1.0	*D/d*=0.46 H_i/L = 0.01-0.10 *B/L* =0.12-0.60	C_t = 0.08-0.58
Behzad M. and Akbari M. (2007)	Moored Pontoon Type FBW	B = 0.72, D = 0.3-0.4	33 x 5.5 x 1.5, *d* = 1.0	*D/d*=0.14-0.23 H_i=0.20-1.20 *B/L* =0.20-2.20	C_t = 0.55-0.89
Vital Hedge A. et al. (2007)	Horizontal Interlaced Multilayer Moored Pipe FBW	B=0.77-4.91 ,number of layers, n=3, spacing-to-diameter, S/d=5	45 x 0.75 x 1.0, *d* = 0.5	H_i = 0.06-0.18 T=1.20-2.20 *B/L* = 0.40-1.20	C_t = 0.65-0.77
Wang H.Y. and Sun Z.C. (2010)	Porous FBW (Directional Mooring)	B=0.68, l=0.32, h=0.2, porosity=0.63,D=0.4-0.44	50 x 0.7 x 1.0, *d*=0.44	H_i = 0.06 T=0.60-1.40 *B/L* = 0.132-0.569	C_t = 0.10-0.94 C_r = 0.09-0.25 C_l = 0.40-0.99
Wang H.Y. and Sun Z.C. (2010)	Porous FBW (Directional Mooring)	B=0.68, l=0.32, h=0.2, porosity=0.63, D=0.4-0.42	50 x 0.7 x 1.0, *d*=0.44	H_i = 0.06 T=0.60-1.40 *B/L* = 0.132-0.569	C_t = 0.01-0.66 C_r = 0.09-0.28 C_l = 0.72-1.00
Fang He et al. (2012)	Rectangular FBW without pneumatic chambers	B=0.75, l=1.42, h=0.4, D=0.235	45 x 1.55 x 1.5, *d* = 0.7	H_i = 0.04 T=1.10-1.80 *B/L* = 0.186-0.404	C_t = 0.35-0.91 C_r = 0.39-0.55 C_l = 0.05-0.72
Fang He et al. (2012)	Rectangular FBW with pneumatic chambers	B=0.75, l=1.42, h=0.4, D=0.235	45 x 1.55 x 1.5, *d* = 0.45-0.90	H_i = 0.04 T=1.10-1.80 *B/L* = 0.187-0.430	C_t = 0.18-0.65 C_r = 0.15-0.72 C_l = 0.45-0.88
The H.M. and Nuzul I.M. (2012)	H-shape FBW	B=0.20, l=0.29, h=0.10, D=0.065	12 x 0.3 x 0.45, *d*=0.20-0.30	*D/d*=0.22-0.325 H_i/L = 0.025-0.125 *B/L* =0.10-0.50	C_t = 0.18-0.70
Nuzul I.M. (2012)	Improved H-shape FBW	B=0.20, l=0.30, h=0.10, D=0.05-0.103	10 x 0.3 x 0.45, *d*=0.20-0.30	*D/d*=0.17-0.52 H_i=0.005-0.075 *B/L* =0.10-0.50	C_t = 0.15-0.65
Present Work (2013)	H-type FBW	B=1.00, l=1.44, h=0.50, D=0.24-0.31	25 x 1.5 x 3.2, *d*=0.7	*D/d*=0.34-0.44 H_i/L = 0.04-0.07 *B/L* =0.22-0.65	C_t = 0.08-0.47 C_r = 0.73-0.87 C_l = 0.44-0.61

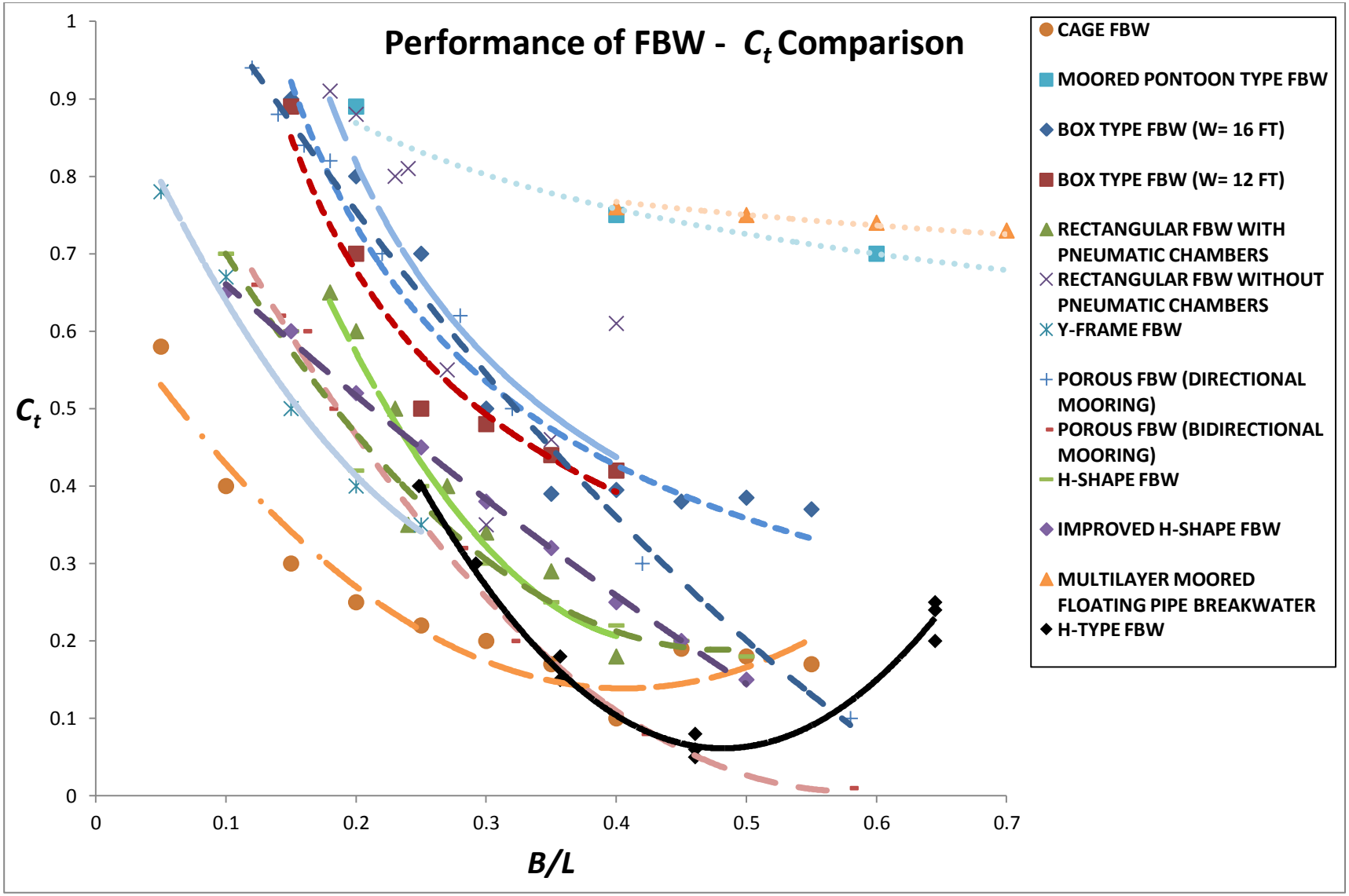

Figure 4.17: Comparison of Transmission Coefficient results with previous studies

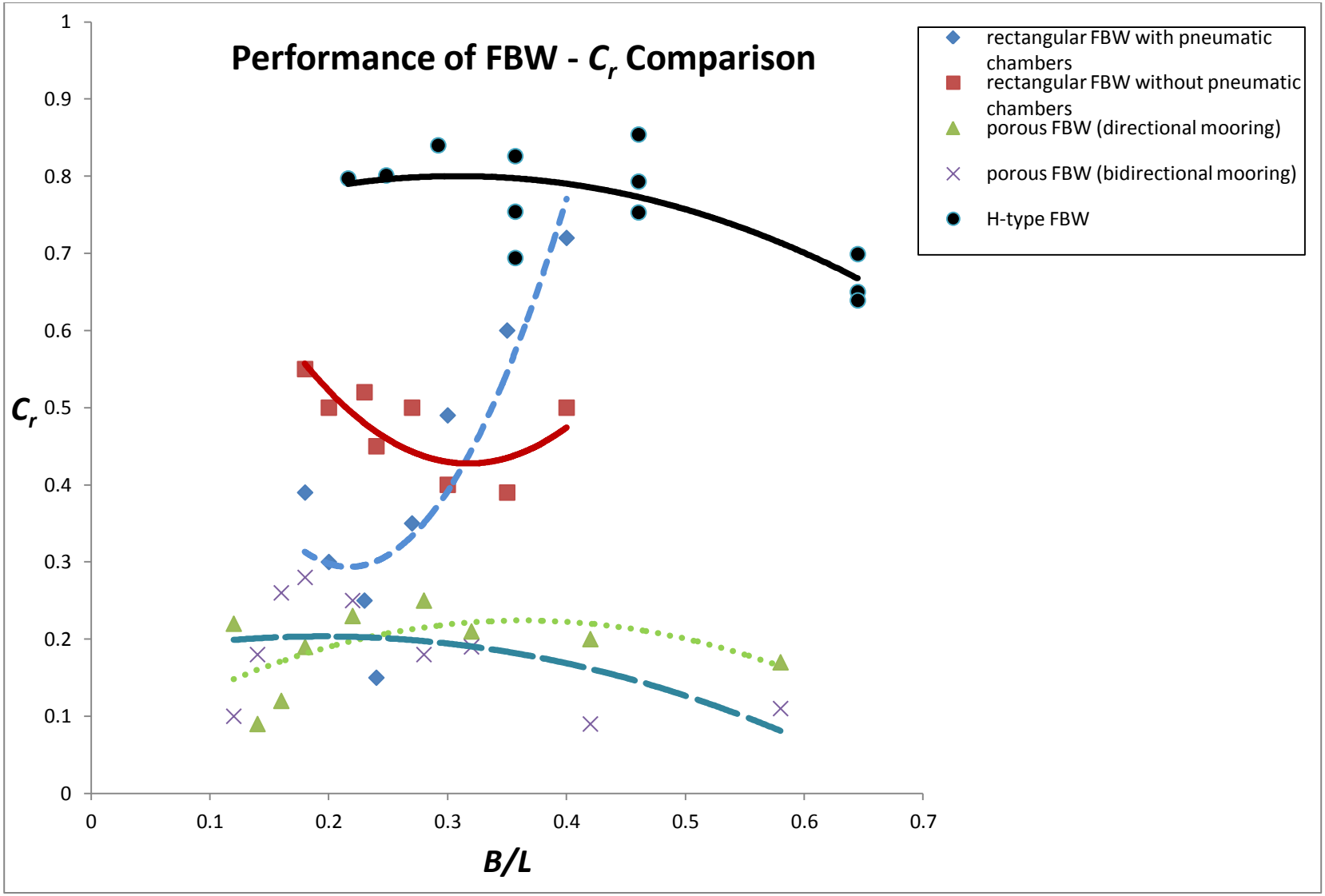

Figure 4.18: Comparison of Reflection Coefficient results with previous studies

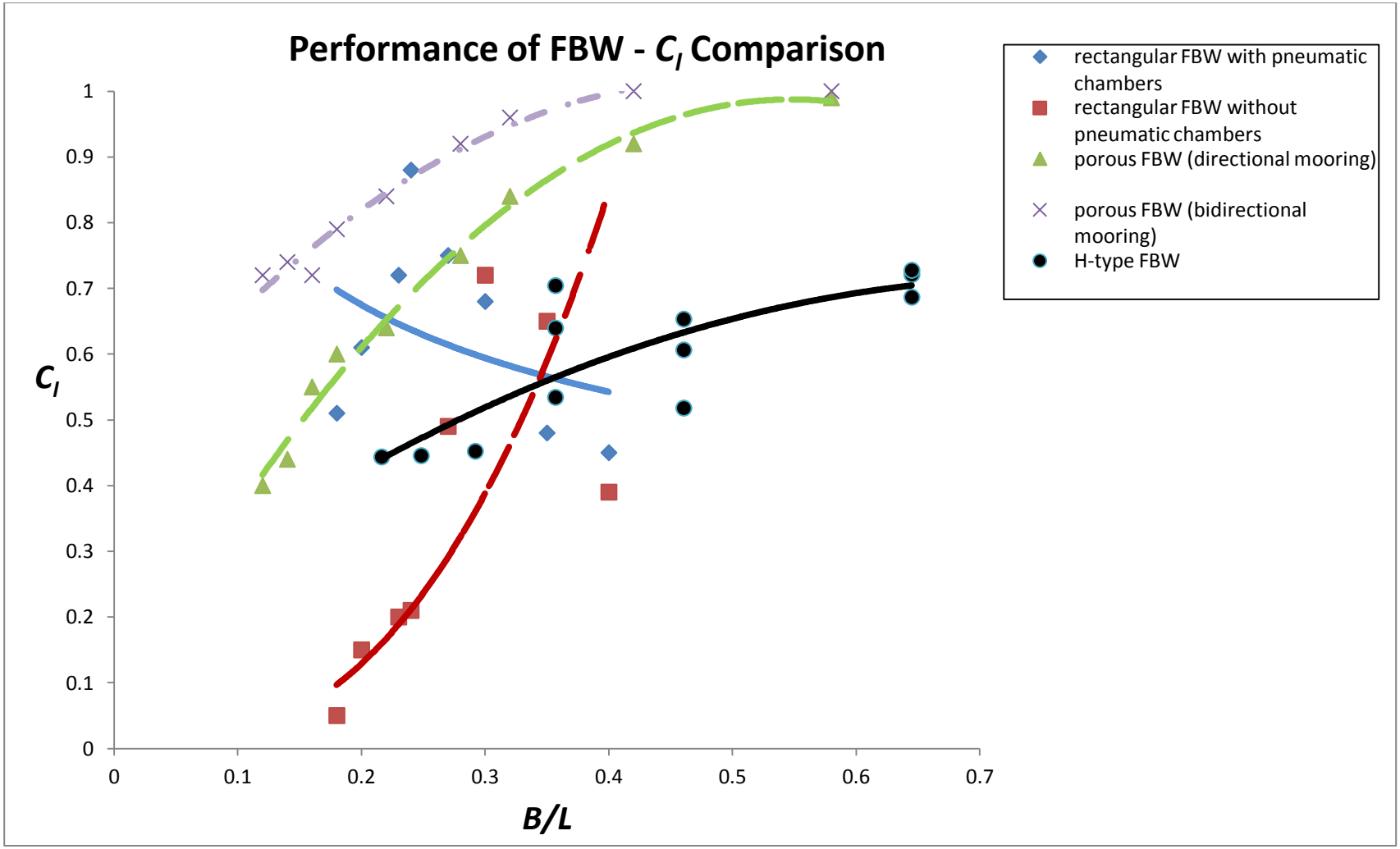

Figure 4.19: Comparison of Energy Loss Coefficient results with previous studies

4.6 Concluding Remarks

The efficiency and hydraulic performance of the H-type floating breakwater was studied via means of physical modeling in both regular and random waves to simulate the realistic sea state. The flume that was used in this experiment was first calibrated and the calibration was also done to other experimental apparatus that will be used when conducting this experiment. The calibration was done to increase the accuracy and the consistencies of the results obtained while at the same time minimize the error that will be encountered throughout the experiment.

The model was designed to test the effect of its scaled up size on its performance in attenuating incoming wave energy. Besides that, it was design to be equipped with the function of draft adjustment to assist in the immersion of the floating breakwater. A number of ballast chambers were installed in the H-type floating breakwater which will then be filled with sand bags to allow the model to be immersed while freely floating on the water surface.

The experimental results show the time series plot of the various test conditions. Using Fast Fourier Transform, these time series plot are then converted to frequency domain plot where the spectral density of the wave interaction can be analyzed. Based on these wave spectra, the energy coefficients of the wave that interact with the H-type FBW can be calculated. The energy coefficients that were being studied are the transmission coefficient, reflection coefficient and energy loss coefficient. The overall results of the energy coefficients were then plotted against the relative breakwater width and also the relative wave steepness parameter separately to study the effects of these manipulated variables towards the energy coefficients. The results obtained shows that the model can restrict more wave transmission in shorter period waves, a good wave reflector when it is deeply immersed and can dissipate more short period waves when it is immersed in shallow water depth.

The results of the experiment were then compared with the floating breakwaters that were developed by other previous researchers and it was deduced that the H-type floating breakwater outperformed most of the floating breakwater in terms of wave

transmission wherein the model only allow less wave to be transmitted to the lee of the breakwater compared to other breakwater model. The H-type is also a good wave reflector as it shows higher scatters of plotted values mainly due to its configuration as well as its immersion ability. However the H-type floating breakwater is not a good wave energy dissipater as it shows a slightly lower trend when compared with other floating breakwater developed by other researchers.

To conclude this study, the H-type floating breakwater shows a hugely promising result but much more investigations are needed to assess the possible enhancement that needed to improve the performance of the floating breakwater further.

CHAPTER 5

CONCLUSION AND RECOMMENDATION

5.1 Conclusion

The H-type floating breakwater has been developed in this study. Some of the major conclusions within the test limits are given below:

- Calibration of the wave flume shows that the test can be conducted at a maximum water depth of 0.7 m and a maximum wave height of 0.20 m due to some limitation by the laboratory apparatus.
- Adjustment of the H-type floating breakwater draft was made possible with the availability of the ballast chambers. The submergence of the model was easily adjusted by simply adding or removing sand bags. However, this will also increase the weight of the model and thus increased the inertia of the model.
- Transmission coefficient analysis reveals that more than 50% of wave energy was restricted by the model from being transmitted with the increase in relative width of the model as well as the increase in incident wave steepness. Moreover, the model performed even better when it is being submerged deeper into the water.
- Reflection coefficient analysis indicates that more wave energy was being reflected by the model when the relative breakwater width was small and also when the incident wave was of low steepness. Increasing the draft of the breakwater also shows that more wave energy can be reflected by the model.
- Energy loss coefficient analysis reveals that for shallow immersion depth, the model was able to dissipate more wave energy in shorter period waves as well as steeper waves.
- Comparison with previous studies indicates that the model outperformed most of the other previously investigated floating breakwater in terms of wave transmission coefficient. The model can attenuate as high as 95% of wave energy when the model was immersed deeply into the water. The model also excels well in reflecting incident waves as more waves were reflected when

compared to other floating breakwater. However, the model was not able to compete well in wave energy dissipation as the other floating breakwater shows higher energy loss coefficients.

- The performance of the H-type floating breakwater was very satisfactory although much more study is needed to be conducted on this model.
- The objective of the study was achieved as the model was tested in a condition that was similar to a typical sea condition.

5.2 Recommendation

The H-type floating breakwater was performing very well in both regular wave as well as random waves. However, few recommendations are needed for the improvement of the H-type floating breakwater such that as shown below;

- The improvement of design was focused mainly on the draft adjustment and larger width on the performance of the floating breakwater but the effect of enlarging the scale was not studied in this experiment. Further study should focus on the effect of model scale on the performance of the model and the result should be compared with previously similar design as well as test conditions.
- The length of the model was quite large in this experiment. This affects the transmission of the waves at the breakwater side due the small clearance between the breakwater and the walls of the wave flume. Future design must focus on redesigning the width of the breakwater so that the transmission the waves will not be blocked at the side of the model.
- Due to the limitation of the wave probes, higher waves steepness could not be recorded, thus, new waves probes that can measure high steepness on incident waves should be used instead of the existing wave probes.
- The experimental studies should be conducted in various ranges of wave period, wave steepness and also water depth to show how well the model will perform in respect to various water depths.
- The model price should be compared with other models price as it was locally made. This will show if the H-type floating breakwater is an effective solution compared to other floating breakwater that was fabricated overseas.
- A shock absorbance material should be installed on the outer surface of the model to prevent the model from being damaged when colliding with the flume wall.

REFERENCES

Adee, B.H., 1976. A Review Of Developements And Problems In Using Floating Breakwaters. *Proceeding of 8th offshore technology conference*, 2, pp.225–236.

Army, U.S.A.C. of E. Department of the, *Engineering and Design, Coastal Engineering Manual*, Washington, DC 20314-1000.

Bayram, A., 2000. Experimental Study Of A Sloping Float Breakwater. *Journal of Ocean Engineering*, 27, pp.445–453.

Behzad, M. M. Akbari, 2007. Experimental Investigation On Responses And Efficiency Of Moored Pontoon Type Floating Breakwaters. *Iranian Journal of Science and Technology, Transaction B, Engineering,*, 31, pp.95–99.

Bishop, C.T., 1982. Floating Tire Breakwater Comparison. *Journal of Waterway, Port, Coastal and Ocean Engineering*, 108(3), pp.421–426.

Brebner, A.O. A. Ofuya, 1968. Floating Breakwaters. *Proceeding of the 5th Coastal Engineering Conference*, pp.1055–1085.

Carver, D.D. R.D. Davidson, 1983. Sloping Float Breakwater Model Study. *Proceeding of coastal structure 83A speciality conference on design construction, maintenance and performance of coastal structure*, pp.417–432.

Carver, R.D., 1979. *Floating Breakwater Wave Attenuation Tests For East Bay Marina, Olympia Harbour Hydraulic Model Investigations*, U.S. Army Engineers, Watermay experiments Station, Vicksburg, Missisipi.

Dong, D.F. G.H. Zheng Y.N. Li Y.C. Teng B. Guan C.T. Lin, 2008. Experimentas On Wave Transmission Coefficient Of Floating Breakwaters. *Journal of Ocean Engineering*, 35, pp.931–938.

Duclos, C. G. Josset C. Clement S.H. Gentaz L. Colmard, 2004. Hydrodynamic Efficiency Of A New Design Of Half-submerged Breakwater Compared To A Rectangular Caisson. *Journal of Waterway, Port, Coastal and Ocean Engineering*, 130(3), pp.127–133.

Falcao, A.., 2010. Wave Energy Utilization: A Review Of The Technologies. *Renewable sustainable energy*, 14(3), pp.899–918.

Fousert, M.W., 2006. *Floating Breakwater: A Theoretical Study Of A Dynamic Wave Attenuating System*, Delft University of Technology, Faculty of Civil Engineering and Geoscience, Section of Hydraulic Engineering.

Gesraha, M.R., 2006. Analysis Of "pie" Shaped Floating Breakwater In Oblique Wave: I. Impervious Rigid Wave Boards. *Journal of Applied Science Research*, 28, pp.327–338.

Hales, L.Z., 1981. *Floating Breakwater: State-of-the-art Literature Review, Technical Report No. 81-1*, U.S. Army, Corps of Engineers, Coastal Engineering Research Center.

He, A.K.L. F. Zhen H.H. Wing, 2012. Hydrodynamic Performance Of A Rectangular Floating Breakwater With And Without Pneumatic Chambers: An Experimental Study. *Journal of Ocean Engineering*, 51, pp.16–27.

He, A.W.-K. F. Huang Z. Law, 2013. An Experimental Study Of A Floating Breakwater With Asymetric Pneumatic Chambers For Wave Energy Extraction. *Journal of Applied Energy*, 106, pp.222–231.

Hedge, A.S. V. Kamath K. Magadum, 2007. Performance Characteristics of Horizontal Interlaced Multilayer Moored Floating Pipe Breakwater. *Journal of Waterway, Port, Coastal and Ocean Engineering*, 133, pp.275–285.

Isaacson, R. M. Byres, 1988. Floating Breakwater Response To Wave Action. *Proceeding of the 21st Conference on Coastal Engineering*, pp.2189–2199.

Kamakar, C. D. Bhattacharjee J. Guedes Soares, 2012. Scattering Of Gravity Wave By Multiple Surface-piercing Floating Membrane. *Journal of Applied Ocean Research*, 39, pp.40–52.

Kato, Y. J. Hagino S. Uekita, 1966. Investigation Of Floating Breakwater To Which Anti-rolling System Is Applied. *Proceeding of the 10th Coastal Engineering Conference*, pp.1068–1078.

Kee, M.H. S.T. Kim, 1997. Flexible Membrane Wave Barrier ii: Floating/submerged Buoy-membrane System. *Journal of Waterway, Port, Coastal and Ocean Engineering*, 123, pp.82–90.

Koftis, P. T. Prinos, On The Hydrodynamic Efficiency Of Floating Breakwater. *Proceedings of the Conference of Arabian Coast, Dubai*.

Koftis, P. T. Prinos, 2005. On The Hydrodynamic Efficiency Of Floating Breakwaters. *Conference of Arabian Coast 2005*.

Koraim, A.S., 2013. Hydrodynamic Efficiency Of Suspended Horizontal Rows Of Half Ppipe Used As A New Type Breakwater. *ocean engineering*, 64, pp.1–22.

Kumar, R. K.S.V. Sundaravadivelu, 2001. Hydrodynamic Characteristics Of Moored Floating Pipe Breakwater. *Proceedings of 1st Asia-Pasific Conference on Offshore System*, pp.159–164.

Liang, C.F. N.K. Huang J.S. Li, 2004. A Study Of Spar Buoy Floating Breakwater. *Journal of Ocean Engineering*, 31, pp.43–60.

Mani, C.R. J.S. Venugopal, 1987. Wave Transmission Characteristics Of Floating Berrier. *Proceeding of 2nd national conference on docks and harbours engineering*, pp.53–59.

Mani, J.., 1991. Design Of Y-frame Floating Breakwater. *Journal of Waterway, Port, Coastal and Ocean Engineering*, 117, pp.105–119.

Mansard, E.R. E.P.D. Funke, 1980. The Measurement Of Incident And Reflected Spectra Using A Least Square Method. *Journal of Coastal Engineering*, pp.154–172.

Martinelli, B. L. Ruol P. Zanuttigh, 2008. Wave Basin Experiments On Floating Breakwaters With Different Layouts. *Journal of Applied Ocean Research*, 30, pp.199–207.

McCartney, B.L., 1985. Floating Breakwater Design. *Journal of Waterway, Port, Coastal and Ocean Engineering*, 111, pp.304–317.

Murali, J.S. K. Mani, 1997. Performance Of Cage Floating Breakwater. *Journal of Waterway, Port, Coastal and Ocean Engineering*, pp.172–179.

Nece, N.K. R.E. Skjelbreia, 1984. Ship-wave Attenuation Tests Of A Prototype Floating Breakwater. *Proceedings of the 19th conference on Coastal Engineering*, pp.2515–2529.

Ozeren, W.P.A. Y. Wren. D.G. A.M.ASCE Altinakar M., 2011. Experimental Investigation of Cylindrical Floating Breakwater Performance with Various Mooring Configurations. *Journal of Waterway, Port, Coastal and Ocean Engineering*, 137, pp.300–309.

Patil, S. S.G. Mandal S. Hedge A.V. Alavandar, 2011. Neuro-fuzzy Based Approach For Wave Transmission Prediction Of Horizontal Interlaced Multilayer Moored Floating Pipe Breakwater. *Journal of Ocean Engineering*, 38, pp.186–196.

Purusthotham, R. S. Sundar V. Sundaravadivelu, 2001. Hydrodynamic Characteristics Of Moored Floating Pipe Breakwater. *Proceedings of 1st Asia-Pasific Conference on Offshore System, Kuala Lumpur*, pp.165–170.

Rahman, K. M.A. Mizutani N. Kawasaki, 2006. Numestudy Modeling Of Dynamic Responses And Mooring Forces Of Submerged Floating Breakwater. *Journal of Ocean Engineering*, 53, pp.799–815.

Sannasiraj, R. S.A. Sundar V. Sundaravadivelu, 1998. Mooring Forces And Motion Responses Of Pontoon-type Floating Breakwaters. *Journal of Ocean Engineering*, 25, pp.27–48.

Seymour, D.M. R.J. Harnes, 1979. Performance Analysis Of Tethered Float Breakwater. *Journal of Waterway, Port, Coastal and Ocean Engineering*, 105(3), pp.265–279.

Shih, R.-S., 2012. Experimental Study On The Performance Characteristics Of Porous Perpendicular Pipe Breakwater. *Journal of Ocean Engineering*, 50, pp.53–62.

Sorensen, R.., 1978. *Basic Coastal Engineering*, Singapore: John Wiley & Sons.

Takahashi, S., 1996. *Design of Vertical Breakwater*, Port and Airport Research Institute, Japan.

Tang, W.M. H.J. Hung C.C. Chen, 2011. Dynamics Of Dual Pontoon Floating Structure For Cage Aquaculture In A Two-dimensional Numerical Wave Tank. *Journal of Fluids and Structure*, 27, pp.918–936.

Teh, H. H.M. Ismail, 2013. Hydraulic Characteristics Of A Stepped-slope Floating Breakwater. *Proceedings of the 4th International Conference on Energy and Environment*.

Teh, M.F. H.M. Nuruddin M.F. Hisham, 2006. Experimental Study On The Wave Attenuator Performance Of A Floating Breakwater. *International Seminar on Civil and Infrastructure Engineering*.

Teh, N.I. H.M. Mohammed, 2012. Wave Interactions With A Floating Breakwater. *Proceedings of the IEEE Colloquium on Humanities, Science and Engineering 2012*.

Vethamony, P., 1995. Wave Attenuation Characteristics of a Tethered Float system. *Journal of Ocean Engineering*, 22, pp.111–129.

Wang, Z.C. H.Y. Sun, 2010. Experimental Study Of A Porous Floating Breakwater. *Journal of Ocean Engineering*, 37, pp.520–527.

Williams, A.G. A.N. Abul-Azm, 1997. Breakwaters Floating Breakwater. *Journal of Ocean Engineering*, 24, pp.465–478.

Williams, Z. A.N. Lee H.S. Huang, 2000. Floating Pontoons Breakwater. *Journal of Ocean Engineering*, 27, pp.221–240.

Yamamoto, T., 1981. Moored Floating Breakwater Response To Regular And Irregular Waves. *Journal of Applied Ocean Research*, 3(1), pp.114–123.